ISSN 2709-4529
Volume 5, Number 2,
December 2024

Journal of Digital Food, Energy & Water Systems [JD-FEWS]

About the Journal

The Journal of Digital Food, Energy & Water Systems (JD-FEWS) is a peer-reviewed bi-annual publication that publishes recent and innovative deployment of emerging digital technologies in Food, Energy, and Water Systems. Food, energy, and water resources are interconnected scarce resources that require systems and technologies to foster sustainable management and effective utilization. The journal is also interested in articles that explore the nexus between at least two of these resources. The journal considers the following topics as long as they are deployed in the Food, Energy & Water space:

- Advanced Metering Infrastructure (AMI)
- Algorithm development
- Artificial Intelligence
- Blockchain and distributed ledger technology
- Case studies
- Cybersecurity
- Data mining & Big data
- Human-Computer Interaction
- Intelligent Forecasting
- Internet of Things
- Machine Learning
- Mathematical Optimization
- Robotics
- System architectures
- Wireless Sensor Networks

Editorial Team

Journal of Digital Food, Energy & Water Systems [JD-FEWS]

Table of Contents

Volume 5 Number 2, December 2024

ARTICLES

Journal of Digital Food, Energy & Water Systems [JD-FEWS]

JDFEWS 5 (2): 1-16, 2024
ISSN 2709-4529

Micro-Grid Wind Energy Conversion System: Conventional and Modern Technologies - A Review

Mutiu AGBOOLA,

Federal Polytechnic Ede, Nigeria; agboolamutiu10@gmail.com

K. A. HASSAN

Federal Polytechnic Ede, Nigeria.

T. O., AJEWOLE

Osun State University, Nigeria.

Received: 30 July 2024

Review: 26 October 2024

Accepted: 13 December 2024

Published: 16 December 2024

Abstract - This paper thoroughly looks at how well the introduction of modern technology, especially an artificial neural network-based control mechanism, works compared to other conventional control methods in the applications of electric microgrid wind energy conversion systems. The study uses data analytic method to compare modern proposed technology (MPT) and conventional conversion systems (CCS) for controlling wind turbine systems by examining their advantages and disadvantages via data analysis methodology. Furthermore, the study explained the key factors influencing power quality output during the conversion process, such as pitch angle control, power coefficient, and tip speed ratio, across both methodologies. Poorer power quality results from the conventional conversion technologies' requirement to use mechanical sensors to alter the turbine rotor's rotational velocity. However, with the advent of artificial neural networks, mechanical sensors are no longer necessary, and power quality output is improved with little to no impact on wind turbine rotors. Therefore, compared to the conventional wind energy conversion system (WECS), introducing artificial neural networks with microcontrollers has demonstrated positive outcomes as one of the latest technologies. Hence, this study aims to identify key research areas and assist researchers and experts in gaining a current and thorough understanding of the efficacy of neural network applications in wind energy conversion systems.

Keywords*:* Artificial *Neural Network, Wind Energy Conversion System, modern technologies, conventional methods*.

JDFEWS 5 (2): 1-16, 2024
ISSN 2709-4529

1.0 Introduction

Recent research has demonstrated that incorporating renewable energy sources (RES), including wind energy, into microgrid systems has attracted significant interest because of its multiple advantages, including less reliance on fossil fuels and lowered carbon emissions [1]. Given the rising demand for electricity and the exhaustion of traditional energy sources, it is imperative to augment electricity production by utilizing renewable energy sources such as wind and solar energy, among others [2]. Also, due to the need for an efficient and clean power system and the challenges associated with conversion, it is crucial for researchers to concentrate on the reliability and stability of system control within a power conversion framework. This study categorizes energy generation systems into two primary groups based on their potential exhaustibility: renewable power systems and conventional power systems, to ensure power quality from the green energy system. In reaction to the increasing demand for electricity in the 21st century, power generation systems scaled up, utilizing wind energy across capacities from several kilowatts to numerous megawatts [3]. This research examines green energies, mainly wind energy conversion systems (WECS), in the context of both conventional and modern harvesting methods. Research indicates that wind turbines are the primary component of the WECS, and they function primarily through rotors and blades. Characteristics such as pitch angle, power coefficient, and tip speed ratio influence the efficiency of these elements. The tip speed ratio (TSR) within regulatory limits can optimize turbine performance, particularly when the ratio is smaller than 1 [4].

Considering the difficulties posed by the wind turbine and its blades when controlled conventionally, conventional control is linked to mechanical control using sensors, which typically entail mechanical losses that lead to an output of low quality [5]. However, to remove the sensor influence on the mechanical output of wind turbines, it is necessary to implement contemporary technologies like grid-side converters (GSC), fuzzy logic controllers (FLC), and particle swarm optimisation (PSO). Also, to address these issues, researchers have presented an artificial neural network algorithm to regulate wind turbines. The effectiveness of this algorithm is thus evaluated by comparing previous research in this area using data analytical techniques.

2.0 Research Methodology

The number of publications on the application of conventional and modern technology in wind energy conversion system applications was investigated in this study through WEB sources via a data analysis methodology, which is synonymous with a systematic literature review (SLR). Pitch angle, tip speed ratio, and power coefficient—three key factors affecting the power output quality—are the main areas of focus for the artificial neural network controller's effectiveness on the wind turbine and its blade. The work of [6] shows that in global estimates, WECS is among the rapidly expanding technologies for energy sources, based on existing data regarding wind abundance in natural phenomena. Furthermore, the study of Ref [7] offers valuable insights into assessing the efficacy of WECS that employ both conventional and modern harvesting techniques. Consequently, in addressing the issue of mechanical strain on the turbine blade, a conventional approach is proposed for adjustments of both full-load and partial-load conditions. The operational series of a WECS dependent on wind speed is shown in Figure 1 and affects the performance of TSR tracking [8][9]. This calls for a more advanced technique for monitoring the maximum power point in WECS, as shown in the sketch, which involves determining the cut-out and cut-in speeds at a rated wind speed [10].

JDFEWS 5 (2): 1-16, 2024
ISSN 2709-4529

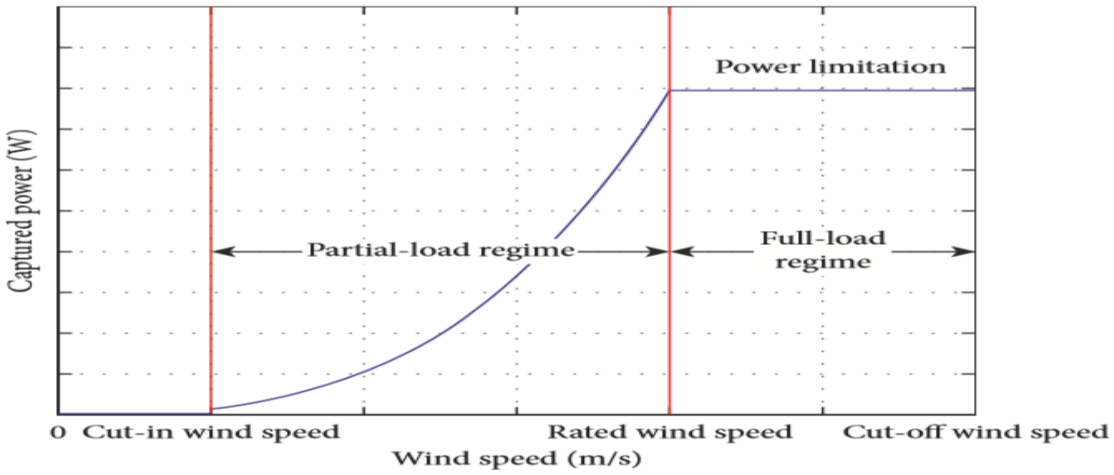

Figure 1 Wind Speed Operational Mode [14].

3.0 Wind energy conversion system under conventional systems

Figure 2 illustrates the mechanism through which the blade, located on the rotor hub, transforms the wind's kinetic energy into mechanical energy. The low-speed shaft, functioning as the principal shaft, firmly connects the hub. The generator transforms mechanical energy into electrical energy via the drive train. Electricity converter systems perform an intermediary between the grid and the generators, enabling the flow of electricity from the generator to the grid. These mechanisms are chiefly accountable for the conversion process, as corroborated by [2] in conventional technology. Ref [11], in their work's on conventional methodology, established that WEC system comprises two primary electrical components: the generator and the power converter. The author presents a realistic operation of the wind turbine power converter for WECS, utilizing independently stimulated DC motor control for converting kinetic energy into electrical energy with little mechanical losses.

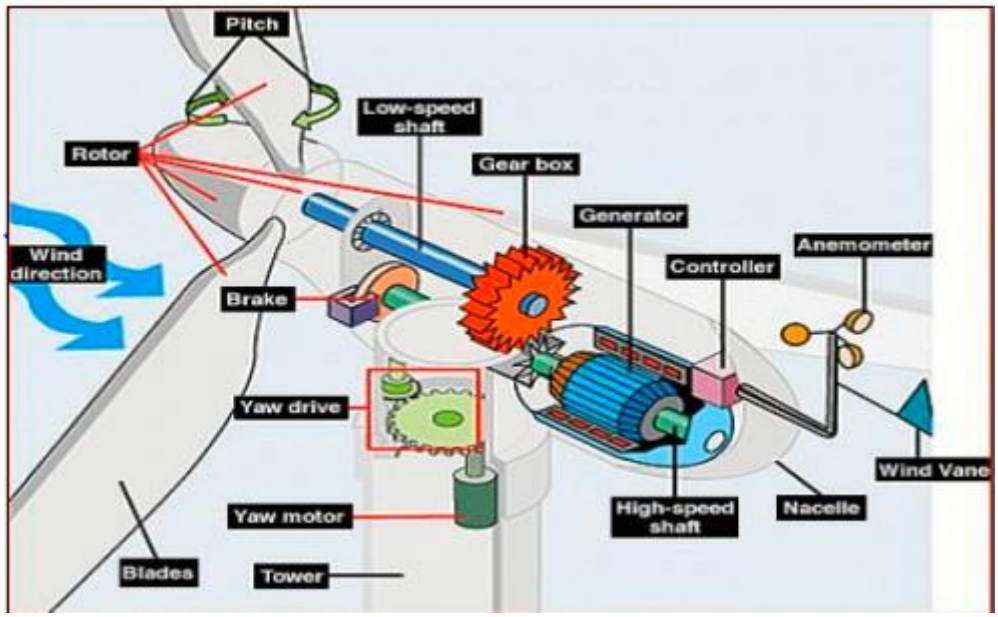

Figure 2: Side View of a Typical WEC System [2]

JDFEWS 5 (2): 1-16, 2024
ISSN 2709-4529

Also, in the work of [12], the author established that due to the unpredictability of wind, the voltages generated by the generator display persistent swings in both frequency and amplitude and lead to power loss in the energy generation. Ref [13] proves that the generated electric power is unsuitable for standard operational loads due to the parameters' variability, leading to so much energy wasted.

Also, a crucial aspect of the conversion process involves pitch control, power management, and synchronous grid operations, as illustrated in Figure 3, which depicts the entire wind turbine generator and its converter in operation [15]. When wind speeds exceed the specified threshold, the pitch angle control mechanism activates, thereby ensuring stable power generation [16] by modifying the turbine blade angle in relation to the wind speed rating value, which serves as the power control variable that may lead to unstable mechanical power output [17] under the conventional system. [18]. The TSR has a big impact on the power efficiency of WEC and an important part of wind turbine design because it quantifies the correlation between wind velocity and the velocity of the blade tips [19]. To study how blade solidity affects micro scale wind turbines with lower TSR, the blades need to be made stronger to overcome the torque frictions for their mechanical part and start working [20]; otherwise, the mechanical power output efficiency will be affected. Also, using conventional approaches, many control methods have been developed to obtain high-quality power from wind turbine generators. A good example is the adjustment of wind turbines using permanent magnet generators (PMG), adjusting the turbine rotor speed, and synchronizing the generators, among others. All these innovations aim to evaluate the efficiency of energy generation by improving control over the primary parameters influencing wind turbine operation in the WECS under conventional evaluations but come with imitations [14].

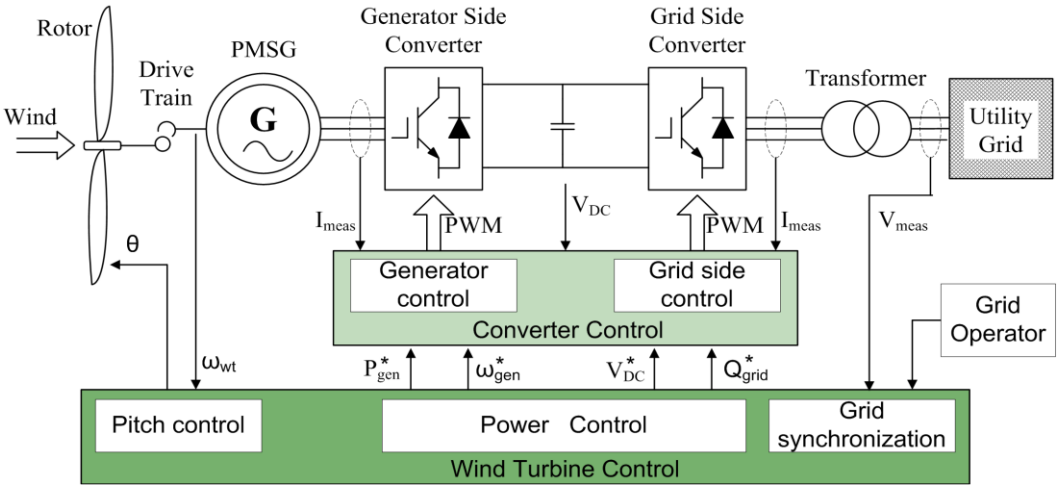

4.0 Power Coefficient, Pitch Angle, and Tip Speed Ratio Operations

Pitch angle, tip speed ratio, and power coefficient are the three main control factors that can be managed using various algorithms or contemporary controllers like maximum power point tracking (MPPT), maximum power control (MPC), magnetic synchronous controls (MSC), generator synchronous controls (GSC), pitch angle control (PAC), power coefficient (PC), and artificial neural networks (ANN), among others, in light of the many difficulties with the current methods and controls of wind energy harvesting in the WECS.

The International Electrotechnical Commission (IEC) designated the power coefficient (Cp) as a critical metric for assessing wind turbine performance [21]. The Cp quantifies the correlation between actual power output and the wind power available to the turbine blades. The results indicate that the electrical power generated by wind turbines is mostly affected by the performance coefficient, but the mechanical power is exactly proportional to the cube of the wind speed [22]. The Cp of a horizontal axis turbine is often affected by various factors, including

JDFEWS 5 (2): 1-16, 2024
ISSN 2709-4529

the number of blades, the TSR (λ), and the blade pitch angle (β). The Cp of a turbine is defined as the coefficient power tip speed ratio and pitch angle, respectively Cp (λ, β), which indicates the turbine's efficiency, together with the blade TSR and the pitch angle, respectively [23] and [24]. Blade pitch actuators control the speed of the rotor, which lowers the wind turbine's mechanical torque output and performance coefficient. The three-blade and the horizontal-axis models have been proven to be the most common types of wind turbines [25]. In [26], the authors show how to use a proportional-integral (PI) controller to control the pitch angle with the goal of keeping the output voltage constant. Pitch angle control is the most efficient technique for modifying a wind turbine's aerodynamic thrust when wind speed surpasses the rated speed conventionally. Incorporating sliding mode control, feedforward, and feedback systems into the robust wind turbine systems' robust controller improves pitch angle control's reliability [27]. The blade element momentum (BEM) method, Buhl's wake state model, and the Viterna-Corrigan post-stall model, all can enhance the Cp of a tiny wind turbine rotor. This subsequently enhances the efficiency of energy production, as indicated by [28].

Another crucial parameter is the TSR, whose operation significantly impacts the quality of power production in the WECS. Figure 4 presents a standard TSR control block diagram with an implementation of the TSR controller. The results demonstrated that an increase in the TSR correlates with a drop in the ideal maximum power, indicating a direct influence of the TSR on power production. It has been shown that a simulated Savonius turbine reached its highest power coefficient of 0.31 at a TSR of 0.97, proving that a hybrid turbine works well [29]. Ref [30] looks at how TSR affects the performance of Savonius wind turbines with flexible blades using a quasi-2D model and a two-way fluid-structure interaction method, with the goal being to improve aerodynamic efficiency. It has also been demonstrated that the TSR influences the aerodynamic noise of a small wind turbine while maintaining an optimal power output [31]. To enhance energy output while maintaining a low rotor speed, it is unwise to use a uniform turbine-specific rating across all turbines in a wind farm [32].

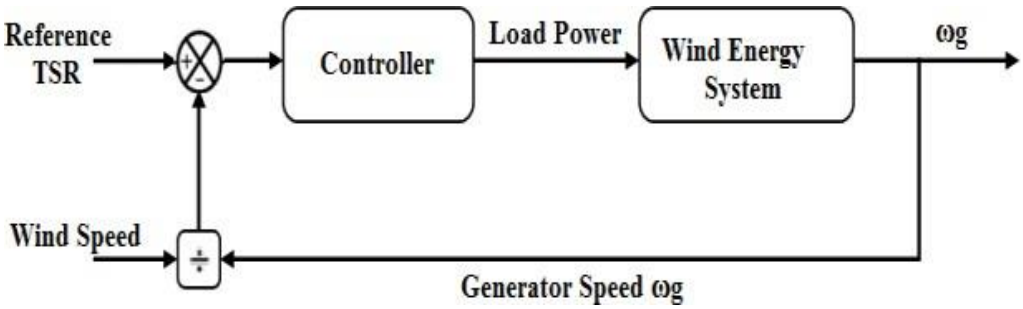

Figure 4. Block diagram of TSR-based MPPT control [29].

5.0 Artificial Neural Network Based Control

Having examined and evaluated different controllers on WECS, an artificial neural network is evaluated and proposed in this review work. An ANN is a computational model that simulates the human brain's operations to provide novel solutions. The term "Modern operating systems" refers to specialized operating systems made for systems, like FreeRTOS, VxWorks, Embedded Linux, and ANN. Numerous fields, such as industrial automation, robotics, power control systems, and energy systems, use modern technology.

According to Ref [33], to enhance power quality (PQ) in wind energy conversion systems (WECS), the author used a neural network (NN) controller for pitch angle management by backpropagation training, as illustrated in Figure 5. Using a multi-layer perceptron backpropagation ANN (MLP-BP ANN) and a dynamic voltage restorer (DVR) as a series compensator, the author created a model matrix in his study that produces an enhanced mechanical power output. By tracking wind speed faster than an anemometer WECS operation, ANN can efficiently monitor turbine maximum power in static and dynamic circumstances [34].

JDFEWS 5 (2): 1-16, 2024
ISSN 2709-4529

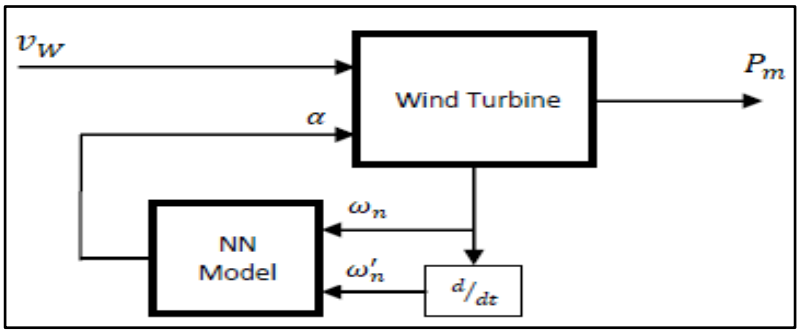

Figure 5 Block Diagram of NN Control Based of pitch angle in WEC system [33]

6.0 Wind Energy Integrations to the Grid with modern technology

Rapid industrial knowledge advancement has led to improved control algorithms in connecting WECS to the grid [35, 36]. Research indicates that in early wind turbine systems, it was common to directly link a wind turbine to the electrical grid, a method occasionally termed the "Danish concept." The AC grid can interconnect a wind farm at multiple voltage levels, ranging from low to very high. A high-voltage alternating current (HVAC) transmission system and an insulated bipolar voltage-source converter (VSC), both suitable for grid connections, can achieve this [37]. Ref [38] proposed that a grid connection with a soft start efficiently decreases peak currents, alleviating stress on the gearbox and limiting the impact on the power system, along with related expenses. During an inquiry, [39] advocates for energy transition using power-electronic systems to incorporate energy from renewable sources into the electric grid. The findings reveal that the integration of renewable energy sources with power electronics, which represents one of the traditional methods of integration in WECS, significantly impacts system stability in multiple ways [40]. The low inertia of wind turbines inside synchronous renewable grids hinders reliable power modulation in the traditional system, but rapid power reserve management, an alternative approach, facilitates this without requiring exact grid frequency measurements [41]. While [42] submitted that a power grid often uses phase-locked loop (PLL) procedures to connect to the main electrical network when it is operating under a certain control scheme, [43] suggested that a genetic algorithm could be used on a double-fed induction generator (DFIG) to add power to the power grid using modern methods. Figure 6 depicted the representation and regulation of a wind energy system connecting to the grid through doubly fed induction generators. A rotor-side filter, a grid-side filter, an MPPT controller, a DC-link capacitor, and three-phase voltage source converters (VSCS) and their controller are some of the parts that make up the system of DFIG-based wind turbines.

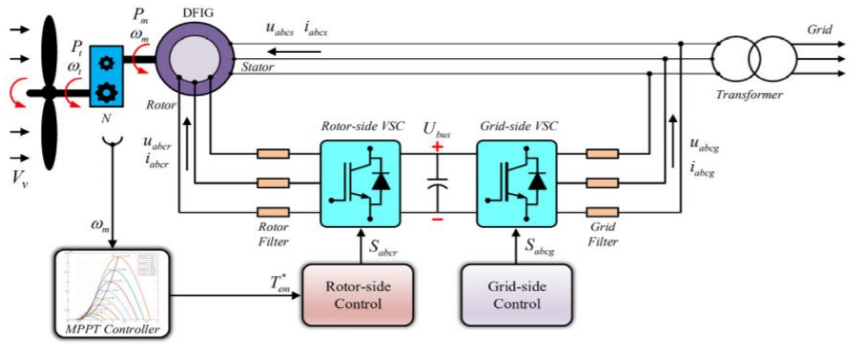

Figure 6. Designing Speed Wind Turbine with (DFIG). [43].

This advanced technology's output response demonstrates enhanced power delivery efficiency [44]. However, [45] posits that using a multipole permanent magnet synchronous generator (PMSG) with MPPT controller is better than a DFIG. This is because the PMSG doesn't need a gearbox, has lower losses, requires less maintenance, and is lighter, more efficient, more reliable, and does not need an external excitation current when connecting to

JDFEWS 5 (2): 1-16, 2024
ISSN 2709-4529

the grid [46]. In conclusion, Ref [47] said that a sliding-mode controller (SMC) design makes it easier to control nonlinear systems and gives stable systems strong and flexible responses. Similarly, [48] confirms this assertion.

The study in [49] develops a Sliding Mode Control (SMC) for wind turbine systems employing a dual-output asynchronous generator directly connected to the power grid, enhancing stability in both frequency and voltage. Ref [50] found that system faults, device failures, load disconnections, and changes in generated power all influence the power balance of electric networks. However, modern controller technology can help fix these problems. However, a later study shows that adding wind energy to the power grid greatly affects how well the system works. Because of this, Ref [51] suggested that using the Distribution Static Compensator (DSTATCOM) and Battery Energy Storage System (BESS) together can improve the power quality of the grid-connected WECS. Ref [52] proposes integrating a fuzzy logic controller with a phase-locked loop (PLL) approach to improve the quality and efficiency of electricity transmission to the grid. Although solid-state transformers (SSTs) can integrate voltage conversion, reactive power correction, and active power transmission, no study has comprehensively examined the full utilization of all SST compensatory functions, as found in [53]. Thus, the authors introduce a novel type of wind farm design utilizing an SST interface, which basically replaces the traditional reactive power compensator and grid connections [54].

The various types of WECS that were empirically examined to determine which generated the most power and which performed better with contemporary technology than the earlier approaches are listed in Table 1. Similarly, there are contemporary methods like artificial neural networks (ANN), magnetic synchronous controls (MSC), generator synchronous controls (GSC), pitch angle control (PAC), power coefficient (PC), maximum power point tracking (MPPT), maximum power control (MPC), and more.

Journal of Digital Food, Energy & Water Systems [JD-FEWS]

JDFEWS 5 (2): 1-16, 2024
ISSN 2709-4529

Table 1: The empirical summary table

Author's Names and Year of Publication	Wind Energy System	Algorithm/Controller	Methodology/Software Used	Inference Drawn/GAP	Performance Metrics
Guediri et al. (2023).	WT+DFIG	Hybrid Genetic Algorithm (GA) controller	Multilevel Inverter (MLI) technique; MPPT technique Active and reactive energy control MATLAB/SIMULINK	GA offers greater efficiency, significant results and enhanced stability to WT, compared to classic PI regulator	WT stability improvement Power quality enhancement
Chen et al. (2023)	WT-driven PMSG	Gray Wolf Optimization (GWO) algorithm Blade Pitch controller	Model predictive control technique Blade pitch control MATLAB	Direct control of WT output power was realized across various wind speeds. GWO exhibited slightly fast minimization times compared to MATLAB's unconstrained optimization function. The approach offers WT independent control and mechanical stability.	WT stability augmentation. Regulation/maximization of load output power. Enhancement of power generation efficiency.
Sharma (2023)	PV-Wind hybrid RES	Modified Fuzzy Logic controller (FLC)	Shunt active power filtering MPPT technique Electromagnetic control method MATLAB/SIMULINK	Electromagnetic control's effectiveness depends on DC link capacitor voltage control.	Power quality enhancement System voltage profile enhancement Overall system power factor Reduction of system peak losses.

Journal of Digital Food, Energy & Water Systems [JD-FEWS]

JDFEWS 5 (2): 1-16, 2024
ISSN 2709-4529

Rawa et al. (2023)	Hybrid RES	DVR-PI controller Gorilla Troops Algorithm (GTA)	DVR control MATLAB/SIMULINK	DVR-PI controller exhibited fast response and minimal objective function. The control technique excelled in voltage quality and harmonic rejection.	Power quality enhancement. System voltage profile enhancement.
Junejo, Gilal, and Doh (2023)	H-type VAWT	Physics-informed optimization Multi-objective Grey Wolf Optimization (GWO)	Advanced Direct Vector control WT rotational speed control Matrix Inequality (MI) technique SIMULINK, CFD tools	WT power efficiency significantly increased. Low-inertia turbines ideal for maximum power conversion.	Enhancement of WT power efficiency Improvement of power output and system stability Improvement of active power gain Optimization of WT power conversion
Aghaei et al. (2023)	VAWT	Radial Basis Function Neural Networks (RBFNN) controller Markov chain Monte Carlo (MCMC) algorithm	Reinforcement Learning (RL) technique MATLAB	Proposed method specifically addressed limitations typically associated with conventional solutions. Algorithm-controller combination outperforms MPPT. Total energy output was maximized, rather than instantaneous output power.	Maximization of WT output power Optimization of WT power output Improvement of power capturing
Pourrajabian et al. (2022)	HAWT	GA optimization algorithm	Blade Geometry control Tip Speed Ratio (TSR) control MATLAB	GA optimization minimized emitted noise along with the maximized power coefficient.	Maximization of WT output power.

Journal of Digital Food, Energy & Water Systems [JD-FEWS]

JDFEWS 5 (2): 1-16, 2024
ISSN 2709-4529

Hosseini et al. (2022)	WT	Jensen Wake Model + Particle Swarm Optimization (PSO)	Tip Speed Ratio (TSR) control Computational Fluid Dynamics (CFD) tools/Large-Eddy Simulation (LES)	TSR reduction mitigates noise, bird/bat collisions, and leading-edge erosion; it addresses environmental concerns.	Reduction of wake losses Turbine downwind power maximization
Chhipą et al. (2022)	Grid-connected DFIG-based WECS	MPPT controller Vector controller	Vector control; Active and reactive power control MPPT technique MATLAB/SIMULINK	Proposed system performs well with variable wind speed control. THD was maintained within IEEE 519 standard's permissible limits.	Improvement of WT power conversion
Pehlivan et al. (2022)	PMGS-based WECS, (VSVPWT)	FLC with GA	Pitch angle control MATLAB/SIMULINK	GA optimized specified pitch angle controller for multiple coefficients. FLC with GA achieved optimal power output quickly and sustainably.	Maximization of WT output power Optimisation of WT power output
Palanimuthu et al. (2022)	Grid-connected Permanent Magnet Vernier Generator (PMVG)-based WT	Integral Sliding-Mode DC-Link Voltage Controller	Active and reactive power control Variable Exponential Reaching Law-based Sliding Mode control	Control schemes stabilized DC-link voltage and converter peak current.	Fault ride-through (FRT) capability Reduction of system peak losses.
Iqbal et al. (2020)	VSWT	Fuzzy based Model-Predictive controller	Pitch angle control MATLAB/SIMULINK	Fuzzy logic controller offers higher performance than conventional PI controller	Reduction of WT loading effect Improvement of power capturing/conversion

Journal of Digital Food, Energy & Water Systems [JD-FEWS]

JDFEWS 5 (2): 1-16, 2024
ISSN 2709-4529

				This technique sustains rotor speed within its limit	Optimisation of WT power output
Mousa et al. (2020)	5-ϕ PMSG-based VSWT (VSVPWT)	Integral Sliding Mode Controller (ISMC)	MPPT technique Pitch angle control MATLAB/SIMULINK	ISMC offers higher performance than conventional PI controller.	Overall system power factor Overall system efficiency Maximization of WT generated power Optimisation of WT power output Reduction of mechanical stress/instability
Hussain et al. (2019)	Grid-connected Wind Power Plant	Distribution Static Compensator (DSTATCOM) controller	Voltage Source Converter (VSC) control PI controller based PLL technique MATLAB/SIMULINK software	DSTATCOM controller improved power factor. The controller provided real and reactive power compensation. Controller was effective for voltage regulation.	Power quality enhancement. Overall system power factor. System voltage profile enhancement.
Zhou & Liu (2018)	WECS	Pitch controller	Pitch angle control Nonlinear PI/PD control method MATLAB/SIMULINK	WECS output power was highly sensitive to pitch angle changes. Nonlinear control reduces power fluctuations better than fixed control. PI control achieved precise speed tracking and accurate pitch adjustment	Optimisation of WT power output Improvement of power capturing/conversion WT stability improvement Reduction of mechanical stress
Yao et al. (2017)	FSIG-based PMSG-based Wind Farms	StatComs	Capacity Configuration method	The controller provided reactive power compensation.	Fault ride-through (FRT) capability Power quality enhancement

Journal of Digital Food, Energy & Water Systems [JD-FEWS]

JDFEWS 5 (2): 1-16, 2024
ISSN 2709-4529

				Controller was effective for voltage regulation.	WT output voltage regulation
Memije et al. (2016)	WT Generator	Newton Raphson algorithm Perturb & Observe (P&O) algorithm	MPPT technique Wind speed control MATLAB/SIMULINK	The Newton-Raphson method provided rapid and accurate wind speed estimates. Wind speed estimation improved MPPT performance.	Power output improvement. WT stability improvement. Reduction of mechanical stress.
Wei et al. (2015)	PMSG-based VS WECS	ANN-based Reinforcement Learning (RL) MPPT algorithm	MPPT control RL technique	Learned MPPs generate optimal speed-power curve for fast MPPT. RL allows WECS to operate without turbine or wind data.	Optimisation of WECS power generation
Barzola et al. (2015)	PMSG-linked WT	Damping control algorithm Proportional-Integral (PI) Controller	Bidirectional DC-DC converter control PSCAD software	Bidirectional DC-DC converters effectively managed energy flow between the system and the grid. Controlling of bidirectional DC-DC converter effectively maintained voltage stability and optimized power output.	Improvement of power oscillation damping. Improvement of active power gain. Voltage stability improvement. Reduction of mechanical stress. Cost saving
Rekha & Immanuvel (2014)	1-ϕ Grid-connected Wind Energy Generation system	FLC	MPPT & SVPWM technique Modified Phase Locked Loop (PLL method)	Modified PLL method reduced Total Harmonic Distortions (THD) in single-phase wind generation.	Power quality enhancement Optimisation of WT power output

Journal of Digital Food, Energy & Water Systems [JD-FEWS]

JDFEWS 5 (2): 1-16, 2024
ISSN 2709-4529

Khajuria & Kaur (2012)	VSWT	Speed controller	Pitch angle control MATLAB/SIMULINK	Speed controller adjusted blade pitch for accurate power output.	WT output voltage regulation
Beltran et al. (2012)	DFIG-based WT	Higher-order sliding mode controller	MPPT technique WT simulator FAST	Controller rapidly stabilized WT to desired operating point.	Improvement of WT power conversion. WT stability improvement. Reduction of mechanical stress. Cost saving.
Li et al. (2011)	PMSG-based WT	Vector control mechanism. Machine- and Grid-Side Converter controller (MSC and GSC).	Two side-by-side voltage source PWM converter control. Direct-Current Vector control (DCVC). Integrated control of PMSG maximum power extraction, reactive power, and grid voltage support controls. MATLAB/SIMULINK.	The DCVC approach offers improvement to power quality and stability of the electricity supplied to the grid.	Improvement of power capturing/conversion Power quality enhancement Optimization of WT power output Reduction of mechanical stress
González et al. (2010)	PMSG-based WT	Modified Perturb&Observe (P&O) algorithm	MPPT technique Sensorless wind speed control PSIM software	Large reduction of turbine mechanical stress. Modification of P&O algorithm yielded improved MTBF.	Improvement of system MTBF System voltage profile enhancement Reduction of mechanical stress Cost saving
Arifujjaman et al. (2006)	Small WT Emulator	Maximum Power controller	WT speed and rotor speed control	The controller enables WT operation at optimum tip-speed ratio.	Improvement of power capturing/conversion

JDFEWS 5 (2): 1-16, 2024
ISSN 2709-4529

5.0 Conclusions

Researchers have looked closely at the control of conventional and modern wind energy conversion systems, focusing on artificial neural network techniques. To fill in the gaps in the literature and offer a framework for further research, this paper evaluates a few of the control strategies used in wind turbine operations. The paper closely examines the primary contemporary wind energy techniques, including grid-side converters (GSC), fuzzy logic controllers (FLC), and particle swarm optimisation (PSO), among other algorithms. The methods were the focus of this study, revealing several application areas for better use and decision-making. The studies and evaluations conducted demonstrate the significant potential of modern technology in the field of wind energy. According to the study, using artificial neural networks in conjunction with microcontrollers has proven to be a successful modern technology compared to the conventional wind energy conversion system (WECS) in solving the problem related to mechanical sensors connected to wind turbines and leading to poor power output. This thorough analysis aims to assist academics and experts in gaining a current and comprehensive understanding of the efficacy of applications of artificial neural network algorithms in wind energy conversion systems. Thus, more research on applying alternative algorithms for parameter control, development complexity, memory restrictions, and computational complexity, especially for tip speed control—may be necessary.

References

[1] Elgendi, M., AlMallahi, M., Abdelkhalig, A., & Selim, M. Y. (2023). A review of wind turbines in complex terrain. *International Journal of Thermofluids*, *17*, 100289.

[2] Ajewole, T. O. (2010). Fault Analysis on Grid-Integrated Photovoltaic Power System". *Unpublished Master of Science Thesis, Faculty of Technology, Obafemi Awolowo University, Ile-Ife, Nigeria*.

[3] Syahputra, R. (2013). A neuro-fuzzy approach for the fault location estimation of unsynchronized two-terminal transmission lines. *International Journal of Computer Science & Information Technology*, *5*(1), 23.

[4] Junejo, A. R., Gilal, N. U., & Doh, J. (2023). Physics-informed optimization of robust control system to enhance power efficiency of renewable energy: Application to wind turbine. *Energy*, *263*, 125667.

[5] Tiwari, R., & Babu, N. R. (2016). Recent developments of control strategies for wind energy conversion system. *Renewable and Sustainable Energy Reviews*, *66*, 268-285.

[6] Raouf, A., Tawfiq, K. B., Eldin, E. T., Youssef, H., & El-Kholy, E. E. (2023). Wind energy conversion systems based on a synchronous generator: comparative review of control methods and performance. *Energies*, *16*(5), 2147.

[7] Momoh, J. A. (2012). *Smart grid: fundamentals of design and analysis* (Vol. 33). John Wiley & Sons. 1111

[8] Zhou, F., & Liu, J. (2018). Pitch controller design of wind turbine based on nonlinear PI/PD control. *Shock and Vibration*, *2018*(1), 7859510.

[9] Rodriguez, J., Blaabjerg, F., & Kazmierkowski, M. P. (2023). Energy transition technology: The role of power electronics. *Proceedings of the IEEE*, *111*(4), 329-334.

[10] Aghaei, V. T., Ağababaoğlu, A., Bawo, B., Naseradinmousavi, P., Yıldırım, S., Yeşilyurt, S., & Onat, A. (2023). Energy optimization of wind turbines via a neural control policy based on reinforcement learning Markov chain Monte Carlo algorithm. *Applied Energy*, *341*, 121108.

[11] Wu, B., Lang, Y., Zargari, N., & Kouro, S. (2011). *Power conversion and control of wind energy systems*. John Wiley & Sons.

[12] Mousa, H. H., Youssef, A. R., & Mohamed, E. E. (2020). Optimal power extraction control schemes for five-phase PMSG based wind generation systems. *Engineering science and technology, an international journal*, *23*(1), 144-155.

[13] Rekioua, D., & Rekioua, D. (2014). Modeling of Storage Systems. *Wind Power Electric Systems: Modeling, Simulation and Control*, 107-131.

[14] Li, S., Haskew, T. A., Swatloski, R. P., & Gathings, W. (2011). Optimal and direct-current vector control of direct-driven PMSG wind turbines. *IEEE Transactions on power electronics*, *27*(5), 2325-2337.

[15] Memije, D., Rodriguez, J. J., Carranza, O., & Ortega, R. (2016, November). Improving the performance of MPPT in a wind generation system using a wind speed estimation by Newton Raphson. In *2016 IEEE International Autumn Meeting on Power, Electronics and Computing (ROPEC)* (pp. 1-6). IEEE.

[16] Arifujjaman, M., Iqbal, M. T., & Quaicoe, J. E. (2006, December). Maximum power extraction from a small wind turbine emulator using a DC-DC converter controlled by a microcontroller. In *2006 International Conference on Electrical and Computer Engineering* (pp. 213-216). IEEE.

[17] Chen, Y., Shaheed, M. H., & Vepa, R. (2023). Active blade pitch control and stabilization of a wind turbine driven PMSG for power output regulation. *Wind Engineering*, *47*(1), 126-140.

[18] Bhayo, M. A., Yatim, A. H. M., Khokhar, S., Aziz, M. J. A., & Idris, N. R. N. (2015, October). Modeling of Wind Turbine Simulator for analysis of the wind energy conversion system using MATLAB/Simulink. In *2015 IEEE Conference on Energy Conversion (CENCON)* (pp. 122-127). IEEE.

JDFEWS 5 (2): 1-16, 2024
ISSN 2709-4529

[19] Morgan, E. F., Abdel-Rahim, O., Megahed, T. F., Suehiro, J., & Abdelkader, S. M. (2022). Fault ride-through techniques for permanent magnet synchronous generator wind turbines (PMSG-WTGs): a systematic literature review. *Energies*, *15*(23), 9116.

[20] González, L. G., Figueres, E., Garcerá, G., & Carranza, O. (2010). Maximum-power-point tracking with reduced mechanical stress applied to wind-energy-conversion-systems. *Applied Energy*, *87*(7), 2304-2312.

[21] Hwangbo, H., Johnson, A., & Ding, Y. (2017). A production economics analysis for quantifying the efficiency of wind turbines. *Wind Energy*, *20*(9), 1501-1513

[22] Nouira, I., Khedher, A., & Bouallegue, A. (2012). A contribution to the design and the installation of a universal platform of a wind emulator using a DC motor. *International Journal of renewable energy research*, *2*(4), 797-804.

[23] Lubosny, Z., & Lubosny, Z. (2003). *Wind turbine operation in electric power systems: advanced modeling* (p. 259). Berlin: Springer.

[24] Castillo, O. C., Andrade, V. R., Rivas, J. J. R., & González, R. O. (2023). Comparison of power coefficients in wind turbines considering the tip speed ratio and blade pitch angle. *Energies*, *16*(6), 2774.

[25] Palanimuthu, K., Mayilsamy, G., Lee, S. R., Jung, S. Y., & Joo, Y. H. (2022). Fault ride-through for PMVG-based wind turbine system using coordinated active and reactive power control strategy. *IEEE Transactions on Industrial Electronics*, *70*(6), 5797-5807.

[26] Khajuria, S., & Kaur, J. (2012). Implementation of pitch control of wind turbine using Simulink (Matlab). *International Journal of Advanced Research in Computer Engineering & Technology*, *1*(4), 196-200.

[27] Apata, O., & Oyedokun, D. T. O. (2020). An overview of control techniques for wind turbine systems. *Scientific African*, *10*, e00566.

[28] Yilmaz, O. (2022). Increasing power coefficient of small wind turbine over a wide tip speed range by determining proper design tip speed ratio and number of blades. *Proceedings of the Institution of Mechanical Engineers, Part C: Journal of Mechanical Engineering Science*, *236*(23), 11211-11230.

[29] Pehlivan, A. S., Bahceci, B., & Erbatur, K. (2022). Genetically optimized pitch angle controller of a wind turbine with fuzzy logic design approach. *Energies*, *15*(18), 6705.

[30] Brandetti, L., Liu, Y., Mulders, S. P., Ferreira, C., Watson, S., & Van Wingerden, J. W. (2022, May). On the ill-conditioning of the combined wind speed estimator and tip-speed ratio tracking control scheme. In *Journal of Physics: Conference Series* (Vol. 2265, No. 3, p. 032085). IOP Publishing.

[31] Marchewka, E., Sobczak, K., Reorowicz, P., Obidowski, D., & Jóźwik, K. (2022, November). Influence of Tip Speed Ratio on the efficiency of Savonius wind turbine with deformable blades. In *Journal of Physics: Conference Series* (Vol. 2367, No. 1, p. 012003). IOP Publishing.

[32] Hosseini, A., Cannon, D. T., & Vasel-Be-Hagh, A. (2022). Tip speed ratio optimization: More energy production with reduced rotor speed. *Wind*, *2*(4), 691-711.

[33] Ajewole, T., Agboola, M., Hassan, K., Alao, A., & Momoh, O. (2023). Neural Network Approach to Pitch Angle Control in Wind Energy Conversion Systems for Increased Power Generation. *Journal of Digital Food, Energy & Water Systems*, *4*(2).

[34] Rawa, M., Mohamed, H. N., Al-Turki, Y., Sedraoui, K., & Ibrahim, A. M. (2023). Dynamic voltage restorer under different grid operating conditions for power quality enhancement with the deployment of a PI controller using gorilla troops algorithm. *Ain Shams Engineering Journal*, *14*(10), 102172.

[35] Kani, S. P., & Ardehali, M. M. (2011). Very short-term wind speed prediction: A new artificial neural network–Markov chain model. *Energy Conversion and Management*, *52*(1), 738-745.

[36] Karabacak, K., & Cetin, N. (2014). Artificial neural networks for controlling wind–PV power systems: A review. *Renewable and Sustainable Energy Reviews*, *29*, 804-827.

[37] Carrasco, J. M., Franquelo, L. G., Bialasiewicz, J. T., Galván, E., PortilloGuisado, R. C., Prats, M. M., ... & Moreno-Alfonso, N. (2006). Power-electronic systems for the grid integration of renewable energy sources: A survey. *IEEE Transactions on industrial electronics*, *53*(4), 1002-1016.

[38] Chen, Z., Guerrero, J. M., & Blaabjerg, F. (2009). A review of the state of the art of power electronics for wind turbines. *IEEE Transactions on power electronics*, *24*(8), 1859-1875.

[39] de Freitas, T. R., Menegáz, P. J., & Simonetti, D. S. (2016). Rectifier topologies for permanent magnet synchronous generator on wind energy conversion systems: A review. *Renewable and Sustainable Energy Reviews*, *54*, 1334-1344.

[40] Varalakshmi, K., Bharathi, B. K., & Himaja, T. (2021, August). Study of Soft-Starter Based Induction Generator for Wind Energy Conversion System. In *2021 Asian Conference on Innovation in Technology (ASIANCON)* (pp. 1-4). IEEE.

[41] Meegahapola, L., Sguarezi, A., Bryant, J. S., Gu, M., Conde D, E. R., & Cunha, R. B. (2020). Power system stability with power-electronic converter interfaced renewable power generation: Present issues and future trends. *Energies*, *13*(13), 3441.

[42] Dall'Asta, M. S., & Lazzarin, T. B. (2024). A Review of Fast Power-Reserve Control Techniques in Grid-Connected Wind Energy Conversion Systems. *Energies*, *17*(2), 451.

[43] Golestan, S., Guerrero, J. M., & Vasquez, J. C. (2016). Three-phase PLLs: A review of recent advances. *IEEE Transactions on Power Electronics*, *32*(3), 1894-1907.

JDFEWS 5 (2): 1-16, 2024
ISSN 2709-4529

[44] Guediri, A., Hettiri, M., & Guediri, A. (2023). Modeling of a wind power system using the genetic algorithm based on a doubly fed induction generator for the supply of power to the electrical grid. *Processes*, *11*(3), 952.

[45] Chhipą, A. A., Chakrabarti, P., Bolshev, V., Chakrabarti, T., Samarin, G., Vasilyev, A. N., ... & Kudryavtsev, A. (2022). Modeling and control strategy of wind energy conversion system with grid-connected doubly fed induction generator. *Energies*, *15*(18), 6694.

[46] Alnasir, Z., & Kazerani, M. (2013). An analytical literature review of stand-alone wind energy conversion systems from generator viewpoint. *Renewable and Sustainable Energy Reviews*, *28*, 597-615.

[47] Baroudi, J. A., Dinavahi, V., & Knight, A. M. (2007). A review of power converter topologies for wind generators. *Renewable energy*, *32*(14), 2369-2385.

[48] Yao, J., Guo, L., Zhou, T., Xu, D., & Liu, R. (2017). Capacity configuration and coordinated operation of a hybrid wind farm with FSIG-based and PMSG-based wind farms during grid faults. *IEEE Transactions on Energy Conversion*, *32*(3), 1188-1199.

[49] Beltran, B., Benbouzid, M. E. H., & Ahmed-Ali, T. (2012). Second-order sliding mode control of a doubly fed induction generator driven wind turbine. *IEEE Transactions on Energy Conversion*, *27*(2), 261-269.

[50] Kundur, P. S., & Malik, O. P. (2022). Power System Stability and Control, Second Edition. McGraw Hill Professional.

[51] Hussain, J., Hussain, M., Raza, S., & Siddique, M. (2019). Power quality improvement of grid connected wind energy system using DSTATCOM-BESS. *International Journal of Renewable Energy Research*, *9*(3), 1388-1397.

[52] Rekha, S. S., & Immanuvel, K. A. J. (2014). Power Quality Improvement in Wind Energy Generation using Fuzzy Logic Controller. *Advanced Materials Research*, *984*, 730-739.

[53] Huang, A. Q., Crow, M. L., Heydt, G. T., Zheng, J. P., & Dale, S. J. (2010). The future renewable electric energy delivery and management (FREEDM) system: the energy internet. *Proceedings of the IEEE*, *99*(1), 133-148.

[54] Hannan, M. A., Al-Shetwi, A. Q., Mollik, M. S., Ker, P. J., Mannan, M., Mansor, M., ... & Mahlia, T. I. (2023). Wind energy conversions, controls, and applications: a review for sustainable technologies and directions. *Sustainability*, *15*(5), 3986.

Journal of Digital Food, Energy & Water Systems [JD-FEWS]

JDFEWS 5 (2): 17 - 42, 2024
ISSN 2709-4529

Smart Battery Storage Integration in An IoT-Based Solar-Powered Waste Management System

Olatunbosun A., AJIBOLA
University of Lagos, Lagos, Nigeria.

Omolola A., OGBOLUMANI
University of Lagos, Lagos, Nigeria.
oaogbolumanischolar@gmail.com

Received: 20 November 2024
Review: 7 December 2024
Accepted: 13 December 2024
Published: 16 December 2024

Abstract - The global waste crisis is worsening, with more than 33% of the world's 2.01 billion Tonnes of annual solid waste being poorly managed, which could reach 3.40 billion Tonnes by 2050. Low-income countries are projected to triple their waste production by this time, adding further burdens to traditional waste management systems, which are often very inefficient and environmentally damaging. Hence, this research integrates smart battery storage into an IoT-based solar-powered waste management system to improve efficiency and sustainability. A model system was developed and simulated using the Proteus circuit design, which integrates IoT sensors, solar panels, and smart battery storage. The key components of the project include ultrasonic sensors for bin fill-level monitoring, GPS modules for bin location, weight sensors for precise waste measurement, GSM modules for real-time alerts, and DHT11 sensors for battery condition tracking. The system demonstrated reliable performance, achieving real-time bin and battery status monitoring. Alerts were triggered under presumed conditions, such as near-full bin capacity. The smart battery system was designed to ensure continuous operation by managing solar energy efficiently for power, reducing downtime and energy waste. Performance testing and validations were done to reduce operations inefficiencies, improve resource allocation, and advance decision-making. These results are very important for advancing sustainable waste management practices, providing a framework for scalable IoT-based applications in urban waste management and beyond.

Keywords: *Smart Waste Management, Solar Power, Sustainability, Smart Battery Storage, Real-Time Monitoring, Internet of Things (IoT), Prototype Development.*

Journal of Digital Food, Energy & Water Systems [JD-FEWS]

JDFEWS 5 (2): 17 - 42, 2024
ISSN 2709-4529

LIST OF ABBREVIATIONS

- **GPS**: Global Positioning System
- **GSM**: Global System for Mobile Communications
- **ToF**: Time-of-Flight
- **Li-Po**: Lithium-Polymer
- **DHT** Sensor: Digital Humidity and Temperature Sensor
- **BMS**: Battery Management System
- **DC**: Direct Current
- **GPRS**: General Packet Radio Service
- **SMS**: Short Message Service
- **SIM**: Subscriber Identity Module
- **LTE-TDD**: Long-Term Evolution - Time Division Duplex
- **LTE-FDD**: Long-Term Evolution - Frequency Division Duplex
- **HSPA+:** High-Speed Packet Access Plus
- **EDGE**: Enhanced Data rates for GSM Evolution
- **UART**: Universal Asynchronous Receiver-Transmitter
- **USB**: Universal Serial Bus
- **I2C**: Inter-Integrated Circuit
- **GPIO**: General Purpose Input/output
- **GNSS**: Global Navigation Satellite System
- **IoT**: Internet of Things

Journal of Digital Food, Energy & Water Systems [JD-FEWS]

JDFEWS 5 (2): 17 - 42, 2024
ISSN 2709-4529

I. Introduction

Rapid urbanization and industrialization of modern societies have resulted in the rise of an increasingly complex problem: waste management. Many existing approaches toward managing solid waste prove inefficient, usually resulting in environmental pollution and a high operation cost. IoT technologies coupled with renewable energy provide a promising approach to handling such problems. These problems bring about this topic of interest: designing and implementing a smart battery storage system integrated into an IoT-based solar-powered waste management system.

Currently, at least 33% of about 2.01 billion tons of solid waste produced worldwide yearly is not managed environmentally sustainable. By 2050, 3.40 billion tons of waste will be produced worldwide. The waste generated by a person daily worldwide ranges from 0.11 to 4.54 kilos, with an average of 0.74 kilograms. By 2050, it is predicted that the total quantity of waste produced in low-income countries will have more than tripled. [1]. Proper waste management should be given top attention to protect public health and minimize environmental contamination. Waste management and awareness are new ideas in developing nations. Appropriate waste management is required to guarantee sustainable growth and a healthy environment. However, inadequate infrastructure and unsustainable methods have worsened waste management in underdeveloped countries, contaminating the environment [2]. Significant health hazards, such as skin infections and chronic illnesses, result from open dumping and waste pickup at open dumpsites. The issue worsens in slums due to the high human density. It suggests linked environmental/health concerns and improper waste management[3].

The sustainable and proper management of produced solid wastes by various nations worldwide has been a significant problem (4). However, it is more noticeable in developing countries like Nigeria than in industrialized ones. Many developing countries have failed to adequately manage their generated solid waste because they are preoccupied with the rapid speed of industrial and economic growth [5].

Lagos is Nigeria's second most populous state and central urban area after Kano, as well as the country's most economically significant state. The state creates around 12,000 metric tons of waste daily (0.72 kg/person) [6]. To address budget constraints, the Lagos State Government established the Lagos State Waste Management Authority (LAWMA) to oversee waste management policy, including implementation, monitoring, advocacy, and enforcement [7]. As part of its responsibilities, the agency hired a private service provider (PSP) to properly handle the invoice for waste services. LAWMA collects income centrally and remits the agreed-upon 60% of waste levies to individual PSP accounts based on the expected waste collected [6].

In recent years, innovative and environmentally friendly options for waste management techniques have emerged across various industries thanks to the convergence of renewable energy sources and Internet of Things (IoT) technologies [8]. Solar energy can reduce carbon emissions and reliance on non-renewable energy sources; solar power has attracted interest in waste management [7], [9], [10]. However, relying on solar energy for waste management systems can be challenging due to its inconsistent nature. To fully harness the benefits of solar energy in smart waste management systems, there is a need to find a reliable way to store it. This will ensure a consistent power supply for IoT-based waste management systems, allowing them to operate smoothly and maximize the use of renewable energy.[11]. Integrating smart battery storage is vital for storing excess solar energy generated during peak sunlight hours and releasing it when there's little or no sunlight. Batteries allow regulated energy usage across various sectors, including transportation, manufacturing, and power. Optimizing battery life cycle performance to improve battery longevity is a continuous problem for all industries [12]. Incorporating intelligent battery storage systems with solar-powered waste management systems is an exciting prospect. This convergence contributes to more innovative, greener urban environments by addressing the critical need for better waste and energy management. Sustainable power sources such as solar, wind, and hydro-energy are the lights of the future because traditional sources such as fossil, coal, and oil reserves are limited and running out due to rising demand [13]. This study aims to contribute to

JDFEWS 5 (2): 17 - 42, 2024
ISSN 2709-4529

the current IoT interface architecture in waste management systems that run on solar power, taking cognizance of the following aspects:

- Real-time Energy Monitoring.
- Dynamic Energy Switching.
- Predictive Analytics for Optimization.

The design, simulation, and development of smart battery storage integration in Internet of Things-based solar-powered waste management systems are carried out. This study intends to add to the expanding body of knowledge that seeks to address the energy issues in waste management while promoting environmental sustainability by utilizing insights from previous research and industry advances.

Furthermore, integrating IoT and solar-powered smart battery storage in waste management is a big leap toward solving global environmental and operational challenges. Inefficient collection schedules, high operation costs, and reliance on non-renewable energy sources characterize traditional waste management systems. This study's design offers a sustainable alternative through real-time monitoring and energy switching that will change contemporary waste management practices. One major significance of this study is its contribution to environmental sustainability. By harnessing solar energy as a primary power source, the system reduces the traditional dependence on fossil fuels, thereby minimizing carbon emissions. The smart battery storage enables energy storage during periods of low sunlight, thus ensuring the system's continuous operation. This design initiative aligns with the global goals to mitigate climate change and promote [14] adoption.

This paper also demonstrates a practical application of IoT in waste management system. The system optimizes waste collection schedules with real-time data collection and analysis, reducing unnecessary trips and conserving resources. This enhances operational efficiency, lowers costs, and reduces environmental impact. Predictive analytics further enable proactive resource allocation, extending system life and reducing maintenance needs. It is also a scalable and flexible study since architecture could be applied to other urban systems, such as water management or traffic monitoring. Thus, this shows the potential of facing any brilliant city challenge. Equipped with renewable energy and top-notch technologies, the study represents the benchmark for sustainable infrastructure development. Thus, this work points to the inefficiency in waste management and serves long-term environmental goals, reducing operational costs and fostering sustainable IoT-based solutions for urban ecosystems.

II. Related Works

This section highlights the work related to designing and implementing a smart battery storage system integrated into an IoT-based solar-powered waste management system. Having the knowledge that the poor waste management system threatens the environment. The increasing volume of waste generated by urban areas is difficult to manage by traditional waste management systems, which frequently rely on manual labour and inefficient management methods. So, scholars and experts have recommended incorporating the Internet of Things (IoT) into waste management systems to improve waste management.

2.1 IoT Smart Waste Management

IoT is an emerging area that is changing smart cities' solid waste management practices. The scenes of pilled waste and ineffective collection routes are all gone now. These state-of-the-art technologies, integrated with sensor networks, offer real-time data regarding temperature, tilt angles, and fill levels inside the waste can. [15]. This information is then transmitted wirelessly to a central hub, where it is analyzed to determine optimal collection schedules and routes, leading to a form of waste management for cities that are far more efficient, cleaner, and greener. This is because researchers are now looking into various Internet of Things-based waste management techniques. A system using weight and ultrasonic sensors to measure the fill level of the bins and detect overflow instances uploads the data

JDFEWS 5 (2): 17 - 42, 2024
ISSN 2709-4529

collected to a server for web-based monitoring, thus enabling waste management organizations to deal with waste overflow before it happens [16].

Another method used is the gas sensors and ultrasonic sensors [17]. The system will detect dangerous gasses that are released from waste and bin filling levels. Waste management bodies can monitor the waste bin status using real-time data, allowing them to respond to different waste situations on time. More advanced systems use many sensor nodes to monitor bin fill levels and the location of home and public bins [18]. Waste collection agencies reduce time wasted traveling from one place to another, thus reducing fuel consumption by routing optimization using rich data. Furthermore, extra efficiency advantages can also be made possible by using predictive insights and dynamic route adjustments with the help of this rich data using machine learning algorithms. Finally, some systems advance with server-less structures and edge computing [19].

Innovative technologies bring opportunities to a better future for the earth and cities by promoting efficiency, supporting environmental sustainability, and guaranteeing cleaner environments. Researchers are exploring other ways to use IoT in waste management. One example is a home waste management system that uses machine learning, specifically K-Nearest Neighbors (KNN), to sort and compost biodegradable waste [20]. A system that predicts waste bin fill levels based on university class distribution has been developed at the university level. This system uses graph theory and machine learning (ML) with logistic regression (LR) to predict waste buildup. It also uses route optimization for efficient waste collection, has a low-cost circuit design, and LoRa integration. Also, the system uses pressure sensors to measure how full waste bins are. When a bin is almost full, an alert is sent. This helps ensure waste is collected on time, keeping the environment clean. Online apps and text messages are used to send these alerts on specific bin conditions [21]. These methods prove IoT technology can help create cleaner environments, collect waste more efficiently, and protect the environment.

2.2 Smart Battery Storage in Smart Waste Management

Solar-powered Internet of Things (IoT) waste management systems are the foundation of a more sustainable and data-driven method of waste collection. These systems use solar energy to power sensors used in the bins and continuously monitor fill levels, temperature, and even tilt angles. Real-time data is sent through an IoT network to a monitoring system for analysis and route optimization [22]. This technology has several advantages, broadening waste management possibilities. One of the main advantages is using a more environmentally friendly energy source. By using solar energy, this solution minimizes dependence on traditional electricity sources, resulting in a greener approach. This also reduces greenhouse gas emissions related to electricity generation by traditional means and promotes energy independence for waste collection systems [23].

Consequently, Solar power and the Internet of Things (IoT) can improve waste collection. By tracking how full bins are, companies can plan their routes more efficiently, avoiding unnecessary trips and saving money. The data can also help in understanding how waste is generated and where to place bins strategically. A study even showed a 20% reduction in fuel use for city collection vehicles by using real-time bin data to plan routes.[24].

Several studies emphasize the importance of efficient energy. The authors in the cited work [25] proposed a solar-powered method of waste management but highlighted that power consumption needs to be optimized through sensor selection and communication protocol. Ref [26] wrote on the unstable nature of solar energy and suggested using duty cycling for sensors and low-power communication technologies like LoRaWAN. Ref [27] researched the use of rechargeable batteries as a backup, highlighting battery degradation as an issue and the need for effective battery management techniques. The studies highlight the importance of optimizing power consumption for the sustainable use of these systems.

Moreover, solar-powered IoT waste management systems promote data-driven planning. The collected data provides an outlook on waste generation patterns, including differences based on seasonality or population density [28]. This information can be used to plan waste management infrastructure and resource allocation. For example, areas that consistently generate high amounts of waste, planning additional processing facilities, or using targeted waste

JDFEWS 5 (2): 17 - 42, 2024
ISSN 2709-4529

reduction campaigns. Research was done, and data was used to identify areas with high food waste generation. This information was used to start composting initiatives in those areas, reducing waste sent to landfills [29].

The present research has been on using solar or battery power in waste management systems, paying little attention to the Internet of Things (IoT) and its essential part in smart battery storage. This oversight limits the amount of data the system can gather, resulting in incomplete and inconsistent datasets that decrease the system's efficiency. One problem discussed is the inability to check the battery's health or control it remotely without using the Internet of Things (IoT). This shows how important it is to study this and ensure IoT is part of solar or battery-powered waste management systems, hence this study. Using IoT helps us use energy better, making waste management more efficient and eco-friendlier. It does this by improving data collection and letting us monitor and fix batteries from a distance.

III. Methodology

This section provides a systematic approach to designing, developing, and implementing a smart solar-powered waste management system. This process included the definition of system requirements, the selection of appropriate hardware and software components, and the creation of detailed system architecture. Much emphasis was put on integrating IoT technologies, sensors, and smart battery storage for real-time monitoring and efficient energy use. Each stage involves prototyping and simulation to properly deploy the field for functionality and reliability. The methodology consists of various test methods and validation to assess system performance, making it robust and adaptable for sustainable waste management practices.

3.1 Design Process

Developing an innovative waste management system requires system concept, component selection, architectural design, prototyping, testing, integration, deployment, and constant enhancement. Figure 1 below outlines a structured process for developing a smart waste management system. From conceptualization through deployment and improvement, each stage is significant in ensuring the system's success. The system's specifications and objectives are first established, focusing on effective waste monitoring, location tracking, efficient communication, and sustainability. These factors pick components with dependability, compatibility, and energy efficiency given top priority. These components include microcontrollers, GPS/GSM modules, and ultrasonic sensors.

Journal of Digital Food, Energy & Water Systems [JD-FEWS]

JDFEWS 5 (2): 17 - 42, 2024
ISSN 2709-4529

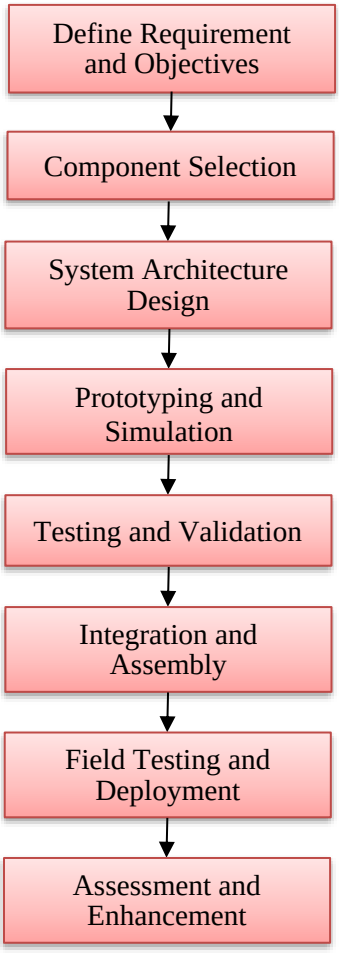

Fig. 1. Design process chart

Next, an efficient system architecture is determined, detailing component interconnections, data flow, and functional needs. Hardware and software components are constructed for optimum performance and integration. Circuit diagrams and virtual prototypes are made to verify the design, spot possible problems, and improve the system.
Then, testing is done at both the component and system levels to ensure peak system performance. Power management, communication stability, and sensor accuracy are tested. Next, the system is assembled using sensors, microcontrollers, communication modules, and parts for power management.

Field testing simulates real-world implementation and provides user input and system performance data. The optimization process is guided by data analysis and user input, improving user interaction, efficiency, and dependability. To maintain system effectiveness and adjust to changing demands, constant review and improvement are necessary to simulate real-world implementation that efficiently handles environmental issues, maximizes waste collection, and offers valuable data for well-informed decision-making.

3.2 System Architecture

In Figure 2, the considered smart waste management system comprises five (5) layers, each having a role to play in ensuring sustainability and effective operation. The system's core is the sensor interface layer, which consists of a

JDFEWS 5 (2): 17 - 42, 2024
ISSN 2709-4529

microprocessor to which several sensors are connected, such as ultrasonic, weight, temperature, and humidity sensors. The microcontroller receives data from these sensors, allowing it to track the bin's status (weight of the waste bin, the amount of waste within it, and the conditions of the battery unit). The microcontroller is fitted with a GPS/GSM module, which makes up the Communication Layer that updates the central server with the status and position of the bin. The user interface layer handles user interaction, and the system features a mobile application that displays information about the bin's status and battery conditions.

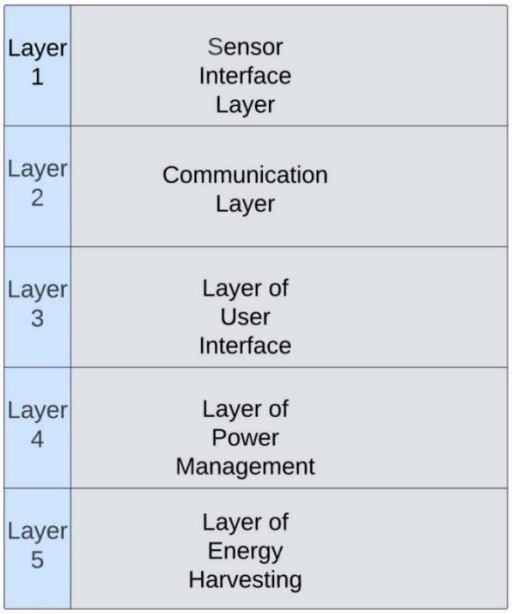

Fig. 2. System architecture diagram

The power management layer maintains reliable operation, and a power module is responsible for managing the distribution of power to the various components of the system. This includes a battery charger controller, which is in charge of the charging process to ensure a stable power supply, which works hand-in-hand with the energy harvesting layer, which boosts sustainability and autonomy; the system incorporates a solar panel that harnesses solar energy to supplement or recharge the battery. This renewable energy source reduces dependence on external power and enhances the system's environmental friendliness.

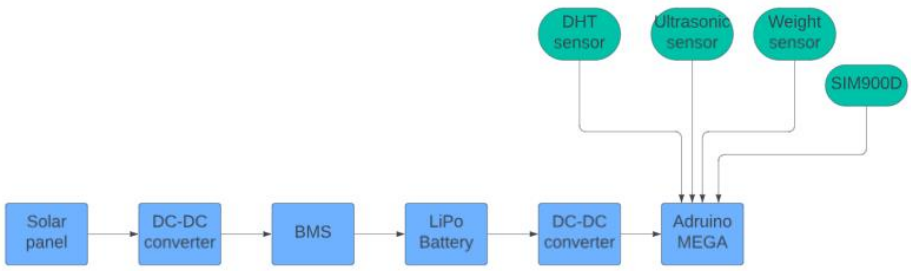

Fig. 3. Block diagram of system architecture

Figure 3 above shows the energy and data flow in the smart waste management system, where solar energy captured via a solar panel feeds directly into a DC-DC converter, regulating it in voltage for storage in a Li-Po battery via

JDFEWS 5 (2): 17 - 42, 2024
ISSN 2709-4529

Battery Management System control. However, using another DC-DC converter, this stored energy powers the system with stabilized voltage for the use of the Arduino MEGA microcontroller.

The Arduino MEGA acts as the system's central processing unit, interfacing with sensors such as the DHT sensor for temperature and humidity, the ultrasonic sensor for bin fill level, and the weight sensor for waste weight. It also communicates via a SIM900D GSM module for data transmission to a remote server. This architecture ensures sustainable energy use, precise data collection, and seamless communication, thus enabling efficient operations about waste management. See Figure 4 (Proteus system schematic) for more information on the circuitry connections of the hardware prototype components.

3.3 Hardware Components Selection

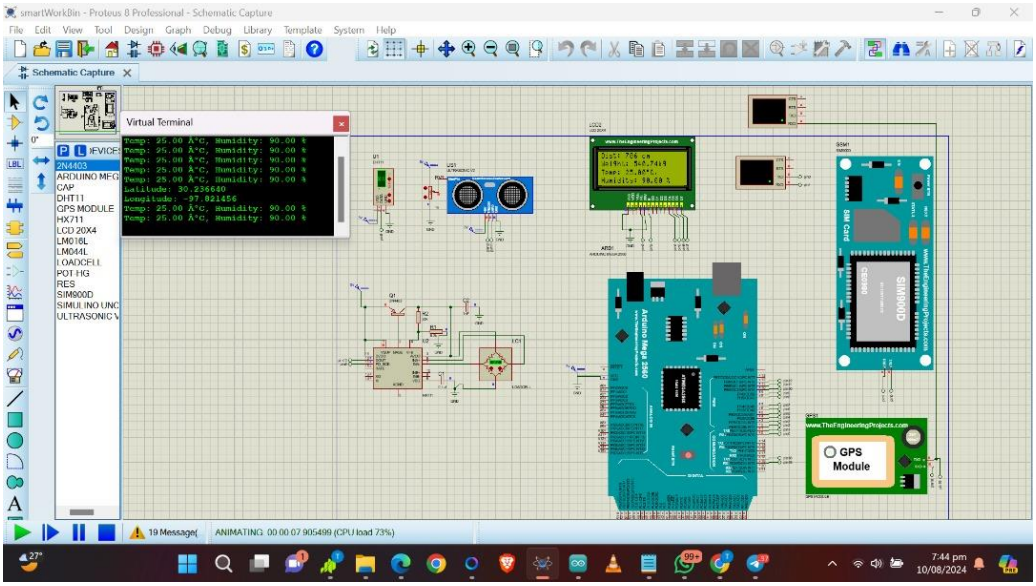

Fig. 4. Proteus system schematic

3.3.1 Microcontroller (Arduino-nano)

The microcontroller, a tiny computing device integrated into a chip, lowly operates the waste management system's peripherals. The microcontroller of choice for both final board design and prototyping is the Arduino-nano. The microcontroller interfaces with the ultrasonic sensor, weight sensor, voltage sensor, temperature sensor, charge controller, and Li-Po battery. Figure 5 below shows the image of the microcontroller used in the project development.

Journal of Digital Food, Energy & Water Systems [JD-FEWS]

JDFEWS 5 (2): 17 - 42, 2024
ISSN 2709-4529

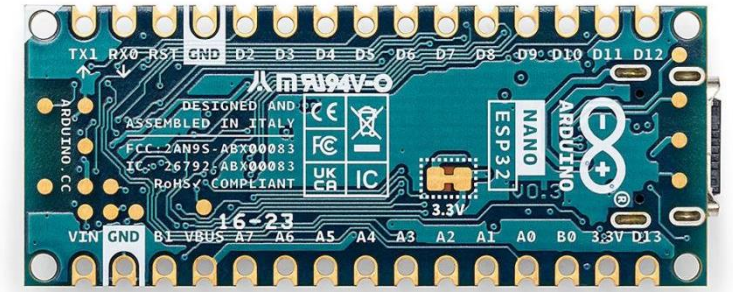

Fig. 5. Arduino-nano microcontroller

3.3.2 Ultrasonic Sensor (HC-SR04)

Ultrasonic sensors use sound waves to measure distances, making them essential for monitoring waste levels. They also enable bin-fill data to be gathered, which is necessary to optimize resource allocation and waste management. An ultrasonic sensor measures the time-of-flight (ToF) of an acoustic wave. Figure 6 below shows the image of the HC-SR04 ultrasonic sensor used in the project development.

Fig. 6. HC-SR04 Ultrasonic sensors

Time-of-Flight Equation of the Ultrasonic Sensor

The fundamental equation governing the operation of an ultrasonic sensor is:

$$\text{Distance (d)} = \frac{\text{Speed of sound (c)} \times \text{Time-of-flight (t)}}{2} \quad (1)$$

Where:

d represents the distance to the object.
c represents the speed of sound in the medium (typically air), and
t represents the time elapsed for the ultrasonic pulse to travel to the object and return.

3.3.3 Weight Sensor (HX711)

Weight sensors make accurate measurement and waste management processes possible. They offer real-time data on waste weight, which is essential for a user reward system based on waste weight. The fundamental concepts of strain gauge technology, especially load cell mechanics, regulate the weight sensor's operation. A weight sensor monitors the force applied to a load and transforms it into an electrical signal that is processed to calculate the weight. Figure 7 below depicts a typical image of an HX711 weight sensor with a load cell used in this project design.

JDFEWS 5 (2): 17 - 42, 2024
ISSN 2709-4529

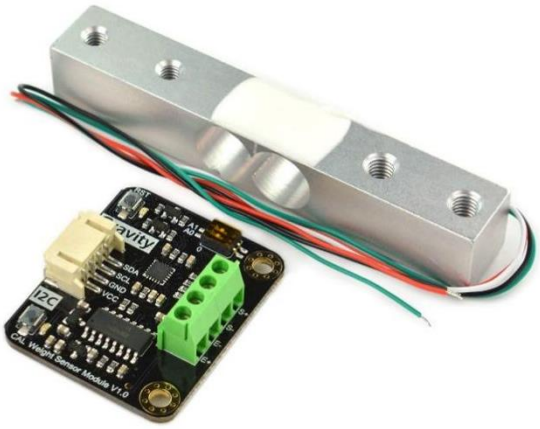

Fig. 7. Weight sensor (HX711) with Load Cell

The governing equation for the operation of a weight sensor can be expressed as follows:

$$V_{out} = S \times F_{applied} \quad (2)$$

Where:

V_{out} is the output voltage of the weight sensor (in volts).
S is the sensitivity of the sensor, also known as the calibration factor (in volts per unit force), and
$F_{applied}$ is the applied force or weight (in newtons or grams, depending on the calibration).

Conversion of Force to Weight: In real-world applications, the acceleration caused by gravity, or g (or 9.81 m/s^ on Earth), is frequently considered when converting the applied force, or F, to weight. Thus, the following relation may be used to find the weight if the output voltage matches a force:

$$W = \frac{V_{out}}{S} = F_{applied} = m \, . \, g \quad (3)$$

In this case, mass is denoted by m and gravitational acceleration by g.

3.3.4 Voltage Sensor

Voltage sensors monitor electrical potential variations to provide a steady power supply to the system. They improve system dependability and enable timely interventions via real-time voltage change detection. Fig. 8 below shows a typical image of a voltage sensor used in this project development.

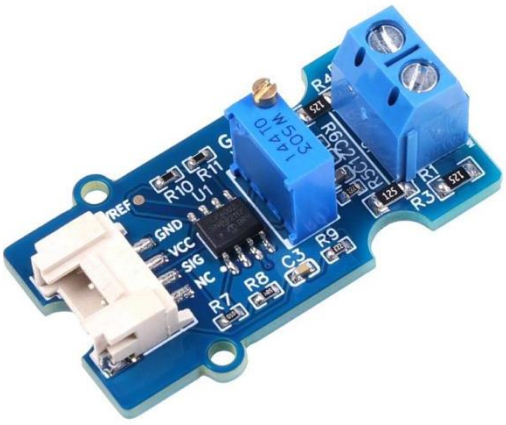

Fig. 8. Voltage Sensor

JDFEWS 5 (2): 17 - 42, 2024
ISSN 2709-4529

3.3.5 DHT Sensor Unit

The DHT sensors unit integrates temperature and humidity sensors to monitor environmental conditions within the waste bin's battery unit. These sensors play a crucial role in ensuring that the operational environment remains within safe and optimal limits, thereby enhancing the longevity and performance of the battery system. Figure 9 below shows a typical example of a DTH11 sensor used in this project development.

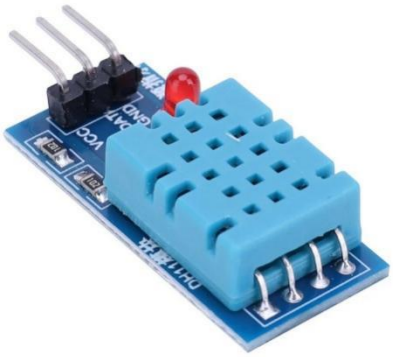

Fig. 9. DTH11 Sensor

Temperature Sensor: The DHT unit's temperature sensor measures the ambient temperature inside the waste bin battery enclosure.

Humidity Sensor: The DHT unit's humidity sensor measures the relative humidity inside the waste bin battery enclosure.

3.3.6 SIM900D

SIM900D in Figure 10 is a small and reasonably priced GSM/GPRS module that allows devices to communicate over cellular networks through features like SMS, voice calls, and GPRS data transmission. Because of its low power consumption, small size, and ease of integration, the SIM900D is used in IoT projects, remote monitoring systems, and mobile-based applications. It works especially well in smart systems, providing cellular communication capabilities that let the system send and receive commands remotely. The SIM900D creates a wireless link to the cellular network by combining a SIM card and a GSM module. This allows real-time communication with external servers, management platforms, or mobile applications.

JDFEWS 5 (2): 17 - 42, 2024
ISSN 2709-4529

Fig. 10. SIM900D Diagram

3.3.7 SIM7600H

The SIM7600H is an LTE Cat 4 module that supports LTE-TDD/LTE-FDD/HSPA+/GSM/GPRS/EDGE networks and provides fast wireless connection. This is shown in Figure 11. It has a 50 Mbps upload speed and a 150 Mbps maximum download speed. This allows easy migration and flexible product design due to the SIM7600H's compact LCC1 size and compatibility with previous module generations. The module combines high-accuracy GNSS location technologies with several satellites. Its support for several network protocols and compatibility with different operating systems make it adaptable and user-friendly. It also has a wide array of interfaces, which include UART, USB, I2C, and GPIO.

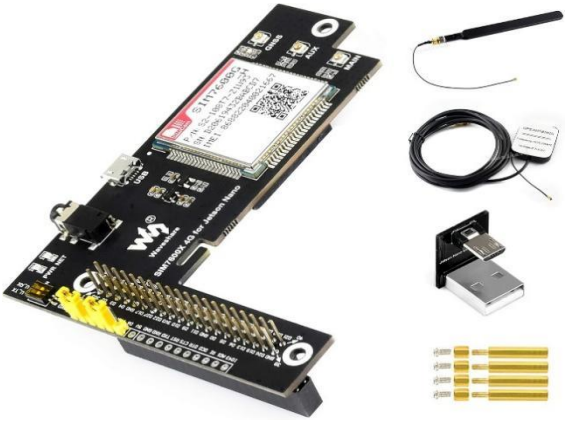

Fig. 11. SIM7600H Diagram

JDFEWS 5 (2): 17 - 42, 2024
ISSN 2709-4529

3.4 Battery Management System

A battery management system (BMS) manages the charge and discharge of a battery to keep it in safe operating condition. In general, it monitors and keeps the battery in good health. The system integrates circuitry for charge protection, discharge protection, temperature protection, and battery health monitoring, having the following features:

i. Over-voltage Protection
ii. Over-current Protection
iii. Under-voltage Protection
iv. Charge Balancing

Over-Voltage Protection

This voltage protection feature under charge protection protects from overcharging, acquiring a voltage level greater than the manufacturer's rated voltage upper limit. With this feature, the circuit ensures the battery can charge each cell to a nominal voltage and cuts off or stops charging the battery before it reaches its maximum specified voltage to prevent overcharge.

Over-current protection

The BMS also protects the battery against loads that draw excessive amounts of current, such as capping or setting a boundary to the maximum current supply.

Under-Voltage Protection

The BMS also protects the battery from usage beyond its rated under-voltage specification, beyond which the battery would be damaged. It cuts off discharge when the voltage drops to this level. For a single cell, the under-voltage rating is about 2.5V.

Charge Balancing

This is also a feature under charge protection for the battery. The BMS also ensures that approximately the same voltage level is reached across all the cells, preventing a case of one cell having a higher or lower voltage than another.

3.5 DC to DC Converter

The DC-to-DC step-down converter adjusts the solar panel or battery unit's voltage levels to meet the needs of the smart waste bin system. It ensures compatibility with electrical components operating at lower voltage levels by effectively converting greater input to lower output voltages. The step-down converter maximizes energy economy and system performance by controlling voltage output, filtering noise, and supplying steady power to delicate devices. The DC-to-DC step-down converter increases overall system dependability and prolongs battery life in renewable energy-based applications by improving energy conversion and use.

3.6 LI-PO Battery

Lithium polymer (LiPo) batteries are the main energy storage option with their great energy density and dependability. They are perfect for smart battery storage applications because of their extended cycle life and rechargeability. To determine the size of the battery, several factors need to be considered; see calculations in section 3.7 below.
The LiPo battery is integrated with a BMS to ensure the solar charging system works safely and efficiently. This is the model that controls the charging balancing/control for overcharging and undercharging control. The BMS works

JDFEWS 5 (2): 17 - 42, 2024
ISSN 2709-4529

in synergy with the solar controller and DC-DC converters for regulating power flow from the solar panel to the battery and connected devices.

3.7 Calculations

Calculations on the Amount of Energy Consumed per Cycle

The Arduino Nano operates for 10 seconds to connect to Wi-Fi and transmit data, then sleeps for 10 minutes. The power consumption for the sensors is constant while the Arduino Nano is active. Given:

- Arduino nano: 130mA
- Ultrasonic Sensor: 6.3mA
- Weight Sensor: 16.7mA
- Temperature Sensor: 20mA
- Voltage Sensor: 15.5mA

Total current draw when active, Pt

$$Pt = 130mA + 6.3mA + 16.7mA + 20mA + 15.5mA = 188.5mA.$$

The active time per cycle, T is 10 seconds every 10 minutes, and the deep sleep time is negligible. The energy consumed per cycle is;

$$Pt \times \mathrm{T} = 188.5mA \times 10s = 1885mAs$$

Therefore, the energy consumed in an hour is;

$$Pt \times \mathrm{T} \times 6 = 6 \times 1885mAs = 11310mAs$$

In battery charge capacity it consumes;

$$\frac{11310}{3600} mAh = 3.141667mAh$$

In a year it consumes (16hours run time);

$$3.141667 \times 16 \times 365 = 18347.33528mAh$$

Therefore, the battery needs to store at least $18347.33528mAh$ all year.

Calculation of Solar Panel Size

When calculating the solar panel size for the system, the following factors were considered to determine the solar panel size:

i. Power Consumption of Components
ii. Operating Hours
iii. Efficiency Losses
iv. Sunlight Availability
v. Battery Capacity
vi. Safety Margin

$$\text{Solar Panel Size (W)} = \frac{\text{Total Daily Energy Consumption (Wh)}}{\text{Average Sunlight Hours per Day} \times \text{Efficiency}} \quad (4)$$

Total Daily Energy Consumption (Wh) = Sum of power consumption of all components multiplied by their operating hours per day.
Efficiency Factor = Factor accounting for efficiency losses in the system (usually between 0.7 and 0.9).
So, Efficiency = 0.9 (selected)
the power consumption of the following is:

1. The Microcontroller unit (ESP 32) = P_1(W)
2. Ultrasonic Sensor Unit = P_2(W)
3. Weight Sensor Unit = P_3(W)

JDFEWS 5 (2): 17 - 42, 2024
ISSN 2709-4529

4. DHT Sensor Unit= P_4(W)
5. SIM800L unit = P_5(W)

$$P_T = P_1(W) + P_2(W) + P_3(W) + P_4(W) + P_5(W) \quad (5)$$

Let the operating hour be **T**

Average sunlight hour per day in Lagos = 5hr

Total Daily Energy Consumption = $P_T \times T$

$$\text{Solar Panel Size(W)} = \frac{P_T \times T}{5 \times 0.9} = \frac{(P_T \times T)}{4.5} = \frac{2}{9}(P_T \times T)\ (\text{W}) \quad (6)$$

Then, the conversion of the solar panel size in watt to meter square:

$$\text{Solar Panel Size}(m^2) = \frac{Solar\ Panel\ Power\ (W)}{SOlar\ Irradiance\left(\frac{W}{m^2}\right) \times Solar\ Panel\ Efficiency} \quad (7)$$

The efficiency of solar panels is about 15%

Solar Irradiance in Lagos is 184.17 (w/m^2)

$$\text{Solar Panel Size}(m^2) = \frac{\frac{2}{9}(P_T \times T)}{184.17 \times 0.15} = \frac{\frac{2}{9}(P_T \times T)}{27.6255} = 8.04(P_T \times T) \times 10^{-3}(m^2) \quad (8)$$

IV. Results

This section presents the designed and developed smart waste management system, emphasizing field performance. Designed performance evaluation of the functionality covers mainly the energy efficiency, accuracy, and reliability of system operations. The findings confirm that the system can improve waste collection and resource optimization through data-driven decision-making. This section outlines the development process after implementing and discussing smart battery storage integration in IoT-based solar-powered waste management systems, expanding on the implementation decisions and the project's outcomes. It delves into the integrated system's essential features and functionalities.

4.1 Performance

The designed smart waste management system showed strong performance in each key component. IoT sensors have been used for real-time monitoring, effectively measuring the bin's fill level, weight, and environmental parameters like temperature and humidity. Similarly, integrating GPS and GSM modules ensured accurate location tracking and efficient data transfer to a central control system. The solar-powered energy setup, complemented by a smart Li-Po battery storage system, provided a consistent power supply, reducing reliance on grid energy. Dynamic energy switching mechanisms effectively optimize power usage, preventing overcharging and undercharging of the battery. Field testing confirmed the system's ability to sustain operations under varying environmental conditions, ensuring uninterrupted functionality. Overall, it greatly improved the efficiency of waste collection and resource use while providing a scalable, sustainable response to waste management concerns. The waste management system's performance is based on the functionality and efficiency of the components performing their tasks individually and as a whole.

Journal of Digital Food, Energy & Water Systems [JD-FEWS]

JDFEWS 5 (2): 17 - 42, 2024
ISSN 2709-4529

4.1.1 Hardware Performance

The SIM7600H module replaced the SIM900D module during the prototype development stage. The requirement for more excellent compatibility and speed led to this choice. The SIM7600H provides noticeably faster 4G connectivity than the SIM900D, a reliable 3G module. This allows for more effective data transfer and real-time communication. Furthermore, the SIM7600H ensures secure connectivity by being compatible with various network standards. The system dynamically switches away from solar energy, stopping the battery charging when it is complete and allowing a transition from solar to battery power. This feature maximizes the solar system's efficiency and helps prolong the battery's lifespan.

The battery system minimized energy drain by ensuring consistent power delivery to all sensors and modules through regulation of energy demand and entry into low-power modes during idleness. The waste bin system functions correctly over extended periods and was supported by recharging and proper maintenance, which were made possible by monitoring battery health and charge state. The Ultrasonic Sensor (HC-SR04), connected with the microprocessor to send the data collected for real-time monitoring, identified the waste bin's fill levels. The Load Cell (HX711) accurately measured the waste's weight, resulting in accurate weight measurements that were collected and displayed successfully. The DHT11 Sensor efficiently monitored the temperature and humidity levels within the waste bin battery unit to ensure that battery conditions could be monitored and sent to the system for analysis.

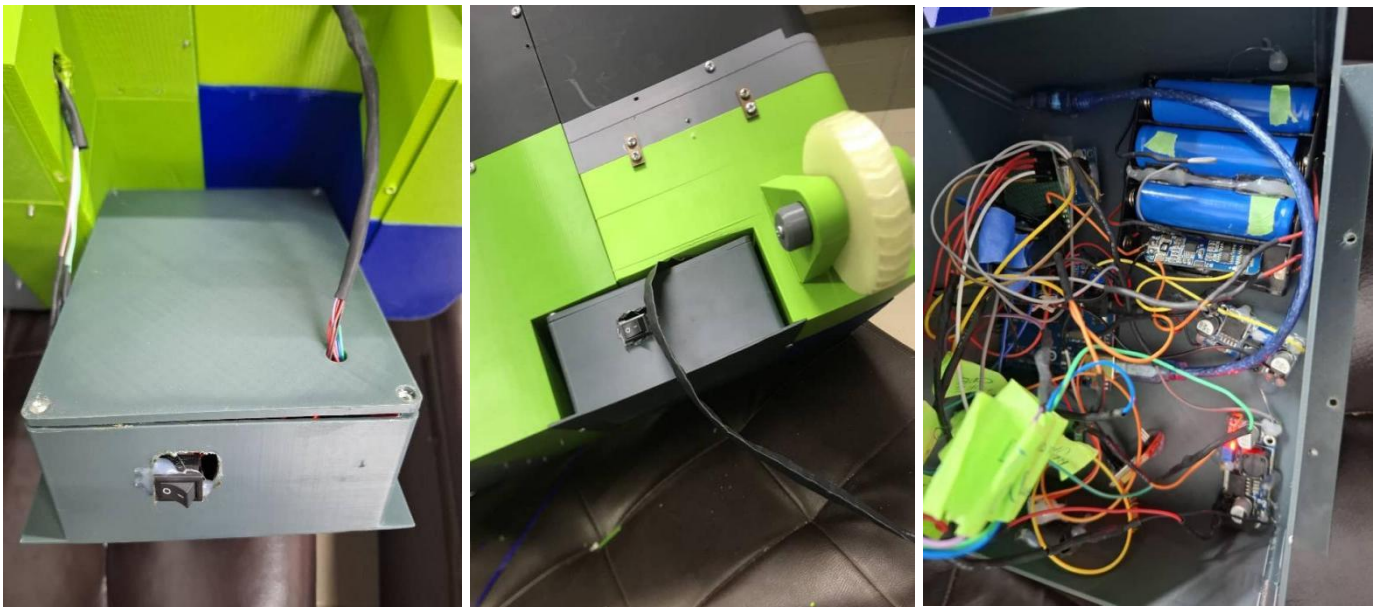

Fig.12. Images showing the circuit inside the developed system (inward and outward view).

Figure 12 above clearly shows the images of the inward view, exposing the inner circuits and components of the system, and the outward view, showing the fully packaged design of the developed system. This unit was placed at the bottom of the designed smart IoT-based solar-powered waste bin.

The GPS Module (TinyGPS++) tracked the waste bin's location, and the alarm system sent alerts at the desired conditions. When specific conditions were met, such as the bin filling up to capacity or specific bin conditions were met, the GSM Module sent out SMS notifications.

Also, Figure 13 below depicts the fully packaged design integrated into an IoT-based solar-powered waste management system with a solar panel on top of the waste bin. Even though the Li-Po battery is the main source of

JDFEWS 5 (2): 17 - 42, 2024
ISSN 2709-4529

energy storage in the system, the integration of solar energy into it plays a vital role in making the smart waste management system work sustainably and efficiently. In other words, the Li-Po battery acts like an energy storage facility, while the solar panels are its primary energy source, making this solution highly reliable, renewable, and cost-effective; rather than changing the batteries at intervals, the solar panel allows for longer system usage.

Fig. 13: Image of the designed smart battery storage system integrated into an IoT-based solar-powered waste.

4.1.2 Software Performance

The system's software parts, such as the custom functions and Arduino libraries, worked together with the hardware's, allowing the system to operate and communicate as intended. The Arduino libraries achieved reliable functioning and data transfer, promoting proper integration and communication between the microcontroller and hardware components. The component functions were done by using custom functions, such as using the ultrasonic sensor to measure distance, processing GPS module position data, and sending SMS notifications when sensor readings met specified conditions. Due to these functionalities, the system could monitor and make decisions in real-time. Figure 14 shows the system's real-time monitoring capabilities using bin sensors' data.

Journal of Digital Food, Energy & Water Systems [JD-FEWS]

JDFEWS 5 (2): 17 - 42, 2024
ISSN 2709-4529

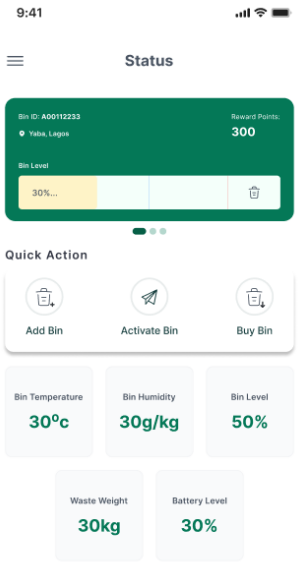

Fig. 14: Mobile app: Monitoring page

4.1.3 System Functionality

The waste bin's fill level was measured using the ultrasonic sensor, and the fill level was displayed on the system database. The load cell weighed the waste, and the database stored the results. Monitoring the battery unit conditions was done by measuring temperature and humidity with the DHT11 sensor. The GPS module provided the location of the bin. The system continually monitored distance, weight, temperature, and humidity to ensure that any predetermined conditions resulted in an SMS alert.

4.1.4 Alert System

The system is designed to send an alert SMS when critical conditions are detected. Alerts are triggered if:

- The waste bin is nearly full (distance < 20 cm).
- The waste weight exceeds 500 g.
- The temperature rises above 50°C.
- The humidity level exceeds 90%.

The alert SMS includes the current distance, weight, temperature, humidity, and GPS location (if valid). This ensures that stakeholders are promptly informed of critical conditions requiring immediate attention.

JDFEWS 5 (2): 17 - 42, 2024
ISSN 2709-4529

Table 1: Waste bin conditions and fill level indication

Condition No.	Threshold	Indication	SMS Sent	Description	Action Required
1	Distance < 20 cm	Nearly Full Bin	Yes	Indicates that the waste bin is nearly full and requires immediate attention to avoid overflow.	Schedule waste collection immediately.
2	Weight > 500 g	Exceeds Weight Limit	Yes	Indicates that the waste bin's weight exceeds the safety limit, risking damage to the system.	Collect and empty the waste bin.
3	Temperature > 50°C	High Temperature Alert	Yes	Indicates an abnormal temperature rise, which could signal fire risk or environmental issues.	Inspect and mitigate overheating.
4	Humidity > 90%	High Humidity Alert	Yes	Indicates excessive humidity levels, which could affect waste decomposition or system hardware.	Investigate and address humidity issue.
5	Valid GPS Location	Location Tracking Active	Yes (included in alerts)	Provides real-time GPS location for the waste bin, ensuring precise location tracking.	Use for planning efficient collection.

Table 1 above highlights the system's ability to promptly detect and respond to critical conditions, ensuring effective waste management. Each SMS includes real-time location, distance, weight, temperature, and humidity data to provide actionable insights.

V. Conclusion

The smart waste management system integrated hardware and software to ensure precise monitoring and efficient data transfer, and the findings showed that it performed reliably across all components. The ultrasonic sensor, load cell, DHT11 sensor, GPS module, and GSM module provided real-time information on the bin's location, weight, fill levels, and environmental conditions. The power management features of the smart battery system further guarantee reliable performance over long periods, cutting downtime and maximizing energy use. The system proved reliable for enhancing waste-collecting procedures via resource efficiency and data-driven decision-making.

This research has successfully integrated IoT and solar energy into the smart waste management system and addressed the key objectives such as real-time monitoring and dynamic energy management and optimization. Real-time monitoring is enabled through the precise tracking of energy metrics and bin status, with seamless source switching enabling the dynamic energy management system for uninterrupted operations and optimization through predictive analytics to bring in improved energy allocation and reduce operational inefficiencies. Therefore, the sustainability and scalability of the system make it promising for addressing modern urban challenges. This may be expanded in further works for use in other smart city systems, implementing machine learning for improved predictive abilities.

JDFEWS 5 (2): 17 - 42, 2024
ISSN 2709-4529

Acknowledgement

We would like to express our sincere gratitude to FBIS Technologies and TreeKle for their financial and technical support, which was instrumental in the success of our project. Their contributions enabled us to carry out this project successfully. We are deeply appreciative of their commitment to seeing this project come to fruition.

JDFEWS 5 (2): 17 - 42, 2024
ISSN 2709-4529

References

[1] K. D. Sharma and S. Jain, "Municipal solid waste generation, composition, and management: the global scenario," *Social Responsibility Journal*, vol. 16, no. 6, pp. 917–948, Jul. 2020, doi: 10.1108/SRJ-06-2019-0210/FULL/HTML.

[2] C. Wan, G. Shen, S. C.-E. of sustainability in higher, and undefined 2019, "Waste management strategies for sustainable development," *Springer*, Accessed: Sep. 12, 2024. [Online]. Available: https://link.springer.com/content/pdf/10.1007/978-3-030-11352-0_194.pdf

[3] M. U. Sohag and A. K. Podder, "Smart garbage management system for a sustainable urban life: An IoT based application," *Internet of Things (Netherlands)*, vol. 11, Sep. 2020, doi: 10.1016/j.iot.2020.100255.

[4] … S. M.-J. of A. E. R. and and undefined 2018, "Importance of municipal solid waste management," *academia.edu*, Accessed: Sep. 12, 2024. [Online]. Available: https://www.academia.edu/download/56757151/49_Importance.pdf

[5] C. C. Ike, C. C. Ezeibe, S. C. Anijiofor, and N. N. Nik Daud, "Solid waste management in Nigeria: Problems, prospects, and policies," *Journal of Solid Waste Technology and Management*, vol. 44, no. 2, pp. 163–172, 2018, doi: 10.5276/jswtm.2018.163.

[6] D. O. Olukanni and O. O. Oresanya, "Progression in waste management processes in Lagos State, Nigeria," *International Journal of Engineering Research in Africa*, vol. 35, pp. 11–23, 2018, doi: 10.4028/www.scientific.net/JERA.35.11.

[7] M. Hussain *et al.*, "A comparative analysis of renewable and non-renewable energy generation to relegate CO2 emissions and general costs in household systems," *Environmental Science and Pollution Research*, vol. 29, no. 52, pp. 78795–78808, Nov. 2022, doi: 10.1007/S11356-022-21121-0.

[8] O. A. Ogbolumani and B. Mabaso, "An IoT-Based Hydroponic Monitoring and Control System for Sustainable Food Production," *Journal of Digital Food, Energy & Water Systems*, vol. 4, no. 2, pp. 106–140, 2023.

[9] B. O. Olorunfemi, N. I. Nwulu, and O. A. Ogbolumani, "Solar panel surface dirt detection and removal based on arduino color recognition," *MethodsX*, vol. 10, p. 101967, Jan. 2023, doi: 10.1016/J.MEX.2022.101967.

[10] O. A. Ogbolumani and N. I. Nwulu, "Multi-objective optimisation of constrained food-energy-water-nexus systems for sustainable resource allocation," *Sustainable Energy Technologies and Assessments*, vol. 44, p. 100967, Apr. 2021, doi: 10.1016/j.seta.2020.100967.

[11] K. Tan, T. Babu, … V. R.-J. of E., and undefined 2021, "Empowering smart grid: A comprehensive review of energy storage technology and application with renewable energy integration," *ElsevierKM Tan, TS Babu, VK Ramachandaramurthy, P Kasinathan, SG Solanki, SK RaveendranJournal of Energy Storage, 2021•Elsevier*, Accessed: Sep. 12, 2024. [Online]. Available: https://www.sciencedirect.com/science/article/pii/S2352152X21003340

[12] P. Liew, P. Varbanov, A. Foley, J. K.-R. and Sustainable, and undefined 2021, "Smart energy management and recovery towards Sustainable Energy System Optimisation with bio-based renewable energy," *ElsevierPY Liew, PS Varbanov, A Foley, JJ KlemešRenewable and Sustainable Energy Reviews, 2021•Elsevier*, Accessed: Sep. 12, 2024. [Online]. Available: https://www.sciencedirect.com/science/article/pii/S1364032120306730

[13] V. Chand, "Conservation of Energy Resources for Sustainable Development: A Big Issue and Challenge for Future," *Environmental Concerns and Sustainable Development*, pp. 293–315, 2020, doi: 10.1007/978-981-13-5889-0_15.

[14] B. O. Olorunfemi, O. A. Ogbolumani, and N. Nwulu, "Solar Panels Dirt Monitoring and Cleaning for Performance Improvement: A Systematic Review on Smart Systems," *Sustainability 2022, Vol. 14, Page 10920*, vol. 14, no. 17, p. 10920, Sep. 2022, doi: 10.3390/SU141710920.

[15] M. Badve, A. Chaudhari, … P. D.-… C. on I., and undefined 2020, "Garbage collection system using iot for smart city," *ieeexplore.ieee.org*, Accessed: Sep. 12, 2024. [Online]. Available: https://ieeexplore.ieee.org/abstract/document/9243387/

[16] K. Nirde, P. Mulay, … U. C.-I. C. on, and undefined 2017, "IoT based solid waste management system for smart city," *ieeexplore.ieee.org*, Accessed: Sep. 12, 2024. [Online]. Available: https://ieeexplore.ieee.org/abstract/document/8250546/

[17] D. Misra, G. Das, T. Chakrabortty, and D. Das, "An IoT-based waste management system monitored by cloud," *J Mater Cycles Waste Manag*, vol. 20, no. 3, pp. 1574–1582, Jul. 2018, doi: 10.1007/s10163-018-0720-y.

[18] S. Vishnu *et al.*, "IoT-enabled solid waste management in smart cities," *Smart Cities*, vol. 4, no. 3, pp. 1004–1017, Sep. 2021, doi: 10.3390/smartcities4030053.

[19] E. Al-Masri, I. Diabate, R. Jain, M. H. Lam, and S. Reddy Nathala, "Recycle.io: An IoT-Enabled Framework for Urban Waste Management," in *Proceedings - 2018 IEEE International Conference on Big Data, Big Data 2018*, Institute of Electrical and Electronics Engineers Inc., Jul. 2018, pp. 5285–5287. doi: 10.1109/BigData.2018.8622117.

[20] S. Dubey, P. Singh, P. Yadav, and K. K. Singh, "Household Waste Management System Using IoT and Machine Learning," in *Procedia Computer Science*, Elsevier B.V., 2020, pp. 1950–1959. doi: 10.1016/j.procs.2020.03.222.

[21] C. S. Srikanth, T. B. Rayudu, J. Radhika, and R. Anitha, "Smart waste management using internet-of-things (IoT),"

JDFEWS 5 (2): 17 - 42, 2024
ISSN 2709-4529

International Journal of Innovative Technology and Exploring Engineering, vol. 8, no. 9, pp. 2518–2522, Jul. 2019, doi: 10.35940/ijitee.g5334.078919.

[22] R. Abujassar, H. Yaseen, A. A.-A.-J. of S. and Actuator, and undefined 2021, "A highly effective route for real-time traffic using an IoT smart algorithm for tele-surgery using 5G networks," *mdpi.comRS Abujassar, H Yaseen, AS Al-AdwanJournal of Sensor and Actuator Networks, 2021•mdpi.com*, vol. 10, p. 30, 2021, doi: 10.3390/jsan10020030.

[23] A. Hoang, X. N.-J. of C. Production, and undefined 2021, "Integrating renewable sources into energy system for smart city as a sagacious strategy towards clean and sustainable process," *Elsevier*, Accessed: Sep. 12, 2024. [Online]. Available: https://www.sciencedirect.com/science/article/pii/S0959652621013809

[24] M. Abdallah, M. Adghim, … M. M.-W. M. &, and undefined 2019, "Simulation and optimization of dynamic waste collection routes," *journals.sagepub.com*, vol. 37, no. 8, pp. 793–802, Aug. 2019, doi: 10.1177/0734242X19833152.

[25] M. Nirmala, K. M.-2021 I. C. on, and undefined 2021, "Solar Powered IoT based Smart Solid Waste Management System," *ieeexplore.ieee.orgM Nirmala, K Malarvizhi2021 International Conference on Advancements in Electrical, 2021•ieeexplore.ieee.org*, Accessed: Feb. 29, 2024. [Online]. Available: https://ieeexplore.ieee.org/abstract/document/9675662/

[26] M. Kabir, S. Roy, M. Ahmed, M. A.-G. J. of Computer, and undefined 2020, "IoT Based Solar Powered Smart Waste Management System with Real Time Monitoring-An Advancement for Smart City Planning," *academia.eduMH Kabir, S Roy, MT Ahmed, M AlamGlobal Journal of Computer Science and Technology, 2020•academia.edu*, Accessed: Feb. 29, 2024. [Online]. Available: https://www.academia.edu/download/64755928/2_IoT_Based_Solar_Powered_Smart.pdf

[27] G. Gunawan, M. Sari, B. Surbakti, G. Kumaravel, and V. Ilankumaran, "IoT based Smart Battery Power and Wastage Level Tracking System for Solar Powered Waste Bin by GSM Technology," *iopscience.iop.orgG Kumaravel, V IlankumaranIOP Conference Series: Earth and Environmental Science, 2022•iopscience.iop.org*, doi: 10.1088/1755-1315/1055/1/012014.

[28] K. Pardini, J. J. P. C. Rodrigues, S. A. Kozlov, N. Kumar, and V. Furtado, "IoT-based solid waste management solutions: a survey," *mdpi.com*, doi: 10.3390/jsan8010005.

[29] B. Wu, W. Widanage, S. Yang, X. L.-E. and AI, and undefined 2020, "Battery digital twins: Perspectives on the fusion of models, data and artificial intelligence for smart battery management systems," *ElsevierB Wu, WD Widanage, S Yang, X LiuEnergy and AI, 2020•Elsevier*, Accessed: Sep. 12, 2024. [Online]. Available: https://www.sciencedirect.com/science/article/pii/S2666546820300161

APPENDIX

MICROPROCESSOR CODE

```
#include <LiquidCrystal.h>
#include <DHT.h>
#include <TinyGPS++.h>
#include <SoftwareSerial.h>
#include <HX711.h>

// Pin Definitions
#define TRIG_PIN 12
#define ECHO_PIN 11
#define DHT_PIN 8
#define LOADCELL_DOUT_PIN 10
#define LOADCELL_SCK_PIN 9
#define GSM_TX 0
#define GSM_RX 1
#define GPS_RX 18
#define GPS_TX 19
// LCD Pins
LiquidCrystal lcd(2, 3, 4, 5, 6, 7);
// DHT11 Setup
#define DHTTYPE DHT11
DHT dht(DHT_PIN, DHTTYPE);
// HX711 Setup
HX711 scale;
```

JDFEWS 5 (2): 17 - 42, 2024
ISSN 2709-4529

```
// GPS Setup
TinyGPSPlus gps;
HardwareSerial &gpsSerial = Serial1; // Using Serial1 for GPS
// GSM Setup
SoftwareSerial gsmSerial(GSM_RX, GSM_TX);
void setup()
{
   // Initialize Serial Monitor
   Serial.begin(9600);
   // Initialize LCD
   lcd.begin(20, 4);
   lcd.print("WELCOME");
   delay(300);
   lcd.clear();
   // Initialize DHT11
   dht.begin();
   // Initialize HX711
   scale.begin(LOADCELL_DOUT_PIN, LOADCELL_SCK_PIN);
   // Initialize GPS
   gpsSerial.begin(9600);
   // Initialize GSM
   gsmSerial.begin(9600);
   delay(10);
}
void loop()
{
   // Read and display ultrasonic distance
   long distance = measureDistance();
   lcd.setCursor(0, 0);
   lcd.print("Dist: ");
   lcd.print(distance);
   lcd.print(" cm");
   delay(50);
   // Read and display weight from HX711
   float weight = scale.get_units(10) / 1000; // Convert to kg
   lcd.setCursor(0, 1);
   lcd.print("Weight: ");
   lcd.print(weight);
   lcd.print("kg");
   delay(50);
   // Read and display temperature and humidity from DHT11
   float temperature = dht.readTemperature();
   float humidity = dht.readHumidity();
   if (isnan(temperature) || isnan(humidity))
   {
      Serial.println("Failed to read from DHT sensor!");
   }
   else
   {
      Serial.print("Temp: ");
      Serial.print(temperature);
      Serial.print(" °C, ");
      Serial.print("Humidity: ");
      Serial.print(humidity);
      Serial.println(" %");
      lcd.setCursor(0, 2);
      lcd.print("Temp: ");
```

JDFEWS 5 (2): 17 - 42, 2024
ISSN 2709-4529

```
    lcd.print(temperature);
    lcd.write(223); // Print the degree symbol (°)
    lcd.print("C, ");
    lcd.setCursor(0, 3);
    lcd.print("Humidity: ");
    lcd.print(humidity);
    lcd.print(" %");
    delay(50);
  }
  // Process GPS data
  while (gpsSerial.available() > 0)
  {
    gps.encode(gpsSerial.read());
  }
  if (gps.location.isUpdated())
  {
    float latitude = gps.location.lat();
    float longitude = gps.location.lng();
    Serial.print("Latitude: ");
    Serial.println(latitude, 6);
    Serial.print("Longitude: ");
    Serial.println(longitude, 6);
  }
  // Check conditions and send alert if needed
  if (distance < 10 || weight > 5000 || temperature > 40 || humidity > 80)
  {
    sendAlert(distance, weight, temperature, humidity);
  }
  delay(100); // Wait for 2 seconds before next loop
}
long measureDistance()
{
  digitalWrite(TRIG_PIN, LOW);
  delayMicroseconds(2);
  digitalWrite(TRIG_PIN, HIGH);
  delayMicroseconds(10);
  digitalWrite(TRIG_PIN, LOW);
  long duration = pulseIn(ECHO_PIN, HIGH);
  long distance = duration * 0.034 / 2;
  return distance;
}
void sendAlert(long distance, float weight, float temperature, float humidity)
{
  // Prepare the alert message
  String message = "ALERT! Bin Full or Critical Condition.\n";
  message += "Dist: " + String(distance) + " cm\n";
  message += "Weight: " + String(weight) + " g\n";
  message += "Temp: " + String(temperature) + " *C\n";
  message += "Humidity: " + String(humidity) + " %\n";
  if (gps.location.isValid())
  {
    message += "Location: https://maps.google.com/?q=";
    message += String(gps.location.lat(), 6) + "," + String(gps.location.lng(), 6);
  }
{
  // Send the message via GSM module
  gsmSerial.println("AT+CMGF=1"); // Set GSM module to text mode
```

JDFEWS 5 (2): 17 - 42, 2024
ISSN 2709-4529

```
  delay(100);
  gsmSerial.println("AT+CMGS=\"+2349039227520\""); // Replace with your phone number
  delay(100);
  gsmSerial.print(message);
  delay(100);
  gsmSerial.write(26); // End SMS command
  delay(100);
}
```

Journal of Digital Food, Energy & Water Systems [JD-FEWS]

JDFEWS 5 (2): 43 - 55, 2024
ISSN 2709-4529

Impact Of Magnetised Water on Nigeria Broiler Chicken Performance and Growth Rate

A.T., BAKER
University of Johannesburg, Johannesburg, South Africa
bakeradebayour@gmail.com

O.I., OJO
Ladoke Akintola University of Technology, Ogbomoso, Nigeria

M.O., DINKA
University of Johannesburg, South Africa

S., RWANGA
University of Johannesburg, South Africa

Received: 20 November 2024
Review: 5 December 2024
Accepted: 13 December 2024
Published: 16 December 2024

Abstract— Poultry farming is vital to Nigeria's economy and provides a key protein source, yet many farms struggle with slow growth and high mortality in broiler chickens. This study aimed to assess the impact of magnetised water on broiler growth. Forty (40) broiler chickens were housed in four groups (T_0-T_3) at the National Integrated Farm Project in Ilorin, Nigeria. The water treatment involved a setup with neodymium magnets and varied exposure times: T_0 (control, no magnetisation), T_1 (55 s), T_2 (110 s), and T_3 (165 s). Each group had ten (10) birds, and weekly weight was recorded over seven weeks. A paired t-test was used to analyze growth differences between treatments. Average weekly weight gains for T_0, T_1, T_2, and T_3 increased progressively, with T_3 showing the highest gain. Paired t-test results indicated significant differences in growth between magnetised and non-magnetised groups, with calculated values above the threshold (ttab = 2.969). This study established that magnetised water increased broiler chicken performance and growth rate. Therefore, magnetized water is recommended to produce broiler chicken for high income from poultry farming.

Keywords— *magnetised water, broiler chicken, mean body weight, growth rate*

Journal of Digital Food, Energy & Water Systems [JD-FEWS]

JDFEWS 5 (2): 43 - 55, 2024
ISSN 2709-4529

1.0 Introduction

Water quality is important for animal production because it is vital to life; it keeps cells healthy, carries nutrients and fluids through the blood, and controls body temperature [1]. Being made up of two positively charged hydrogen atoms joined to an oxygen atom; water is a relatively basic molecule. According to Ref [2], opposite electrical charges attract each other, thereby attracting water molecules. However, when a permanent magnet is placed in contact with water for a long time, the water acquires magnetic properties and becomes magnetically charged [3]. When consumed internally and consistently over an extended period, such magnetically treated water impacts the human body [4]. When water is let to pass through a magnetic field in a pipe or hose, magnetized water—also known as magnetic water or magnetically treated water—is created [5]. Moreover, the purpose of the technique used to provide broiler chicks magnetized water is to increase their development rate (as a growth stimulant), increase their feed conversion ratio, strengthen their immunity, and lessen the unpleasant smell of their droppings [6]. Reducing the bonding angle of the magnetic field from 1040 to 1030 alters the characteristics of magnetized water by decreasing the rate of carbonate deposition in the pipe, increasing its solubility, and decreasing surface tension [5]. One of the methods used to enhance water quality is using magnetic forces to make the water more magnetic. Improvements in crop yields, germination rates, soil and water quality, and the removal of scale formation in pipes are some of the primary advantages of magnetic water in agricultural activities [7]. According to Ref [8], magnetised water improves chicken's biochemical functions and eggs' quality. Also, the research by Ref [9] confirms that using magnetised water accelerates broiler chicken development rate, improves feed conversion ratio, strengthens chicken immunity, and lessens the unpleasant odor of the chicken droppings. Consequently, Nigerian farmers' incomes and the country's economy may both benefit from the profitable industry of raising broiler chickens. In Nigeria, galactosidase and related enzymes have been and continue to be utilized as feed additives to boost broiler chicken productivity. These feed additions, however, are chemical-based, inefficient, and hard for nearby farmers to obtain. Thus, this study employed magnetized water, a (non-chemical) method, and a basic technology that may be used to increase the growth of broiler chickens [10]. Poultry production with magnetized water improves the hens' immunity and lowers the odor in the poultry buildings. In order to increase the growth rate of broiler chickens and lower the degree of objectionable odor in the poultry houses—the primary emphasis of this study—an alternate approach that is cheap for farmers is required.

In addition, digitalization enhances magnetized water usage's effectiveness, monitoring, and scalability in Nigerian broiler production. By combining technology with innovative water treatments, farmers can achieve higher productivity, sustainability, and profitability in poultry farming. In real-time, the Internet of Things (IoT) device was installed to monitor the magnetic field strength, water quality, pH levels, and mineral content. This ensures that the magnetized water remains effective for improving broiler performance. This work has contributed to the study of magnetised water in poultry performance in Nigeria using digitalization to enhance magnetized water's effectiveness, which made it different from previous studies.

Furthermore, the motivation for working on magnetised water for broiler chicken performance in Nigeria stems from various challenges and opportunities within the poultry sector. These include improving productivity, addressing resource constraints, enhancing sustainability, and boosting economic returns. Magnetised water has potential benefits such as reducing stress, improving immunity, and minimizing disease outbreaks, which are critical for maintaining high productivity.

Also, working on magnetised water for broiler chicken performance in Nigeria has several implications that span agricultural productivity, economic development, environmental sustainability, and scientific advancement. Magnetised water can improve broilers' health and nutritional profile, leading to better-quality poultry meat that can fetch higher market prices.

The study observed, among other factors, a lack of Farmer Awareness: Many Nigerian farmers are unfamiliar with the concept and potential benefits of magnetized water and the Cost of Equipment: Magnetising devices may be expensive for smallholder farmers, who dominate the poultry industry in Nigeria. Also, the factor of Smart Farming Solutions: Combining magnetized water with IoT devices, sensors, and AI systems for real-time monitoring and control as the current limitations and future opportunities for the impact of magnetised water on the broiler chicken performance in Nigeria.

1.1 Statement of the Problem

Many poultry farms in Nigeria are associated with the problems of poor growth rate, low production to meet the demand in Nigeria, high mortality rate, environmental pollution (offensive odour) from the poultry droppings and high cost of poultry feeds resulting in high cost of production costs and low marginal profits. According to

JDFEWS 5 (2): 43 - 55, 2024
ISSN 2709-4529

Ref [11], the patented methods used by authors in [12] and [13] for enhancing broiler chicken quality and serving as a growth promoter were organic acids and chemicals by nature, and when taken by people, these chemicals had a negative impact on human health. Therefore, this study used magnetised water, a nonchemical-based method that is non-harmful to humans, to promote the growth rate of broiler chickens.

1.2 Objectives

This study investigated the impact of magnetised water on Nigeria broiler chicken performance and growth rate.

1.3 Materials and Equipment

A total number of 40 broiler chickens were collected from the Aromokeye Veterinary Farm, Ilorin and, weighed on arrival, and stocked on the 15th of September 2023. The materials and equipment used in this study are listed below.
10 x 25 x 50 mm neodymium magnet
Magnetic treatment unit of 250 mm by 200 mm plastic container,
4 units water trough
1 saw blade
4 units feeding trough
50 L water tank
Gum
1-unit 12.7 mm diameter flow control valve
4-unit 12.7 mm (1/2 inch) diameter PVC pipe
6 number elbows
2 number union PVC pipe
150 kg bags of starter feed and 250 kg bags of finisher feeds.

2.0 Materials and Methods

This study was conducted at the National Integrated Farm Project (NIFAP) unit of the National Centre for Agricultural Mechanization (NCAM), Ilorin, Nigeria on longitude 4.61220 East and Latitude 8.41610 north. A total number of 40 broiler chickens were dispersed randomly into four treatment groups of 10 birds each. The system of rearing for the first 4 weeks was a deep litter system in which the treatment houses were constructed using planks and iron sheets and the floor was covered with some wood shavings as the litters, and the remaining 3 weeks, the birds were transferred to the battery cage house. (See Plates 1.4a and 1.4b).
In this housing system, the birds were kept in a litter floor arrangement of 1.90 m by 1.14m dimension. Feed and water were made inside the house and as a general rule of thumb, broiler chicken require 1 kg of starter crumbs of grower pellets and 1.5 kgs of finisher pellets. The total quantity of feed fed to the birds at the end of the 7th week of the study was 150 kg bags of starter feed and 250 kg bags of finisher feed.
Ref [14] calculated the daily water consumption of broilers by multiplying the bird's age in days by 0.00591 liters of water and found that chickens need 0.91 to 1.36 liters of water for every 0.45 kilogram of feed ingested. In this study, broiler chickens in each treatment house were given 10 litres of water per day, and in the 7th week, the total quantity of water provided to the birds was estimated to be 490 litres.

Journal of Digital Food, Energy & Water Systems [JD-FEWS]

JDFEWS 5 (2): 43 - 55, 2024
ISSN 2709-4529

Plate 1.4a: Deep litter house arrangement for the Broiler chicken Plate **1.4b**: Broiler chicken with magnetised water under the Battery cage arrangement.

2.1 Magnetic Treatment Unit

A 10 mm x 25 mm x 50 mm neodymium magnet was used in the development of the magnetic treatment unit. The strongest magnet in the world, the NdFeB magnet, is created by combining neodymium (Nd), iron (Fe), and boron (B). It is a permanent magnet with a magnetic flux density of 1.0 to 1.5 T (1T = 10,000 G) or higher. Neodymium is an effective rare earth magnet that can withstand temperatures as high as 80 °C without demagnetizing, according to [15]. In this study, the magnetic treatment unit utilized the setup of [16], which comprised a pipe (a rectangular clear pipe with a diameter of 20 x 60 mm and a length of 960 mm but built with a plastic container) encircled by 12 neodymium magnet pieces. A 50 L bucket was attached to the magnetic treatment device, and the water flow was controlled by a 25.4 mm pipe control. In order to distribute water to treatment houses two and three, a non-returning valve was attached to a second 20 L bucket along the main line. The magnetic treatment equipment for creating magnetized water was depicted in isometric, orthographic, and pictorial views in Figure 1.4a, 1.4b, and Plate 1.2, respectively.

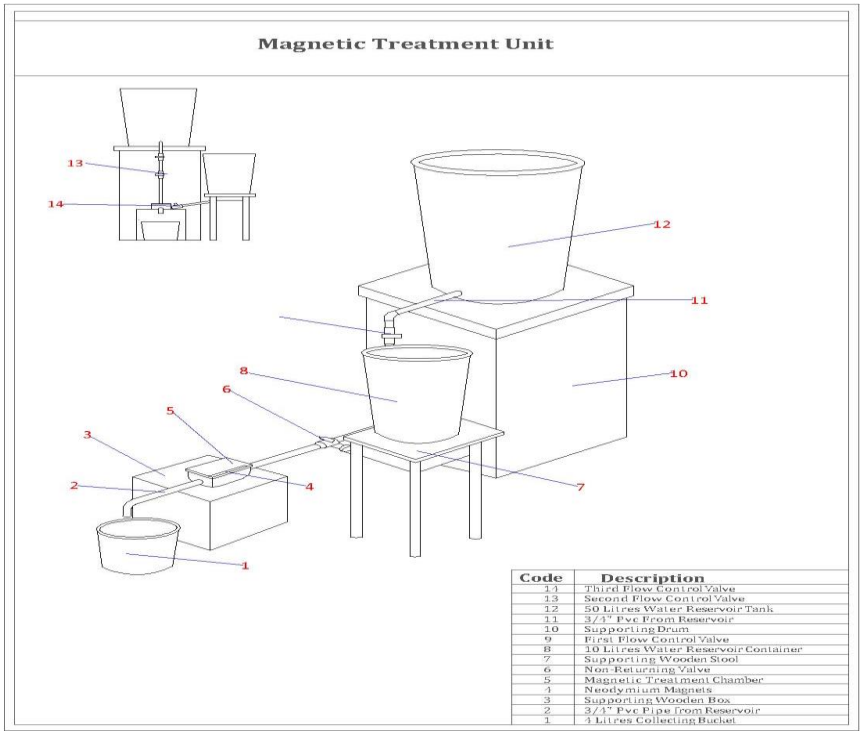

Fig. 1.4a: Isometric image of the magnetised water production equipment

Journal of Digital Food, Energy & Water Systems [JD-FEWS]

JDFEWS 5 (2): 43 - 55, 2024
ISSN 2709-4529

Plate 1.4: An image of the magnetized water production unit's magnetic treatment setup

2.2 Production of Magnetised Water

Various methods for obtaining magnetised water are known and different researchers have used different methods to produce magnetised water according to the aims of their studies. Ref [17] stated that one of these techniques is placing two bottles, jugs, or any other flat-bottomed container in the middle of a magnet with the north pole exposed and the other in the middle of a magnet with the south pole exposed. After a certain amount of time, the magnetism in water or any other liquid pierces it, changing the liquid's characteristics and, consequently, its magnetic. A flowing technique was employed to create the magnetized water used in this study, whereby water was permitted to pass through the magnetic treatment chamber's magnetic field. Broiler chicken was produced using water from the poultry farm's running tap, which was allowed to pass through the magnetic treatment unit once for 55 s. The broiler chicken in treatment house T1 received this water, while the broiler chickens in treatment house T2 received magnetized water that passed through the unit for 110 s, and the broiler chickens in treatment house T3 received magnetized water that passed through the unit for 165 s. Broiler chickens in the control house denoted by T0 were given non-magnetised water. The magnetised water was poured into a drinking trough from which the broiler chickens drank the water.

2.3 Methods

The study used 40 broiler chickens in total, with 10 broiler birds in each of the four treatment homes (see Plates 3.3a and 3.3b). Each treatment house's broiler chickens (designated T0, T1, T2, and T3) were fed the same kind of feed (Starter and Finisher feeds) in the same amount for seven weeks. Water was collected in a graduated cylinder for distribution after being moved through the magnetic chamber at a comparatively slow pace to avoid overflow. The water flow velocity in this configuration was determined to be 0.0058 m/s. As advised by the manufacturers of magnetic funnels (Magnetic Technologies LLC), the water was replaced every 12 hours to guarantee high-quality magnetized water and to make sure it was used within that time frame. Water that has passed through the magnetic field at the funnel can maintain its magnetic characteristics for up to 12 hours, according to [18]. A pH meter was used to measure the water's pH after it had been magnetically treated.

An N52 Neodymium magnet was a type of magnet used in this study where water was magnetically treated by passing it through a magnetic treatment unit made of plastic material following Fleming’s right-hand rule with neodymium magnets placed beside the pipe inside the treatment chamber. The treatment summaries are as follows:

NMW (T0) non-magnetised water group (Control group)
MW 1 (T1) flowed through the magnetic field for 55 s

Journal of Digital Food, Energy & Water Systems [JD-FEWS]

JDFEWS 5 (2): 43 - 55, 2024
ISSN 2709-4529

MW 2 (T2) flowed through the magnetic field for 110 s
MW 3 (T3) flowed through the magnetic field for 165 s


Plate 1.4a: Day-old broiler chicken **Plate 1.4b**: 3 weeks old broiler chicken

2.4 Determination of growth rate and weight gain of broiler chickens

The average growth rate (body weight gain) was determined by measuring the weights of the chickens in each treatment group weekly using an electric weighing device for 7 weeks and recorded as indicated in Plate 1.5. Average weight gain was calculated by dividing the total weight taken by the number of birds in each treatment group. Appendix A shows the % increase in weight gain as well as the growth rate of broiler chickens.


Plate 1.5: Weekly weighing to determine the body weight gain

2.5 The statistical analysis of the paired T-test

The study used a paired t-test statistical analysis to ascertain whether or not the weight and feed conversion ratio of broiler chickens were significantly impacted by magnetically treated water. The average difference between the magnetized and non-magnetized water results was calculated and is shown in Appendices B1–B3 and C. In accordance with [19] description, equations (1), (2), (3), and (4) were used to determine the mean, standard deviation, standard error, and t-test values.

$$\overline{d} = \frac{\sum d}{n} \quad (1)$$

$$\delta = \sqrt{\frac{\sum d^2 - n(\overline{d})^2}{n-1}} \quad (2)$$

$$\delta_{Er} = \frac{\delta}{\sqrt{n}} \quad (3)$$

JDFEWS 5 (2): 43 - 55, 2024
ISSN 2709-4529

$$t_{cal} = \frac{\overline{d}}{\delta_{Er}} \quad (4)$$

where;
$\overline{d}$ = mean of the difference from x1 and x2,

Σd = summation of d

n = number of the observations,

δ = standard deviation

σEr = standard error

tcal = calculated value of t-test.

3.0 Result and Discussion

3.1 Effects of magnetised water on the growth rate of broiler chicken

The broiler chickens that received magnetized water for 165 seconds (T3) gained the most body weight between the first and seventh weeks, increasing by 6.29 percent, and their growth rate increased by 899 g (89.9 g/broiler) overall. In contrast, the control group (non-magnetized water) had the least body weight gain. The trends in the mean body weight of the broiler chickens from week 1 to week 7 are shown in Figures 1.5a. The results of T2 and T3 were very close to each other, and they overlapped, and similarly, T1 and T0 were very close and overlapped as well. The average body weight of the broiler chickens is displayed in Figure 1.5b. By the end of week 7, when the broiler chicks were ready to be sold, the body weight gain was higher due to the magnetized water (Figure 1.5c). Appendix A provides comprehensive findings on how magnetized water affects broiler chicks' body weight gain. This outcome is consistent with Yusuf et al.'s study from 2022, which indicated that magnetized water improved broiler chicken growth rates.

All broiler chickens that were given magnetised water had a higher body weight than broiler chickens given non-magnetised water (control). The percentage increments in body weight gain in the 7th week for T1, T2, and T3 were 5.51 (%), 6.21 (%), 6.29 (%) respectively compared to T0, which showed that magnetised water is economically good and advisable to use to increase the growth performance of broiler chicken. According to this study, the chickens that drank magnetized water gained more body weight, which is consistent with the findings of [6].

The effect of magnetized water on the body weight gain of broiler chickens was statistically significant at $\alpha \leq 0.025$, according to the paired t-test statistical analysis shown in Appendices B1–B3 and C, respectively. This was because the calculated values of the paired t-test were greater than the table value at $\alpha \leq 0.025$ (the table value of the t-test = 2.969 at $\alpha \leq 0.025$, while the calculated values of the t-test for T1, T2, and T3 compared with T0 were 4.599, 5.562, and 5.560, respectively).

Journal of Digital Food, Energy & Water Systems [JD-FEWS]

JDFEWS 5 (2): 43 - 55, 2024
ISSN 2709-4529

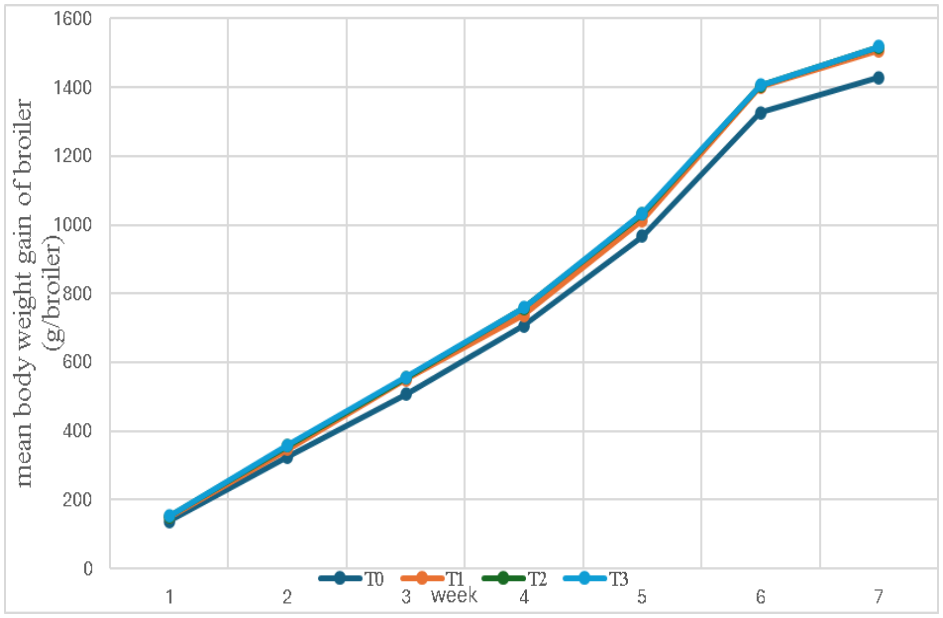

Fig. 1.5a Mean body weight gain of broiler chicken (g/broiler)

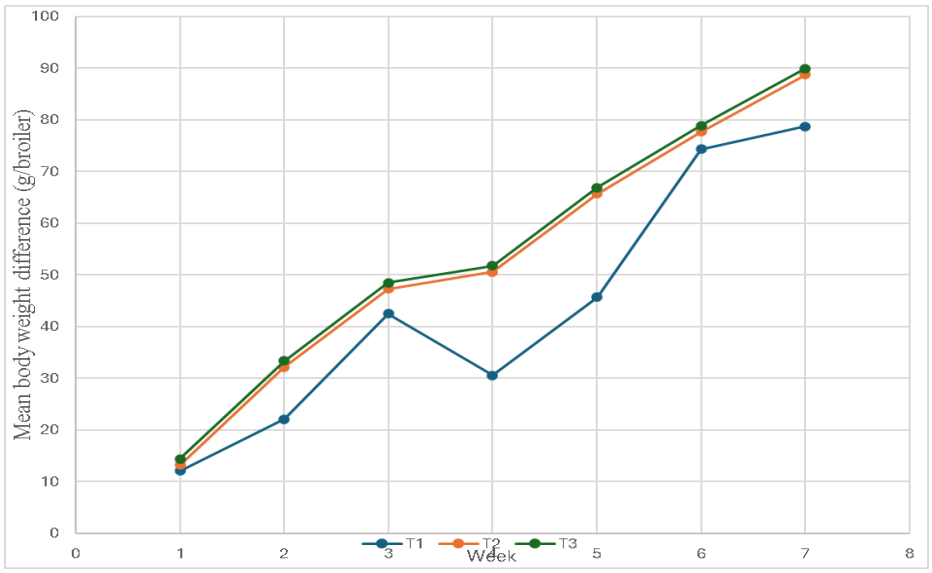

Fig. 1.5b Mean body weight difference (g/broiler)

JDFEWS 5 (2): 43 - 55, 2024
ISSN 2709-4529

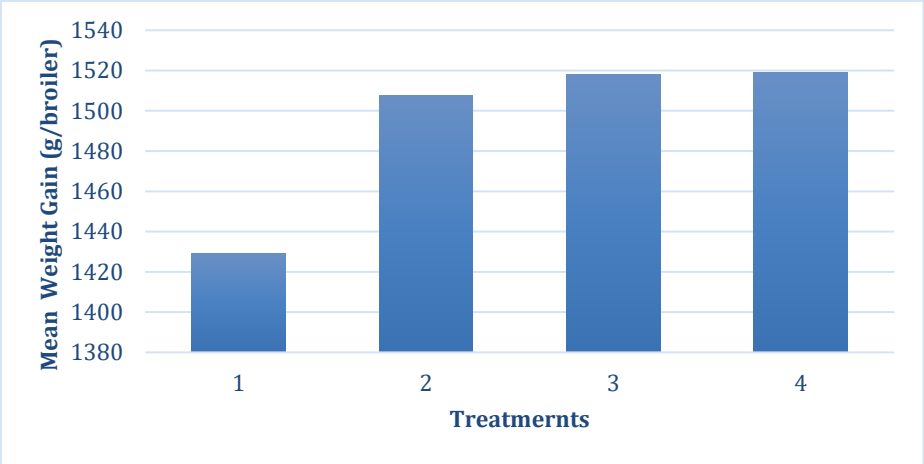

Fig. 1.5c Average weight growth of broiler chickens T_0, T_1, T_2, T_3 at week 7

4.0 Conclusion

Water magnetised for 165 s increased the growth rate of the broiler chicken by 89.9 g/broiler with a percentage increment of 6.29%. The findings of this study highlight the potential impact of magnetised water on broiler chickens' performance and growth rate in the Nigerian production environment. Magnetised water, as a novel technique, appears to offer tangible benefits by enhancing broiler performance metrics, including body weight, feed conversion ratio (FCR), and average daily gain (ADG). The results indicate that broilers given magnetised water exhibited significantly improved growth rates compared to those provided with non-magnetized water, suggesting its positive influence on nutrient absorption and metabolic efficiency.

Moreover, the improvement in growth performance may be attributed to the enhanced physicochemical properties of magnetized water, which are hypothesized to improve cellular hydration, nutrient solubility, and overall feed utilization. This could be particularly relevant in regions like Nigeria, where water quality and feed costs pose significant challenges to poultry production. By improving feed conversion efficiency, the use of magnetized water has the potential to reduce feed costs and enhance profitability for farmers, contributing to more sustainable poultry farming practices.

Furthermore, the study also demonstrates that magnetised water may mitigate stress-related growth depressions, especially in tropical climates characterized by high temperatures, which often impede poultry productivity. This is a particularly valuable observation for Nigerian poultry farmers striving to optimize production under challenging environmental and economic conditions.

However, while the results are promising, certain study limitations need to be addressed. The long-term effects of magnetised water on broiler health, meat quality, and carcass traits were not within the scope of this research and warrant further investigation. Additionally, the economic feasibility of adopting magnetized water on a large scale in commercial poultry operations should be explored to determine its practicality for Nigerian farmers.

In conclusion, magnetised water presents a promising innovation for improving the growth performance and efficiency of broiler chickens in Nigeria. While further research is needed to establish its long-term efficacy and economic viability, its potential as a cost-effective, non-invasive strategy for enhancing poultry productivity makes it an attractive option for addressing the challenges of broiler production in Nigeria and other similar regions.

Journal of Digital Food, Energy & Water Systems [JD-FEWS]

JDFEWS 5 (2): 43 - 55, 2024
ISSN 2709-4529

APPENDIX B - 1

APPENDIX B-1: Determination of Paired t-test

Table 1. T_1 Compared with T_0

Body Weight MW (T_3)	Body weight NMW (To)	d = T_3 – To	d^2
149.6	137.5	12.1	146.41
346.5	324.4	22.1	488.41
549.8	507.3	42.5	1806.25
737.0	706.4	30.6	936.36
1012.2	966.5	45.7	2088.49
1401.2	1326.9	74.3	5520.49
1507.8	1429.1	78.7	6193.69
		$\sum d$ =306.0	**$\sum d^2$ = 17180.1**

APPENDIX B- 2

APPENDIX B-2: Determination of Paired t-test

Table 2. T_2 Compared with T_0

Body Weight MW (T_3)	Body weight NM W (T_0)	d = T_3 – To	d^2
150.7	137.5	13.2	174.24
356.6	324.4	32.2	1036.84
554.6	507.3	47.3	2237.29
757.0	706.4	50.6	2560.36
1032.2	966.5	65.7	4316.49
1404.6	1326.9	77.7	6037.29
1517.8	1429.1	88.7	7867.69
		$\sum d$ =375.4	**$\sum d^2$ = 24230.20**

Journal of Digital Food, Energy & Water Systems [JD-FEWS]

JDFEWS 5 (2): 43 - 55, 2024
ISSN 2709-4529

APPENDIX B - 3

APPENDIX B-3: Determination of Paired t-test

Table 3. T_3 Compared with T_0

Body Weight MW (T_3)	Body Weight NMW (T_0)	d = T_3 – To	d^2
151.9	137.5	14.4	207.36
357.8	324.4	33.4	1115.56
555.8	507.3	48.5	2352.25
758.2	706.4	51.8	2683.24
1033.4	966.5	66.9	4475.61
1405.8	1326.9	78.9	6225.21
1519.0	1429.1	89.9	8082.01
		$\sum d$ =383.8	**$\sum d^2$ = 25141.24**

APPENDIX C

Determination of Statistical Parameters using Paired -test Statistical Analysis

The formular given by Nahm (2005) was used to determine the paired t-test

$$\overline{d} = \frac{\sum d}{n}$$

$$\overline{d} = \frac{383.8}{7} = 54.83$$

$$\delta = \sqrt{\frac{\sum d^2 - n(\overline{d})^2}{n-1}}$$

$$\delta = \sqrt{\frac{25141.24 - 7(54.83)^2}{7-1}} = 26.131$$

$$\delta_{Er} = \frac{\delta}{\sqrt{n}}$$

$$\delta_{Er} = \frac{26.131}{\sqrt{7}} = 9.861$$

$$t_{cal} = \frac{\overline{d}}{\delta_{Er}}$$

$$t_{cal} = \frac{54.83}{9.861} = 5.560$$

at the 5% significant level t_{cal} and t_{tab} values were compared, however, for the paired t-test, the difference was 2.5% ($\alpha = 0.05/2 = 0.025$)

Funding Statement: This study was supported by the research funds from the National Centre for Agricultural Mechanization, Nigeria and conducted under its research program scheme.

Ethical Compliance: All procedures performed in studies involving human participants were in accordance with the ethical standards of the institutional research committee and with 1964 Helsinki Declaration and its later amendments.

Journal of Digital Food, Energy & Water Systems [JD-FEWS]

JDFEWS 5 (2): 43 - 55, 2024
ISSN 2709-4529

Conflict of Interest declaration: The authors declared that they have no affiliations with or involvement in any organization or entity with any financial interest in the subject matter or materials discussed in the manuscript.

JDFEWS 5 (2): 43 - 55, 2024
ISSN 2709-4529

References

[1] Sohal R, Mockett R, and Orr WC. (2002). Mechanisms of aging: an appraisal of the oxidative stress hypothesis. Free Radic Biol Med 33(5): 575-586.
springer.
[2] Shen, D., Duley, W. W., Peng, P., Xiao, M., Feng, J., Liu, L. and Zhou, Y. N. (2020). Moisture-enabled electricity generation: from physics and materials to self-powered applications. *Advanced Materials*, *32*(52), 2003722.
[3] Yacout, H. (2015). Effect of Magnetic Water on the Performance of Lactating Goats. *Journal of Dairy, Veterinary and Animal Research*,*2*(5), 1-14. doi:10.15406/jdvar.2015.02.00048
[4] Lam M (2001). Uses of magnetised water in poultry production
(www.DrLam.com)
[5] Babu, C. (2010) Use of magnetic water and polymer in agriculture. Tropical
research, ID08-806-001.agriculture.pdf https://www.gmxinternational.com
application/agriculture/GMX-on
[6] Al-Mufarrej, S., Al-Batshan, H., Shalaby, M., and Shafey, T. (2005). The Effects of Magnetically Treated Water on the Performance and Immune System of Broiler Chickens. *International Journal of Poultry Science*,*4*(2), 96-102. doi:10.3923/ijps.2005.96.102
[7] Yusuf, K. O. and Ogunlela, A. O (2015). Impact of magnetic treatment of water on growth and yield of tomato. *Journal of Notulae Scientia Biologicae*, 7 (3): 345-348.
[8] Radha, G. H and AL-Sardary, S. Y. T. (2021) Effects of using magnetic matter on egg quality and biochemical composition in commercial layers. IOP Conference Series: Earth and Environmental Science, 761: 1 – 9. doi:10.1088/17551315/761/1/012106
[9] Shah D, and Nagarajan N. (2013). Luteal insufficiency in first trimester. Indian J Endocrinol Metab,17: 44- 49.
[10] Mohamed, A.I. and Ebead, B. M. (2013) Effect of irrigation with magnetically treated water on faba bean growth and composition. International Journal of Agricultural Policy and Research, 1 (2):24-40. https://journalissues.org/wp-content/uploads/2014/07/IJAPR-Ahmed-and-Ebead.pdf
[11] Jassim, E Q., and Aqeel, Ch H. (2017). Effect of alkaline water and /or magnetic water on some physiological characteristics in broiler chicken. *Journal of Entomology and Zoology Studies*,*5*(5), 1643-1647. Retrieved April 4, 2018, from http://www.entomoljournal.com/archives/2017/vol5issue5/PartU/5-5-136-656.pdf
[12] Hussen MA. (2002). Magnetic water treatment is an attractive option. http://www.1st-in-wellness.com).
[13] Smith, K. A., Jackson, D. R., Misselbrook, T. H., Pain, B. F. and Johnson, R. A. (2000) Reduction of ammonia emission by slurry application techniques, Journal of Agricultural Engineering Research, 77 (3): 277-287. https://doi.org/10.1006/jaer.2000.0604
[14] Alhassani, D., and Amin, G. (2012). Response of Some Productive Traits of Broiler Chickens to Magnetic Water. *International Journal of Poultry Science*,11(2): 158-160.
[15] Alhammer AH, Sadiq GT, and Yousif S. (2013). Effect of magnetized water on several biochemical and physical properties in mice. J Babylon Univ Pure Appl Sci, 21(3): 910-916.
[16] Yusuf, K.O, Akande, O.S and Baiyeri, R.M (2022) Effect of drinking magnetized water on offensive odour from poultry droppings of broiler chicken. *Journal of Environmental Research, Engineering and Management;* vol. 78/No 3/2022 pp. 119-128
[17] Ali Y., Samaneh, R., and Kavakebian, F. (2014). Applications of Magnetic Water Technology in Farming and Agriculture Development: A Review of Recent Advances. *Current World Environment*, ***9***(3): 695-703.
[18] Mahdi AS (2012). The effect of using magnetically treated water on some productive and physiological traits of Turkish-Awassi rams. M. Sc. Thesis. Veterinary College, University of Baghdad, Iraq.
[19] Al-Fadul, Muataz F. Mohammed (2007). The Effect of Magnetically Treated Water and diet on the performance of the Broiler Chicks. An *unpublished Ph.D dissertation*, University of Khartoum, Sudan

Journal of Digital Food, Energy & Water Systems [JD-FEWS]

JDFEWS 5 (2): 56 - 64, 2024
ISSN 2709-4529

System Dynamics Approach to Potable Water Management in Eastern Cape Province of South Africa

Motsi Ephrey MATLAKALA
University of Johannesburg, Johannesburg, South Africa
motsim@uj.ac.za

Shelly Thandiwe MONA
Central University of Technology, Free State, South Africa

Received: 26 October 2024
Review: 5 December 2024
Accepted: 13 December 2024
Published: 16 December 2024

Abstract—Water shortage is due to the mismanagement of resources meant to install, operate, and improve water infrastructures. Considering the increase in population and how it affects the water supply and operations of water systems, a management strategy is required to sustain a water supply system for a lengthy period. Hence, the purpose of developing a System Dynamics (SD) model for the water supply chain is to assess water supply systems, enabling a complete understanding of the underlying dynamics and the potential impacts of various interventions in water supply management. The model was applied as a decision-support tool to achieve sustainable water management. It was observed that System dynamics is a suitable approach for comprehending feedback, policy choices, and cause-and-effect interactions. It has been particularly effective in resolving water management issues. SD model for the water supply chain also helped with determining the lengthy period effect of policy alteration on water status. Overall, the development of the SD model was found to be effective in managing water supply systems effectively.

Keywords- *system dynamics, eastern cape, water, infrastructures, water supply, water management, and water access.*

Journal of Digital Food, Energy & Water Systems [JD-FEWS]

JDFEWS 5 (2): 56 - 64, 2024
ISSN 2709-4529

1 Introduction

One of the most crucial issues humans are experiencing in this twenty-first century is the insufficiency of water, which affects ecosystems, public health, and general welfare [1]. The causes of problems in relation to water are caused by either general water scarcity or poor management [1]. Shortage of water affects socio-economic development across the world. For instance, South Africa is one of the countries that struggle with potable water accessibility. Lack of sanitation in other parts of the county, especially in rural areas, contributes to the challenge of water shortage. Water resource management is a complex activity requiring a comprehensive approach to address many factors impacting water supply and demand [4]. This is because centralized water systems are often not upgraded to handle the growing pressures of population growth, urbanization, and climate change [5].

However, system dynamics modelling is significant in modelling economic systems, emphasizing its ability to represent intricate interactions through feedback loops and delays [1]. System dynamics is pivotal for simulating behaviors in various contexts, including financial institutions, highlighting the necessity for adaptive models that can accommodate the nonlinearities inherent in complex systems [2]. The study engages water supply managers in simulations that reflect the dual nature of these systems, comprising both physical infrastructure and the human elements involved in water management [3]. Also, research studies highlight the complexities arising from numerous variables and the stochastic nature of water inflows, advocating for integrated decision models that encompass technical, environmental, and social dimensions. Their work emphasizes that while optimization techniques are evolving, simulation models remain central to practical reservoir management, reflecting a critical need for tools to navigate water resource systems' intricacies [1,3]. This approach has been employed to tackle a range of water management issues, such as sustainable water planning, performance analysis, risk assessment, and water quality monitoring [4]. One key benefit of system dynamics is its ability to model the feedback loops and nonlinear relationships inherent in water systems. By representing the complex interactions between factors like precipitation, runoff, groundwater recharge, and water demand, system dynamics models can simulate the long-term behaviour of water supply systems and identify potential points of intervention [6]. The interlinked nature of the concerns about water has been approached through a SD modeling approach to finding the challenges of the water supply chain. SD models enable the integration of various biophysical, socioeconomic, and policy-related variables, providing a holistic perspective on water resource management [7]. This approach is particularly useful for evaluating the trade-offs and consequences of different water conservation strategies and engaging stakeholders in the decision-making process [8]. SD provides a powerful tool for evaluating water supply systems, enabling a holistic understanding of the underlying dynamics and the potential impacts of various interventions in water supply management.

2 Study Area

The scarcity of freshwater is one of the factors preventing future growth in South Africa. The rural areas of Eastern Cape province of South Africa are the subject of this investigation. Southeast South Africa's Eastern Cape province shares borders with the Western Cape province to the west, the Northern Cape province to the northwest, KwaZulu-Natal province to the northeast, the Free State province and Lesotho to the north, and the Indian Ocean to the southeast, as shown in Figure 1 [9]. With a projected population of 6,676,590 and a land area of 168,966 km2, it is regarded as the second largest province in the nation as of 2021. The climate is generally pleasant at higher elevations in the province's north, although it varies often around the shore [9]. Summers in the province are hot, and winters bring snow to the high Northern mountains [9]. The Eastern Cape is among the most severely affected provinces in the country, where the problem is made worse by antiquated infrastructure and incredibly unskilled water management. It is situated along the southern coast of South Africa and has a population of around seven million, making up 16% (the third largest) of the country's total population [10, 11]. Oliver Tambo, Amatole, Sarah Baartman, Chris Hani, Joe Gqabi, Alfred Nzo, Buffalo City, and Nelson Mandela Bay are the province's eight district municipalities (Figure 1).
Research has shown that approximately 25% of the Eastern Cape population does not have access to clean drinking water, which implies that not all communities in the area have access to clean water 24 hours a day [12]. Access to potable water provides sustainability to agricultural, industrial, household, recreational, and environmental activities, establishing most human water uses.

JDFEWS 5 (2): 56 - 64, 2024
ISSN 2709-4529

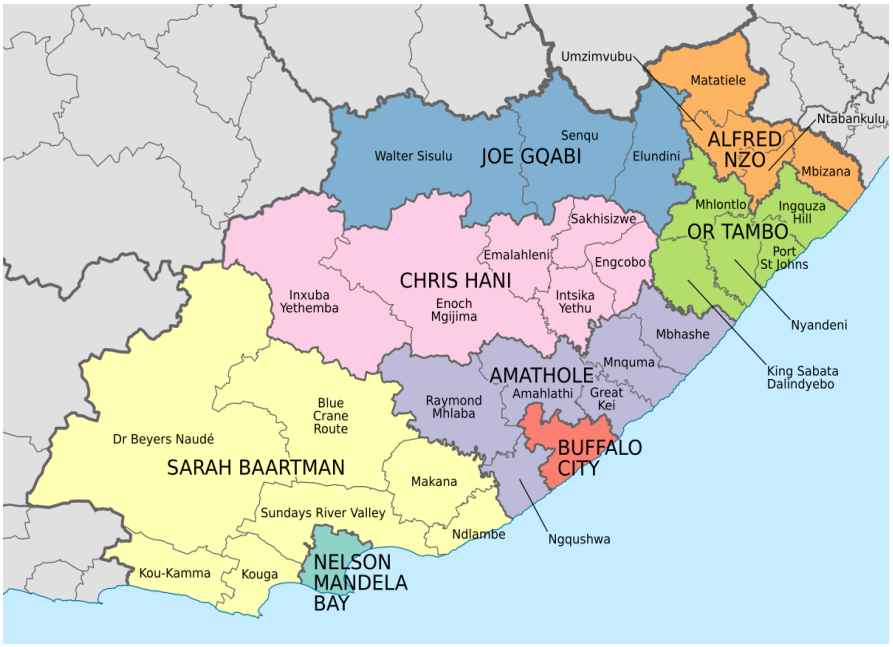

Fig. 1. Map Showing Eastern Cape Province District Municipalities in South African Country Northern [9].

This shortage of clean water in the province is because of the mismanagement of the resources that are meant to install, operate, and improve water infrastructures in the province [13]. Since water resources are complex and interdependent, it is, therefore, difficult to estimate the efficiency of water resource management [14]. Therefore, Effective modeling techniques are crucial for researching and identifying the feedback loops in water resources systems [15, 16]. This research study aims to model the water supply system and identify the types and root causes of water delivery problems. The province should adopt the SD model as a decision-support tool to achieve sustainable water management. SD is suitable for comprehending feedback, policy choices, and cause-and-effect interactions. It has been effectively applied to the resolution of water management issues in particular [11, 17, 18]. (Figure. 1).

3 Method

The research explored the challenges of water access in the Eastern Cape province. Vensim PLE computer software was used to build a computer model based on diagrams of system dynamics. Vensim PLE is a software used for continuous simulation and to produce graphical modelling [11]. This paper introduces the system dynamic approach as a tool for discussing and resolving complicated dynamic issues in the province's water supply and potable water infrastructure management.

The System Dynamics approach effectively solves water problems and ensures the sustainability of the potable water supply through the interaction of local water infrastructures. System Dynamics model is developed in this article to assess the dynamic operations of the water delivery system in Eastern Cape province. The introduction of the System Dynamics model is motivated by the fact that new development and sustainable management of water resources require methods that take into consideration dynamic connections between, among other things, water demand, population, and period effect [19,20,21]. The SD approach can easily solve the delivery of appropriate water service to satisfy human requirements because it helps with the allocation of resources to satisfy the need for water demand. Additionally, the model facilitates the testing of real-world behavior in a synthetic environment [21, 22, 23]. Dynamic simulation examines how a simulated system behaves and reacts to changes over time. Arrows, auxiliary variables, rate, and stock are the components of all SD models [21].

Journal of Digital Food, Energy & Water Systems [JD-FEWS]

JDFEWS 5 (2): 56 - 64, 2024
ISSN 2709-4529

4 System Dynamics Modeling

The system dynamics model is developed to simulate and study issues related to water supply chain, find solutions for water management, and ensure the sustainability of potable water supply. The model was designed to enhance and secure water supply. Some of the main components of the model include water demand, water catchment, water treatment plants, water recycling systems, and population in the province. In this regard, a 30-year simulation of the water supply system was conducted, beginning in 2021 and concluding in 2051. A casual loop diagram and a stock-flow diagram are used to illustrate the system's dynamics concepts. The causal loop diagram, shown in Figure 2, illustrates the positive and negative causation linkages between population growth, the demand for water, and other factors influencing potable water supply. Understanding system behaviors is aided by the causal loop diagram, which promotes further research into system dynamics techniques to increase their usefulness in a variety of fields, including water supply management [5].

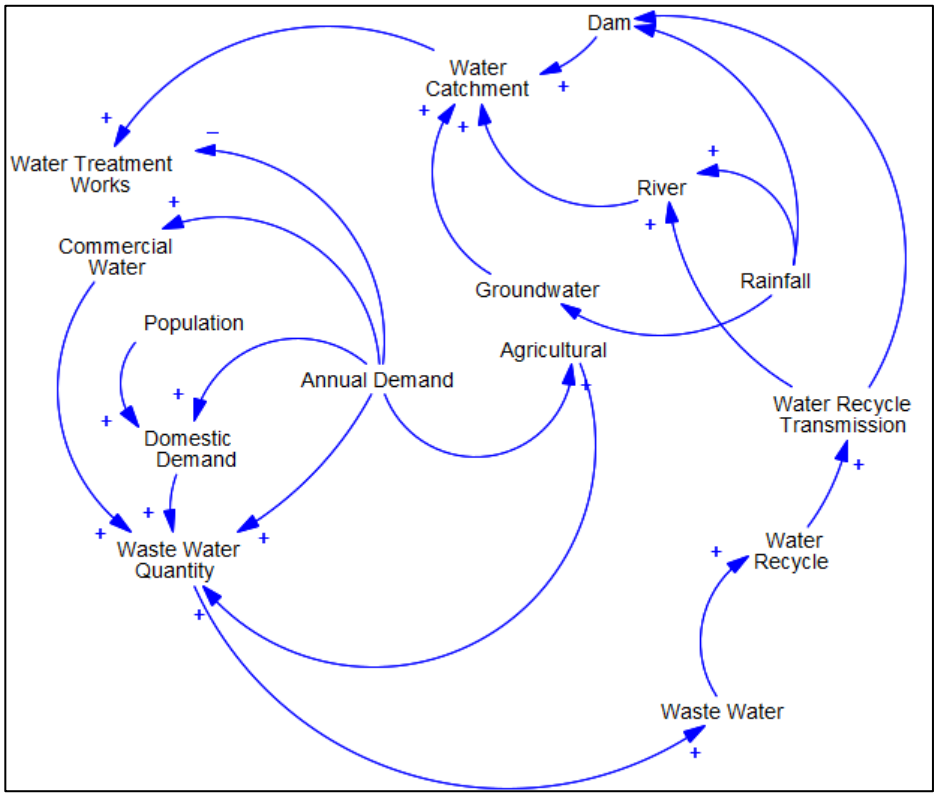

Fig. 2. Casual loop diagram presenting factors contributing to the water supply systems.

The purpose of the stock-flow diagram in Figure 3 is to show how many factors affect the availability and scarcity of water supplies. This analysis of the literature shows a distinct path for applying system dynamics to water supply systems, highlighting the evolution of thought from foundational modelling principles to contemporary integrated approaches that address the complexities of water resource management.

JDFEWS 5 (2): 56 - 64, 2024
ISSN 2709-4529

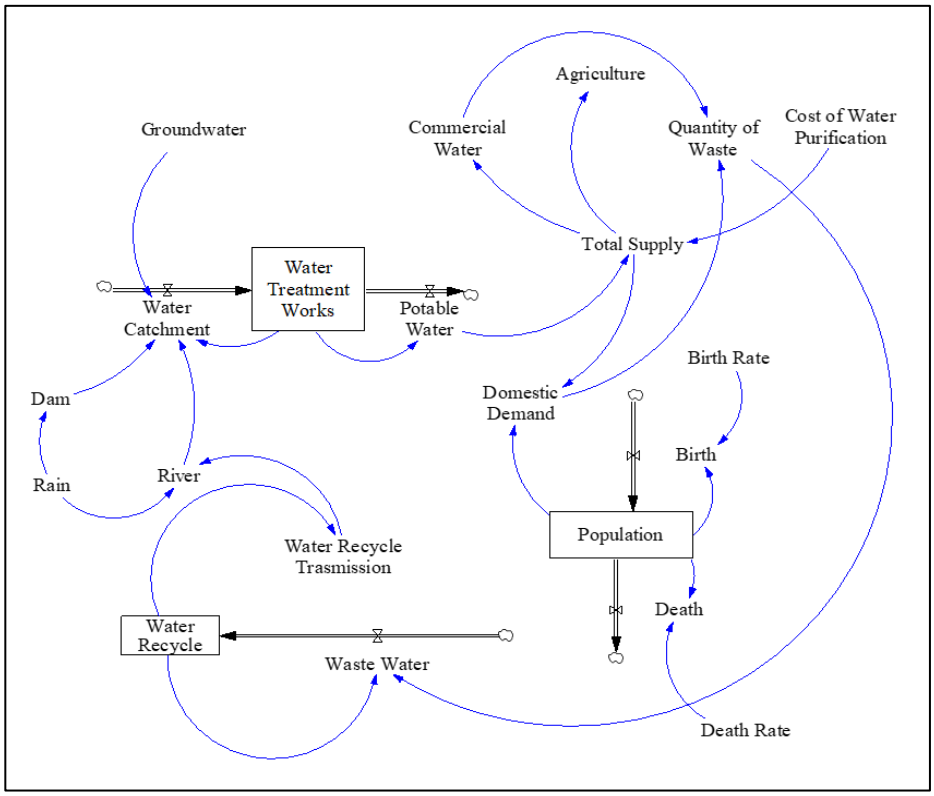

Fig. 3. Stock and Flow Diagram of Water Supply for Eastern Cape Province

5 Results and Discussion

The behaviour in Figure 7 shows the declining trend of domestic water demand, this is due to the increase in population. It is also known that population increase affects the agricultural and commercial sectors; hence, this study focuses on water supply. The total water supply depends on the amount of water from the Water Treatment Works (WTW). It can be seen in Figure 4 that an increase in water being treated increases the total water supply, as shown in Figure 5.

JDFEWS 5 (2): 56 - 64, 2024
ISSN 2709-4529

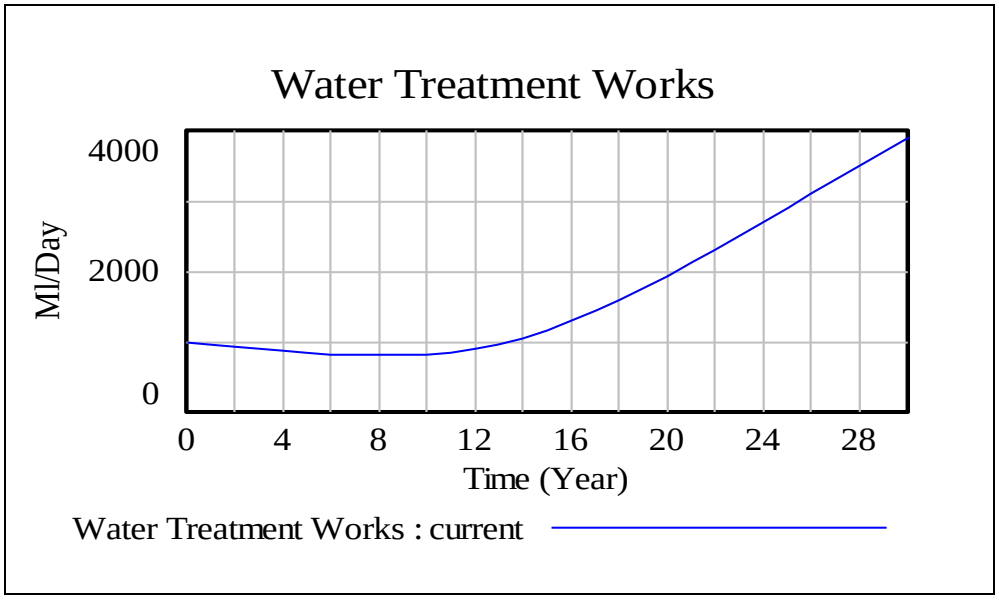

Fig. 4. Simulation Results of Water Treatment Works

In general, an increase in the water supply will also increase the amount of water supply to the agricultural and commercial sectors. On the other hand, the growing population (Figure 6) causes a decline in domestic water demand, as seen in Figure 7. These pose a challenge to water consumers, and if there is no continuous improvement and upgrade of the water systems, there is a risk of water shortage. For this reason, the System Dynamics (SD) model is crucial to help the local municipalities in the province to accurately estimate the amount of water required based on the population increase rate.

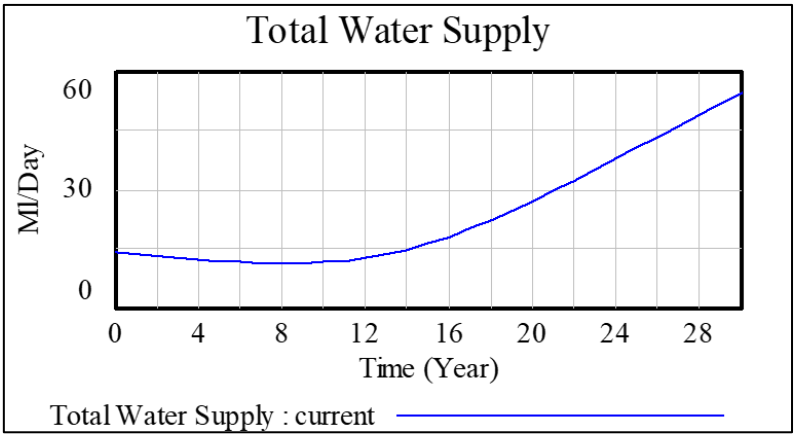

Fig. 5. Simulation Results of Total Water Supply

JDFEWS 5 (2): 56 - 64, 2024
ISSN 2709-4529

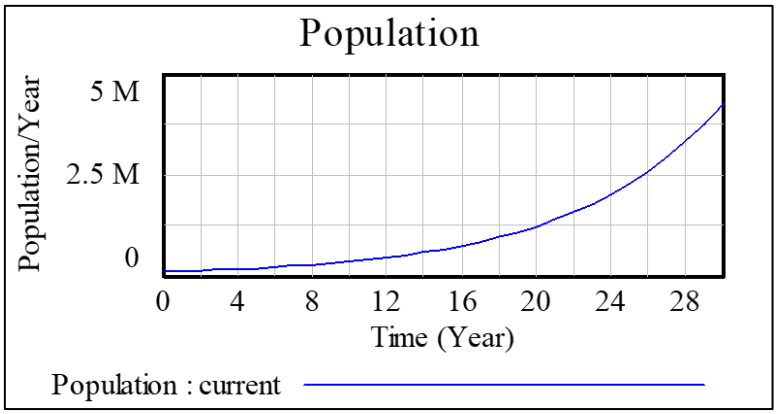

Fig. 6. Simulation Results of Population Rate per Year

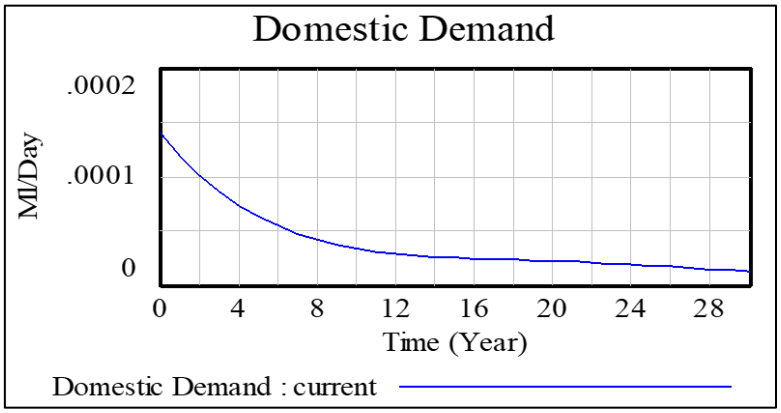

Fig. 7. Simulation Results of Domestic Water Demand

6 Conclusions

In this paper, an SD simulation model was developed to estimate the long-term effect of water supply in Eastern Cape province based on the causal response relationship between population, water demand, and water supply. The result of the simulation model provides a good indicator to the decision-maker on the management of risk of the water system and water distribution networks as the population increases over 30 years. The results show that SD provides a powerful tool for evaluating water supply systems, enabling a holistic understanding of the underlying dynamics and the potential impacts of various interventions in water supply management. SD was enough to develop efficient strategic management for water sustainability. It has been found that with the increase in population, water demand for residential, commercial, and agricultural can be efficiently managed through the development of the SD model. The Eastern Cape has one of the fastest-growing rates of population increase; thus, the SD model for the water supply chain could be used to determine the long-term effect of policy change on the status of water in the province. In addition, the research showed that the SD methodology can help the local government of Eastern Cape province to estimate the amount of water required by its rapidly growing population. The model will also help the local communities from dislocation in their water supply, which shall help in the formation of policy and resource allocation. The result of the optimal allocation model provides a good indicator to the decision-maker on the risk of the water system, water distribution networks, and the cost of the water system. The simulation models could be used as starting points for further research into water management; the models can be improved by incorporating actual data into them. The model can be extended to include more aspects of the water management supply chain, depending on the complexity of the problem being studied.

JDFEWS 5 (2): 56 - 64, 2024
ISSN 2709-4529

7 References

[1] M. I. Rumyantsev, "About Some Applications of Kolmogorov Equations to the Simulation of Financial Institutions Activity," 2009.

[2] G. Watts, B. von Christierson, J. Hannaford, and K. Lonsdale, "Testing the resilience of water supply systems to long droughts," 2012.

[3] J. Meseguer, G. Cembrano, J. M. Mirats, and E. Bonada, "Optimizing Operating Rules Of Multiple Source Water Supply Systems In Terms Of System Reliability And Resulting Operating Costs: Survey Of Simulation-Optimization Modeling Approaches Based On General Purpose Tools," 2014.

[4] Redondo, J. M., Ibarra-Vega, D., Catumba-Ruíz, J., & Sánchez-Munoz, M. P. (2020). Hydrological system modeling: Approach for analysis with dynamical systems. Journal of Physics: Conference Series, 1514(1). https://doi.org/10.1088/1742-6596/1514/1/012013

[5] Tsegaye, S., Missimer, T. M., Kim, J. Y., & Hock, J. (2020). A clustered, decentralized approach to urban water management. Water (Switzerland), 12(1). https://doi.org/10.3390/w12010185

[6] Schenk, C., Roquier, B., Soutter, M., & Mermoud, A. (2009). A system model for water management. Environmental Management, 43(3). https://doi.org/10.1007/s00267-008-9254-8

[7] Cerecedo Arroyo, M. E., & Martínez Austria, P. F. (2021). Dynamic water system modeling: A systematic review. In Water Practice and Technology (Vol. 16, Issue 3). https://doi.org/10.2166/wpt.2021.051

[8] Sun, A. C., Tidwell, V. C., Thomas, R., Brainard, J. R., Kobos, P. H., Malczynski, L. A., & Klise, G. (2006). Collaborative modeling using system dynamics for water resource management. Proceedings of 1st Water Quality, Drought, Human Health and Engineering Conference, WATER2006, 2006. https://doi.org/10.1115/water2006-20019

[9] T. E. E. Britannica, "Graaf-Reinet," Encyclopedia Britannica, 2017 February 23. [Online]. Available: https://www.britannica.com/place/Graaff-Reinet-South-Africa. [Accessed 17 July 2022].

[10] S. Fobisi, "Rural areas in the Eastern Cape Province, South Africa: The right to access safe drinking water and sanitation denied?," Polity.org.za, 2013. [Online]. Available: https://www.polity.org.za/article/rural-areas-in-the-eastern-cape-province-south-africa-the-right-to-access-safe-drinking-water-and-sanitation-denied-2013-01-24. [Accessed 9 June 2022].

[11] M. E. Matlakala and D. V. V. Kallon, "Systems Dynamic of Portable Water Shortage in the Limpopo Province of South Africa," *Proceedings of IEOM Zimbabwe,* pp. 200-207, 2020.

[12] R. Naidoo, "Eastern Cape lags behind with access to drinking water. Infrastructure news and service delivery," Rivonia, Johannesburg, 2016.

[13] L. Amoah, "Water Scarcity and Food Security in Ngqeleni Locality in the Eastern Cape Province- South Africa," *African Journal pf Hospitality, Tourism and Leisure,* pp. 40-53, 2021.

[14] M. E. Matlakala, D. V. V. Kallon, S. P. Simelane and P. M. Mashinini, "Design Parameters on the Performance of Centrifugal Pumps," *Procedia Manufacturing,* vol. 35, pp. 197-206, 2019.

[15] T. Nazarialamdarloo, H. Jamali, B. Nazari, M. Emanjomeh and H. Karyab, "A system dynamics approach for water resources management with focusing on domestic water demand," *Environmental Health Engineering and Management,* vol. 4, no. 7, pp. 229-235, 2020.

[16] M. E. Matlakala and D. V.V. Kallon, "Systems Dynamics Modelling of the Water Supply Problem in the Limpopo Province of South Africa," *Proceedings of IEOM Brazil,* pp. 1589-1597, 2020.

[17] S. Mona, "A system dynamics approach to study the behavior of Cape Town tourism for the next coming 10 years," *Proceedings of the International Conference on Industrial Engineering and Operations Management,* pp. 1006-1010, 2018.

[18] X. Xi and K. Poh, "Using System Dynamics for Sustainable Water Resources Management in Singapore," *Procedia Computer Science,* vol. 16, pp. 157-166, 2013.

[19] S. Park, V. Sahleh and S.-Y. Jung, "A system dynamics computer model to assess the effects of developing an alternate water source on water supply systems management," *Procedia Engineering,* pp. 609-735, 2015.

[20] J. Duggan, "An Introduction to System Dynamics," p. 15, 15 06 2016.

[21] A. Niazi, S. O. Prasher, J. Adamowski and T. Gleeson, "A System Dynamics Model to Conserve Arid Region Water Resources through Aquifer Storage and Recovery in Conjunction with a Dam," *Water,* 7 August 2014.

[22] M. A. Brdys and R. Langowski, "Interval Estimator for Chlorine Monitoring in Drinking Water Distribution System Dyanamics, Inputs and State Measurement Errors," pp. 85-90, 2007.

[23] W. C. d. Araujo, K. P. Esquerre and O. Sahin, "Building a System Dynamics Model to SupportWater Management: A Case Study of the Semiarid Region in the Brazilian Northeast," *Water,* vol. 11, p. 2513, 2019.

JDFEWS 5 (2): 56 - 64, 2024
ISSN 2709-4529

8 Authors

Motsi Matlakala is a PhD candidate in Mechanical Engineering at the University of Johannesburg. He is registered with ECSA as a Professional Engineering Technologist. Mr. Matlakala is working as a Lecturer at the University of Johannesburg (UJ). He is a reviewer for SAIIE Conferences, the International Water Association and the MDPI Journal

Shelly Mona is currently a Deputy Director at Product Development Technology Station (PDTS): CUT, Free State. She is currently studying for a PhD in Industrial Engineering at UJ. She later specialized in Industrial Engineering and Management and obtained a master's degree in engineering management from TUT. She is registered with ECSA as a Professional Engineering Technologist and a member of SAIIE.

Journal of Digital Food, Energy & Water Systems [JD-FEWS]

JDFEWS 5 (2): 65 - 82, 2024
ISSN 2709-4529

Predictive simulation of groundwater contamination due to landfill leachate: A case study on the Robinson Deep Landfill, Johannesburg, South Africa

Osman Abdullahi OSMAN
[1]Department of Civil Engineering, Vaal University of Technology, South Africa
othmanaom@gmail.com

George Mathews OCHIENG
[1]Department of Civil Engineering, Vaal University of Technology, South Africa

Sophia RWANGA
[2]University of Johannesburg, Department of Civil Engineering, South Africa

Received: 15 November 2024
Review: 11 December 2024
Accepted: 13 December 2024
Published: 16 December 2024

Abstract - Groundwater contamination from municipal solid waste landfills is a global issue, including in South Africa. The Robinson Deep landfill (RDL) in Johannesburg needs more leachate collection and handling facilities, has a shallow groundwater table, and no groundwater quality forecast tool. This situation poses a risk of groundwater contamination. This study aimed to construct groundwater flow and contaminant transport models to predict contamination from leachate migration at RDL. Visual MODFLOW Flex (VMOD-Flex) software was used for model construction and verification. Heavy metal concentration observations of Aluminium (Al), Cadmium (Cd), Manganese (Mn), and Lead (Pb) from boreholes BH-1, BH-2, BH-3, and BH-H near the RDL were used to calibrate and validate the contaminant transport model (CTM). The result of the CTM predictive simulations for 2030 show that Mn and Pb concentrations in the BH-H groundwater could reach 4.28 mg/L and 6.85 mg/L, respectively, exceeding permissible limits of 0.01 mg/L for Pb and 0.4 mg/L for Mn. The simulations indicate that the RDL threatens groundwater quality, especially in the northern areas of the landfill. Based on these findings, a recommendation is made for future studies on assessing and modelling groundwater quality to focus on areas where increased concentrations of Pb and Mn are predicted. Further, it is recommended that precautionary preventive measures be implemented to mitigate possible contamination of groundwater in the northern areas of the landfill.

Keywords: *Predictive simulation, groundwater contamination, transport modelling, landfill leachate, Robinson Deep landfill.*

Journal of Digital Food, Energy & Water Systems [JD-FEWS]

JDFEWS 5 (2): 65 - 82, 2024
ISSN 2709-4529

1. Introduction

Groundwater is a globally valued commodity hidden from human eyesight. This invaluable resource only sometimes gets the requisite protection it deserves comparable to its usefulness to human needs [1]. Groundwater contamination has been reported in every global community, from the most developed nations, such as Norway and Switzerland [2], to the least developed countries [3][4]. Although groundwater contamination occurs due to different natural and anthropogenic factors, contamination in the proximity of municipal solid waste landfills (MSWLFs) has been reported in South Africa [5][6][7][8][9][10]; and many parts of the world [2][3][11][12][13][14]. MSWLFs release a liquid waste called 'leachate' that is 'leachate' rich in heavy metals and other emerging contaminants such as Polychlorinated Biphenyls [14]. The stated contaminants are due to a combined effect and presence of soil moisture, rainwater infiltration, groundwater seepage, surface water penetration, low pH in early landfill stages, and biochemical and biomechanical waste degradation [15]. The situation necessitates understanding groundwater flow through modelling systems, monitoring, and implementing protective measures to safeguard this invaluable resource from contamination.

Generally, a model is a simplified representation of a real system, a portion of the complex natural world. Models assist in understanding systems and evaluating management scenarios that cannot be tested in full-scale format [16]. Like any other model, a groundwater model is a simplified version of complex reality, and it simulates spatial and temporal properties of a real groundwater system or one of its parts physically (for example, laboratory sand tank) or mathematically [16][17]. A mathematical groundwater flow model describes the physical processes and boundary conditions of a particular groundwater flow problem, which can be solved deterministically using either an analytical approach if the problem is simple or numerical approaches capable of solving more complex groundwater flow problems [18]. Numerical methods are the best choice for approximate solutions for groundwater flow and contaminant transport problems [19]. According to Kumar [20], the finite difference method (FDM) based numerical models have prevailed in the hydrogeological practice in both academia and industry, and the most prominent FDM-based groundwater modelling program is the modular three-dimensional finite-difference groundwater flow model (MODFLOW) [21]. [22] used MODFLOW and the parameter estimation tool (PEST [23]) within the graphical user interface Visual MODFLOW to construct and calibrate groundwater flow models of a large area in central Limpopo, South Africa. [24] used the multispecies transport model (MT3DMS [25]) to model the groundwater quality of the Atlantis aquifer near Cape Town, South Africa. [26] used MT3DMS to simulate contaminant transport at a sewage farm in Tamil Nadu, India. Both studies [24] and [26] used MODFLOW, MT3DMS, and PEST to construct, calibrate, validate, and perform predictive simulations with their groundwater flow and transport models.

In previous studies of the Robinson Deep landfill (RDL), [8] identified that groundwater monitoring boreholes of the RDL showed higher concentrations of contaminants, including several types of flame retardants. [27], a study of the RDL reports a need for a formally installed landfill liner system at the base of the RDL. [5] and [8] reported that in the case of the RDL, a geosynthetic clay liner system was installed, covering only a portion of the landfill site. From the findings of previous studies on the RDL, it can be inferred that the groundwater beneath the RDL is vulnerable to contamination. [28] corroborated these findings that groundwater beneath the RDL is vulnerable to contamination due to the shallow water table and a lack of groundwater quality forecast tools that can be utilised to develop a proper groundwater management and protection schedule for the RDL and its impacted areas.

From the preceding, it is evident that urgent measures must be implemented to protect groundwater resources in the RDL and its proximate area. In this regard, we opted for this study to apply current technology as a tool to assess groundwater conditions at the RDL. Given the importance and effectiveness of numerical groundwater flow and transport models, groundwater flow and contaminant transport models were set up for the RDL and its proximate area using Visual MODFLOW Flex-8.

This study aims to establish a calibrated groundwater flow and contaminant transport model for the RDL area to predict groundwater quality in and around the RDL. The study's findings may support the landfill's post-closure care so that landfill managers and the government can ensure that this landfill safely stabilises without damaging groundwater quality.

Journal of Digital Food, Energy & Water Systems [JD-FEWS]

JDFEWS 5 (2): 65 - 82, 2024
ISSN 2709-4529

2. Methodology

2.1. Study area description

The study area (RDL and its proximity) is in Johannesburg South, Gauteng Province, South Africa (Figure 1). It encloses an area of 10.08 km^2 that falls under the geographic coordinates of -26.229385S, 28.020817E, and -26.260264S, 28.051153E (Datum: WGS 84).

According to the Johannesburg hydrogeology map, the RDL is in sandy-loam-sandy-clay-loam soil type [29]. The location implies that the area may have slower groundwater movement. In addition, geological maps, including the Geology of Johannesburg, Geological Series-West Rand 2626, Geological Series-East Rand 2628, and the Simplified Geological Map of South Africa and the Kingdoms of Lesotho and Swaziland [30][31][32][33] show some areas where rocks belonging to the Wit-Waters-Rand supergroup are exposed to the surface. These areas may allow a reduced groundwater recharge rate owing to the need for secondary porosity.

The aquifer systems in the study area consist of a shallow Karoo aquifer, a deep Karoo aquifer, and a deeper Wit-Waters-Rand aquifer. The shallow aquifer is considered unconfined to confined; the deep aquifer is confined [34]. Deep and confined aquifers tend to be protected against leachate plumes that migrate from Municipal Solid Waste Landfills (MSWLs). In addition, it is likely that shallow and deep aquifers exchange contaminants if hydraulically connected [35].

This study aimed to construct groundwater flow and contaminant transport models to predict groundwater contamination due to leachate migration from the RDL. The materials and methods are described in the next section.

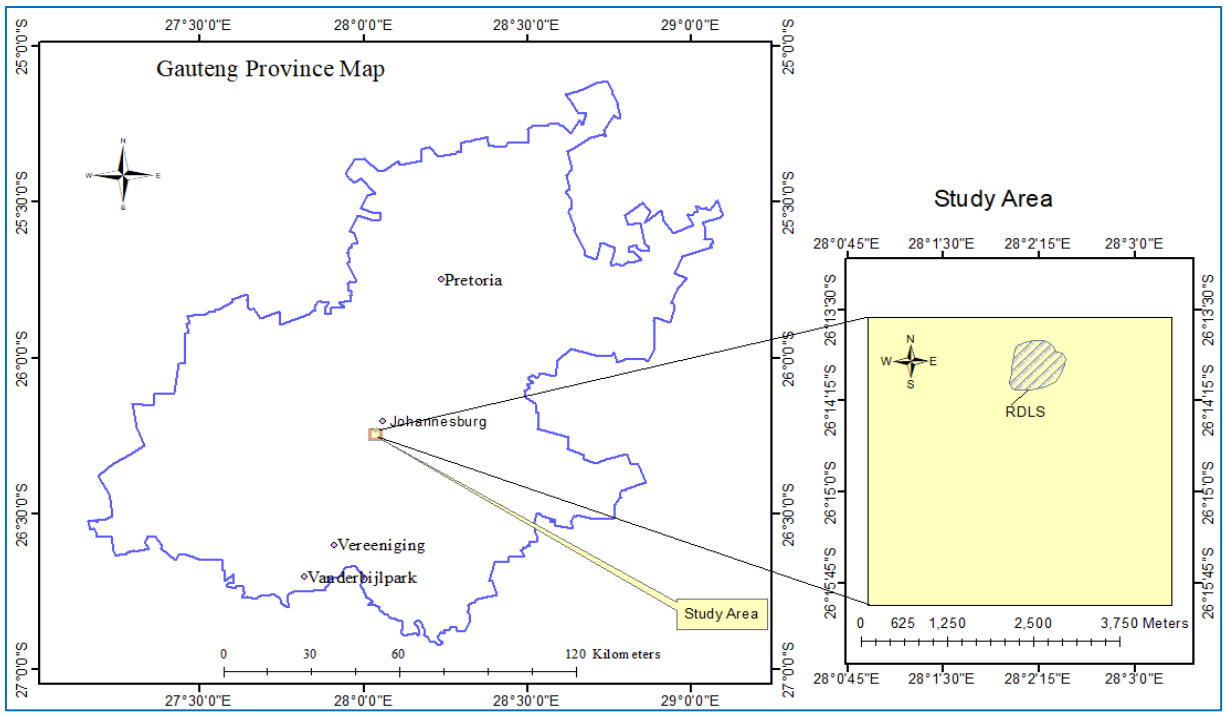

Fig. 1: Location of study area (author)

2.2. Groundwater flow model construction

Groundwater flow (hereafter flow) modelling of the RDL site was performed using Visual MODFLOW Flex Version 8 (VMOD Flex) [36]. The MODFLOW-NWT [37] numerical engine was used to solve the general

JDFEWS 5 (2): 65 - 82, 2024
ISSN 2709-4529

governing equations of the groundwater flow problems. The conceptual modelling approach translated multiple numerical models from a single conceptual model.

2.2.1. Model set up

The extent of the model domain was set to 2800 m × 3600 m × 40 m in the X, Y, and Z dimensions, respectively. The grid discretisation used was a MODFLOW finite difference grid of 144 rows and 112 columns, resulting in 16128 active model cells with a grid spacing of 25 m along the rows and 25 m along the columns. Based on the studies [34][38] and borehole lithology data obtained from the Department of Water and Sanitation (DWS), the thickness of the model domain was set to 40 m comprising three hydrogeological units: sandy loam, sandy clay loam, and fractured rocks—initially, the flow model comprised of the three hydrogeological units mentioned above. However, owing to variations in the groundwater heads in the cells of layer one, the initial heads of some cells in layer one fell below the bottom. MODFLOW-2005 and its Newton–Raphson formulation do not accept that the initial head surface is lower than the bottom of layer one. Therefore, we merged layers one and two into a single layer with reasonably averaged hydraulic properties.

2.2.2. Input parameters and boundary conditions

Input parameters for the flow model consisted of longitudinal, transverse, and vertical hydraulic conductivities (Kx, Ky, and Kz), specific storage (Ss), specific yield (Sy), total porosity (Tp), effective porosity (Ep), and boundary and initial conditions. The flow model contained three boundary conditions and one initial condition: constant Head (CHD), no flow, recharge boundary condition, and initial head condition. The flow model input parameter values and the boundary and initial conditions are listed in Table 1.

Table 1. Flow model input parameters and boundary conditions.

Input parameters	**Parameter value**		**Sources**	
	Layer one	Layer two		
Kx	3.64 x10^{-6} m/s to 1.23 x10^{-5} m/s	9.838 x10^{-6} m/s	[38][39] and borehole lithology	
Ky	3.64 x10^{-6} m/s to 1.23 x10^{-5} m/s	9.838 x10^{-6} m/s	Ky = Kx	
Kz	3.64 x10^{-6} m/s to 1.23 x10^{-5} m/s	9.838 x10^{-7} m/s	Kz = 0.1 x Kx	
Ss	0.0059167 m^{-1} to 0.0265 m^{-1}	0.0065 m^{-1}	Estimated from other parameters	
Sy	0.1065 to 0.053	0.13 or 13%	Estimated parameter	
Tp	0.3 to 0.33	0.18	[38][39]	
Ep	0.25 to 0.26	0.14	[38][39]	
Simulation time in days		9855 days starting from 01/01/1998 to 01/01/2025		
Boundary conditions	CHD	Northern, Southern, and Eastern sides	Same as layer one	Estimated based on initial heads and topography
	No flow	Western and Bottom boundaries	Same as layer one	Assumed
	Recharge	53 to 60 mm annually	Model top	[34]
Initial head condition		Interpolated from water level data obtained from DWS		
Ground surface/model top		Created from the 30 m Shuttle Radar Topography Mission (SRTM) Global DEM from USGS		

JDFEWS 5 (2): 65 - 82, 2024
ISSN 2709-4529

2.2.3. Sensitivity analysis

Sensitivity analysis (SA) is often performed before calibrating and validating the groundwater flow model. In this study, the flow model input parameters and boundary heads were individually increased or decreased to evaluate which parameters significantly impacted the model output (sensitive parameters) and which parameters had no impact on the model output (non-sensitive parameters). Parameter Estimation software (PEST) [23] Version 12.3.1, a VMOD-Flex software component, was used to determine the sensitive parameters of the flow model. Several flow simulation runs were conducted using MODFLOW-NWT with an upstream weighting package (UPW). Then, the sensitive parameters were used in the calibration process of the groundwater flow model.

2.2.4. Calibration and validation

The flow model was calibrated to ensure that the model used for the simulations accurately represented the actual site conditions and produced reasonable results. The most sensitive parameters identified in the sensitivity analysis were used to calibrate the flow model.

Groundwater head and concentration observation data obtained from the DWS were utilised in the calibration process. The borehole data obtained from the DWS contained no production (sink) or injection (source) wells in the model domain. Therefore, there was no well boundary condition defined for the flow model. However, seven observation boreholes recorded water level data on two dates. The seven groundwater level observations listed in Table 2 are the only head observations available in the study area of 10.08 km^2. The head measurements (Gs_5 to Gs_{12}) were used to calibrate the flow model, and (BH-1 and BH-2) were used to validate the flow model.

Table 2. Groundwater head observations used for calibration and validation.

Well Id	X-Coordinate	Y-Coordinate	Elevation (m)	Well bottom	Logger Id	Logger Elevation	Observation time (day)	Observed Head (m)
Gs_5	604294.5667	7098455.676	1708	1680	L5	1688	1095.00	1697.8
Gs_8	603222.4399	7096925.736	1730	1665	L8	1700.4	1095.00	1710.4
Gs_9	603922.1007	7096982.165	1739	1719	L9	1721.2	1095.00	1729.2
Gs_{10}	604141.0464	7098247.565	1707	1687	L10	1689	1095.00	1697
Gs_{12}	603785.2067	7097100.675	1735	1605	L12	1698.69	1095.00	1721.76
BH-1	603754.4359	7097710.576	1715	1695	A1	1700	8907.00	1708.5
BH-2	603096.2822	7097941.353	1708	1688	A2	1690.2	8907.00	1698.2

Source: Wells Gs_5-Gs_{12} (DWS); BH-1 and BH-2 [40].

2.3. Contaminant transport model construction

Contaminant transport modelling of the RDL was conducted using numerical engines built within the software VMOD-Flex-8, such as the MT3DMS. Using the software's graphical user interface (GUI), the output data of the MODFLOW-NWT (flow model) were incorporated into the construction of the contaminant transport model (CTM). The developed CTM was an advection-dispersion-dominated model with no retardation (sorption) or reaction.

JDFEWS 5 (2): 65 - 82, 2024
ISSN 2709-4529

2.3.1 Input parameters and boundary conditions

A constant concentration boundary condition was assigned to add a contaminant source as a point source where the heavy metals measured in the study of [40] continuously percolate from the RDL. Table 3 lists the input parameters, boundary conditions, and initial conditions for the transport model.

Table 3. Transport model input parameters.

Model parameters		Unit	Value
Bulk densities for layers one and two [39].	Sandy loam-sandy clay loam	Kg/m^3	1600
	Fractured sandy shale-		2600
Effective porosity (Ep) [39].	Layer one	--	0.25
	Layer two		0.14
Longitudinal dispersivity [41]. α_L	Layer one	m	7
	Layer two		2
Transverse dispersivity α_{TH} and α_{TV}	Layer one	m	α_{TH}/α_L=0.1 α_{TV}/α_L=0.01
	Layer two		
Source concentrations of the CTM species are assigned as a constant concentration boundary [40].	Aluminium (Al)	mg/L	1.49
	Cadmium (Cd)		0.00141
	Manganese (Mn)		10
	Lead (Pb)		16.6
Initial condition/initial concentrations	Applied to the whole model	mg/L	0

2.3.2. Calibration and validation

Eight concentrations of BH-2 and BH-H (Table 4) were used to calibrate the transport model. The calibration parameters used were longitudinal and transverse dispersivities, which were manually determined because the VMOD Flex-8 does not support the automatic calibration of any transport parameters.

The observed concentrations of BH-1 and BH-3 listed in Table 4 were compared to their simulated counterparts to validate the CTM. The CTM validation run contained the original unaltered calibrated validated flow model and the calibrated transport model. The concentration observations of BH-1, BH-2, and BH-3 were collected by [40]. In contrast, the observations of the BH-H were downloaded from the DWS's National Groundwater Archive (NGA).

JDFEWS 5 (2): 65 - 82, 2024
ISSN 2709-4529

Table 4. Heavy metal concentration observations used for CTM calibration and validation.

Well Id	X (m)	Y (m)	Elevation (m)	Well bottom	Logger Id	Logger Z	Chemical	Observation Time (day)	Concentration (mg/L)
BH-1	603754.43	7097710.5	1715	1695	A1	1700	Al	8907	0.00141
BH-1	603754.43	7097710.5	1715	1695	A1	1700	Cd	8907	0.00141
BH-1	603754.43	7097710.5	1715	1695	A1	1700	Pb	8907	5
BH-1	603754.43	7097710.5	1715	1695	A1	1700	Mn	8907	9.4
BH-2	603096.28	7097941.3	1708	1688	A2	1690.2	Al	8907	0.00141
BH-2	603096.28	7097941.3	1708	1688	A2	1690.2	Cd	8907	0.00141
BH-2	603096.28	7097941.3	1708	1688	A2	1690.2	Pb	8907	3.23
BH-2	603096.28	7097941.3	1708	1688	A2	1690.2	Mn	8907	2.7
BH-3	604960.51	7095096.9	1778	1741	A3	1747	Al	8907	0.00141
BH-3	604960.51	7095096.9	1778	1741	A3	1747	Mn	8907	0.0707
BH-3	604960.51	7095096.9	1778	1741	A3	1747	Pb	8907	0.65
BH-3	604960.51	7095096.9	1778	1741	A3	1747	Cd	8907	0.00141
BH-H	604158.51	7098456.5	1708	1680	A-H	1684	Al	553.5	0.048
BH-H	604158.51	7098456.5	1708	1680	A-H	1684	Mn	553.5	3.254
BH-H	604158.51	7098456.5	1708	1680	A-H	1684	Pb	553.5	0.008
BH-H	604158.51	7098456.5	1708	1680	A-H	1684	Cd	553.5	0.005

Source: BH-1, BH-2, and BH-3 [40]; BH-H (DWS).

The residuals between the observed and simulated head and concentration values were used to calculate the calibration and validation statistics [42][43] such as (i) Mean Error (ME), (ii) Root Mean Square Error (RMS), and (iii) normalised root mean squared error (NRMS), as indicated in the following equations:

$$\mathrm{ME} = \frac{1}{n}\sum_{i=1}^{n}(Xo - Xs)i \qquad 1$$

Where;
ME is the mean of the difference between the observed value (Xo) and the simulated value (Xs).
n is the number of calibration or validation measurements

$$\mathrm{RMS} = \left[\frac{1}{n}\sum_{i=1}^{n}(Xo - Xs)i^2\right]^{0.5} \qquad 2$$

Where;
RMS is the square root of the average squared difference between (Xo) and (Xs)

$$\mathrm{NRMS} = \frac{\mathrm{RMS}}{(Xo)max - (Xo)min} \qquad 3$$

JDFEWS 5 (2): 65 - 82, 2024
ISSN 2709-4529

After the groundwater flow and transport models passed the calibration and validation criteria of a normalised root mean squared error of ≤ 10% [43], the CTM was used to perform predictive simulations to forecast the concentrations of Al, Cd, Mn, and Pb in the groundwater for a simulation period of 11680 days, which corresponds to the period between the start date of the simulation (January 1, 1998) to January 1, 2030.

3. Results and Discussion

3.1 Results

The developed groundwater flow model comprised three horizontal surfaces converted into two structural or property zones, representing the two model layers (Figure 2). The initial description of the hydraulic conductivity for layer one, as shown in Table 1, was based on [38] and [39] findings, which align with the borehole lithology data obtained from the DWS. Then, nine hydraulic conductivity zones were created using the available borehole log data and with the help of the kriging interpolation tool of the VMOD-Flex-8. Zone-based hydraulic conductivities (Figure 3) were preferred to better represent the study area's aquifer characteristics.

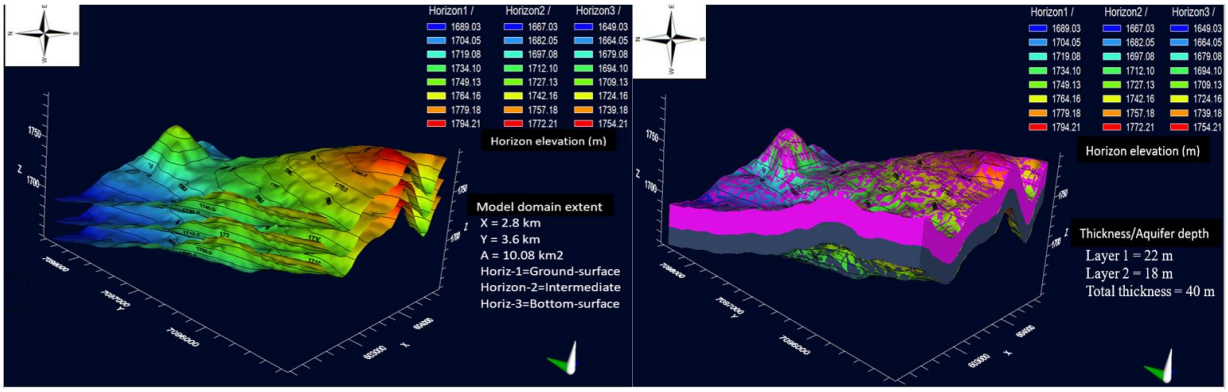

Fig. 2 a): Flow model layer surfaces, **b):** Thickness of the model layers (author).

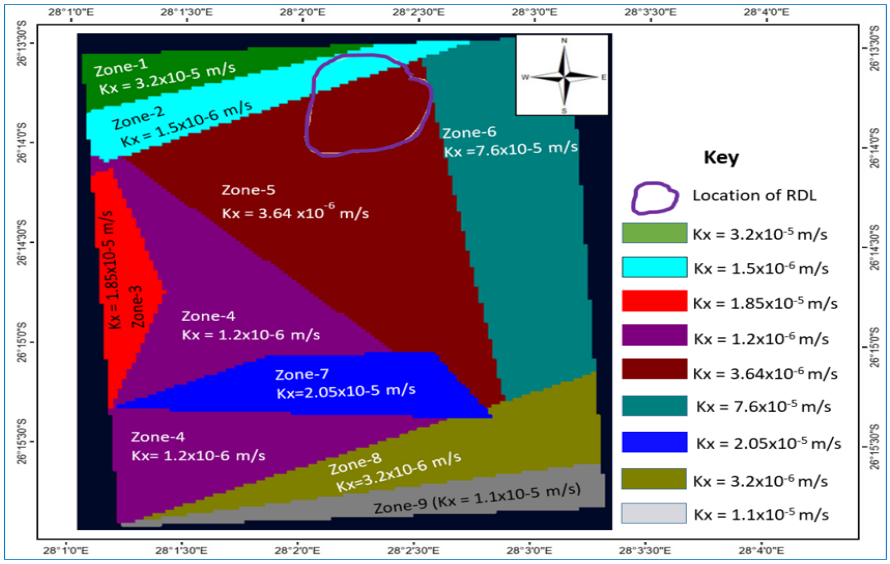

Fig. 3: Zone-based hydraulic conductivities (author).

Journal of Digital Food, Energy & Water Systems [JD-FEWS]

JDFEWS 5 (2): 65 - 82, 2024
ISSN 2709-4529

Regarding the developed CTM, the flow model grid was refined to focus more on the anticipated contaminant source (RDL). Some studies followed similar flow and transport model construction procedures, such as the study of [24] on modelling the Atlantis aquifer of the industrial town of Atlantis, South Africa, and the study of [26] on contaminant transport modelling of a sewage farm located in south Madurai, Tamil Nadu, India.

3.1.1 Sensitivity analysis

Flow model

A parameter sensitivity analysis was performed before model calibration to determine the sensitive parameters to be included in the model calibration process. In the sensitivity analysis, the effect of adjusting the flow model input parameters, such as hydraulic conductivity components, on the match or goodness of fit between the simulated and observed heads was quantified using the PEST component of the VMOD-Flex-8. The measurement of the sensitivity analysis was based on calculating the ratio of the percentage change in output values divided by the percentage change in input values. In this case, it was found that the horizontal (Kx) and vertical (Kz) hydraulic conductivities were influential parameters in the match between the simulated and observed heads; hence, the model was sensitive to these input parameters. A total of 72 pilot points of Kx and Kz (36 pilot points and one parameter group for each) were defined with fixed hydraulic conductivity values deduced from borehole lithology data obtained from the DWS. The pilot points were spatial points in which the initial parameter values were specified, and the PEST software iteratively estimated the best hydraulic conductivity values based on these designated points (Figure 4). The X-axis shows the parameter group (pg) and pilot-point numbers from pg1-1 to pg2-72, whereas the Y-axis shows the parameter sensitivity coefficients. The pilot-point approach to describing aquifer characteristics often outperforms the zonation technique [44]. However, the zonation technique is more reliable than assigning a single parameter value to an entire aquifer system that can be abruptly heterogeneous.

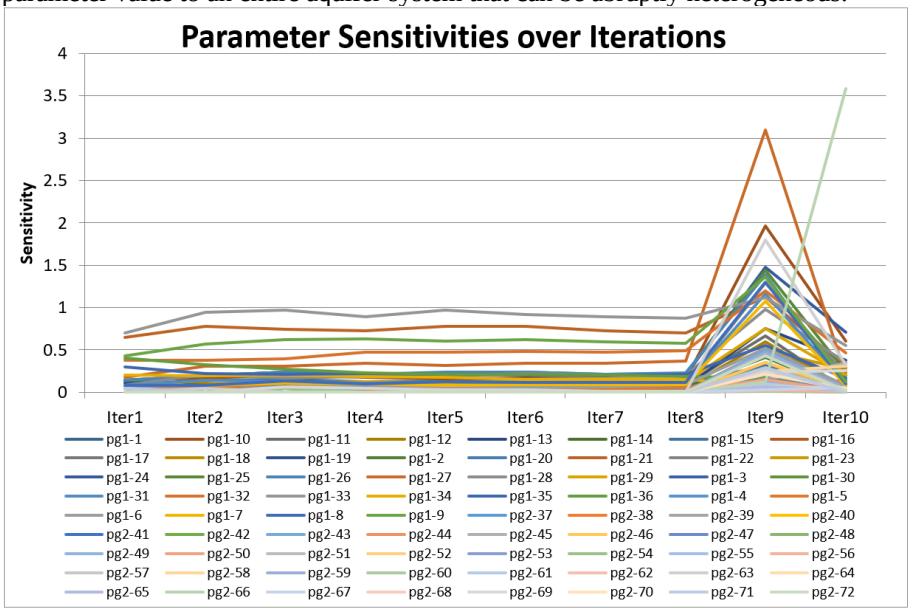

Fig. 4: Kx and Kz pilot-point sensitivities generated by PEST software.

Transport model

Because the automated parameter estimation software (PEST) was not supported in the VMOD-Flex-8 for estimating the transport parameters, manually determining the transport model's sensitive parameters was inevitable. By trial and error, it was found that longitudinal and transverse (horizontal transverse and vertical transverse)

JDFEWS 5 (2): 65 - 82, 2024
ISSN 2709-4529

dispersivities were the important influential parameters for calibrating the contaminant transport model. This indicates that these dispersivity parameters are important in predicting the spread of contaminants in groundwater.

3.1.2. Calibration and validation

Flow model

To objectively quantify the goodness-of-fit between the simulated and observed heads, model calibration statistics (calibration criteria), such as the mean error (ME) of the estimates described in equation (1), the root mean squared error (RMS) equation (2), and the normalised root mean squared error (NRMS) equation (3), were calculated. The steady-state groundwater flow model was calibrated against the five head observation wells in Table 2. The calibration result (Figure 5) was considered acceptable according to the commonly used model calibration criterion of an NRMS of less than or equal to 10% [43].

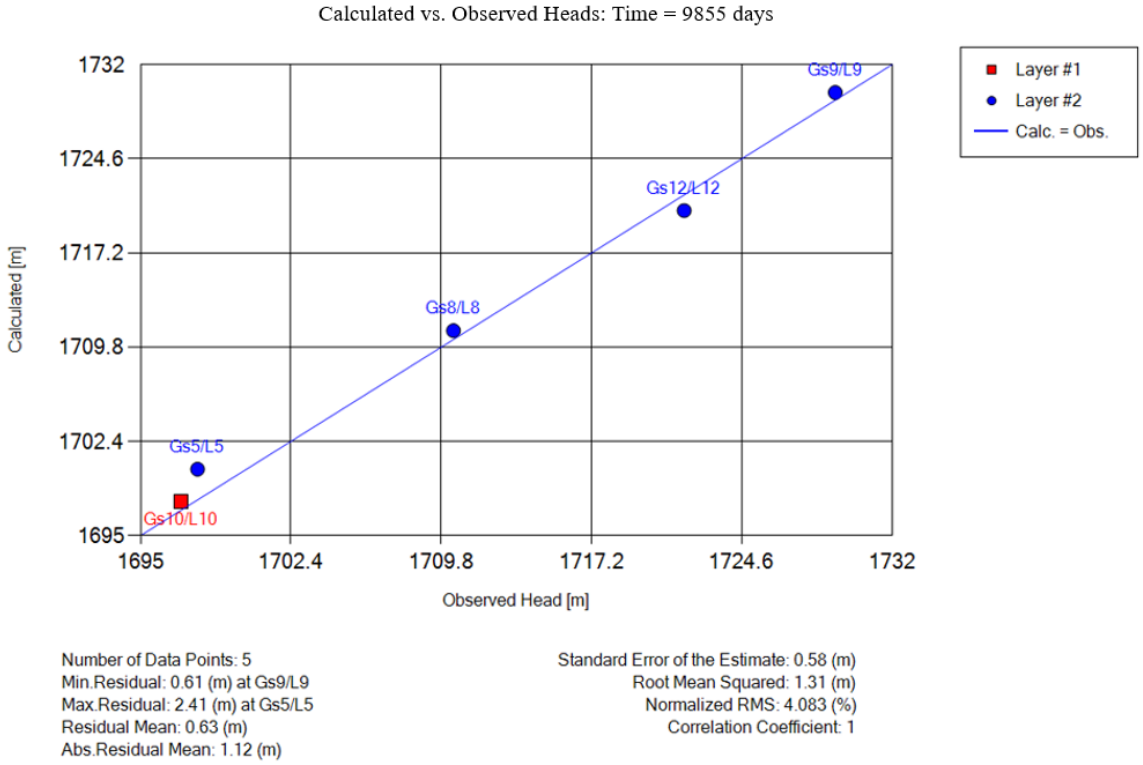

Fig. 5: Calibration curve between calculated and observed heads.

Head observations BH-1 and BH-2 (Table 2), measured on May 24 2022, were used to validate the groundwater flow model. The study performed this measurement using a Solinst TLC meter model 107 (Solinst Canada Ltd) by the study [40].

Validating the groundwater flow model followed the same criteria as the model calibration, requiring an NRMS of less than or equal to 10% [42][43]. The calibrated flow model was validated against the two head observations (BH-1 and BH-2) without adjusting a single flow model parameter because this makes the model uncalibrated. The result of flow model validation is presented in Table 5.

JDFEWS 5 (2): 65 - 82, 2024
ISSN 2709-4529

Table 5. Flow model validation statistics.

Criteria	Results
Number of observations	2
Minimum residual	0 m
Maximum residual	5.25 m
Residual mean	2.62 m
Absolute residual	2.63 m
Standard error	1.25 m
Root mean squared error	3.71 m
Normalised root mean squared error	0.22%
Correlation coefficient	1

Although the number of data points (observations) used is small, the flow model validation statistics presented in Table 5 indicate that the model has high accuracy and reliability.

Transport model

To calibrate the CTM, initial parameter values for longitudinal, horizontal transverse, and vertical transverse dispersivities for model layer one were set at 5m, 0.5m, and 0.05m, respectively, and 2m, 0.2m, and 0.02m for the dispersivities, of layer two respectively. The CTM calibration parameters were adjusted manually more than 50 times better to match the heavy metals' simulated and observed concentrations. The concentration observations BH-2 and BH-H containing eight measurements of Al, Cd, Mn, and Pb were used to calibrate the transport model. Only four concentration observation points were available in the study area, each containing four concentration measurements. Two observation points (BH-2 and BH-H) were used for calibration, and the other (BH-1 and BH-3) for validation.

The transport model was run for a simulation period of 9125 days (25 years) with transport steps of 1, 365, 1500, 3000, 7000, and 9125 days. The PEST tool uses the concentration residuals (Table 6a) to calculate the calibration objective function phi (Φ), the sum of the weighted, squared, and simulated-to-observed concentration discrepancies. The transport model calibration criteria were satisfied; the results are listed in Table 6b.

Table 6a. Concentration residuals.

Observation point	Parameter	Observed (mg/L)	Simulated (mg/L)	Residuals (mg/L)
BH-2	Al	0.00141	0.0865	0.08509
	Cd	0.00141	0.001	-0.00041
	Mn	2.7	2.809	0.109
	Pb	3.23	3.2	-0.03
BH-H	Al	0.048	0.05	0.002
	Cd	0.005	0.0043	-0.0007
	Mn	3.254	2.264	-0.99
	Pb	0.008	0.0077	-0.0003

JDFEWS 5 (2): 65 - 82, 2024
ISSN 2709-4529

Table 6b. Transport model calibration statistics.

Criteria	Results
Number of observations	8
Minimum residual	0.0003 mg/L
Maximum residual	-0.99 mg/L
Residual mean	-0.103 mg/L
Absolute residual	1.2175mg/L
Standard error	0.67 mg/L
Root mean squared error	0.292 mg/L
Normalised root mean squared error	8.977%
Correlation coefficient	0.97

A new set of concentration observations is required to validate the transport model. Borehole one (BH-1) and borehole three (BH-3) concentration observations were used to validate the CTM. Transport model validation (verification) followed the same criteria as the model calibration, requiring the NRMS to be less than or equal to 10%. Table 7 presents the result of the CTM validation.

Table 7. Transport model validation statistics.

Criteria	Results
Number of observations	8
Minimum residual	0 mg/L
Maximum residual	5.62 mg/L
Residual mean	0.34 mg/L
Absolute residual	1.09 mg/L
Standard error	0.81 mg/L
Root mean squared error	2.16 mg/L
Normalised root mean squared error	9.98%
Correlation coefficient	0.91

3.2. Discussion of the Results

The developed groundwater flow and transport models met their calibration and validation criteria [25][42][43]. Therefore, these models are reliable and effective in predicting groundwater contamination in the study area.

The transport simulation period of 9125 days, starting from January 1, 1998, accommodated April 20, 1999, metal concentration observations used for CTM calibration and May 24, 2022, observations used for CTM validation. Notably, the 1999 groundwater quality observation was the only relevant historical observation available in the NGA. The results of the transport simulation showed that the heavy metal plume migration from the RDL was slow and reached the observation boreholes on day 7000 (Figure 6a). Notably, this study assumed that the model domain was initially free from heavy metal contamination and that the landfill started leaking heavy metals at the start of the simulation period. On day 7000, the leachate plume reached BH-2 and moved in the northern direction of BH-H. On day 9125, corresponding to January 1, 2023, a plume containing Mn and Pb concentrations of 4.28 mg/L and 6.85 mg/L crossed the model boundary in the northern direction of the RDL. The simulation result of the heavy metal concentrations is in line with the findings of [40], which indicated a possibility of leachate plume migration towards these boreholes. Though the study of [40] used the same observation points as shown in Figure 6b, that study aimed to assess the spatial correlation between groundwater quality of boreholes (BH-1, BH-2, BH-3, and BH-H) in terms of heavy metal concentration and the distance to the RDL.

Journal of Digital Food, Energy & Water Systems [JD-FEWS]

JDFEWS 5 (2): 65 - 82, 2024
ISSN 2709-4529

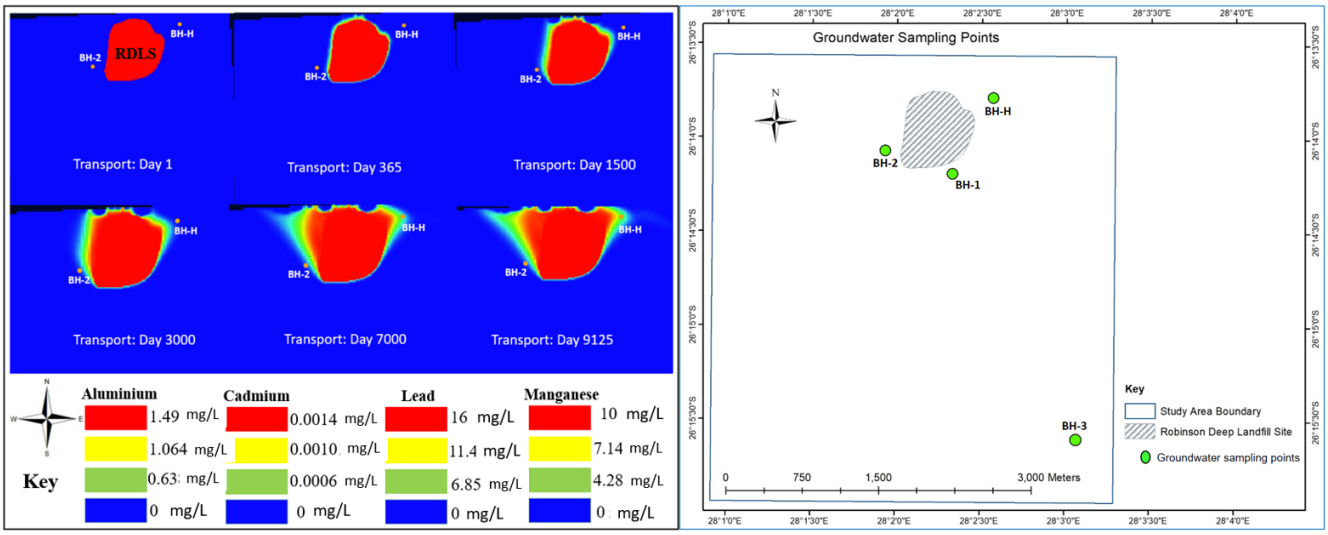

Fig. 6a): Plume migration from day 1 to day 9125, **b):** Observation points [40].

Both the simulated concentrations of Mn and Pb in the groundwater of the boreholes (BH-1, BH-2, BH-3, and BH-H) and the heavy metal concentrations measured by [40] exceed the local water quality guidelines such as the Department of Water Affairs and Forestry [45], the South African National Standards (SANS) for drinking water quality guidelines [46], and international guidelines such as the World Health Organization [47]. As a result, it is evident that the RDL currently threatens groundwater quality in the study area, particularly in areas north of the RDL. Notably, the RDL operates under several permits and licenses required under various South African Environmental laws. The landfill managing company, Pikitup, must submit groundwater monitoring data twice a year to the Department of Water and Sanitation.

The area in the southern direction of the RDL is likely not affected by groundwater contamination due to a leachate plume that comes from the RDL. This is because the southern direction of the RDL is generally upgradient and opposes the direction of the groundwater flow in the study area; moreover, the CTM showed that the dominant transport mechanism in the study area is advection, and mass transport by dispersion has a minimum effect unless a simulation period of more than a century is forecasted. In this study, mass transport by dispersion could not overcome the dominant transport, which is advective transport driven by the bulk motion of flowing groundwater.

The calibrated validated CTM was run one last time for a simulation period of 11,680 days. This simulation period corresponds to 32 years from 01/01/1998 to 01/01/2030, and it was intended to predict how the plume of contaminants from the RDL spreads and the resulting groundwater contamination. The predictive simulation showed that a plume of contaminated groundwater from the RDL spreads toward the BH-H. According to the result of the predictive simulation, the leachate plume or highly contaminated groundwater will not be able to reach boreholes BH-1 and BH-3 in the current simulation period until 2030. However, highly polluted groundwater, which has elevated concentrations of Pb and Mn, was predicted at the location of BH-H, as Figure 7 depicts.

Journal of Digital Food, Energy & Water Systems [JD-FEWS]

JDFEWS 5 (2): 65 - 82, 2024
ISSN 2709-4529

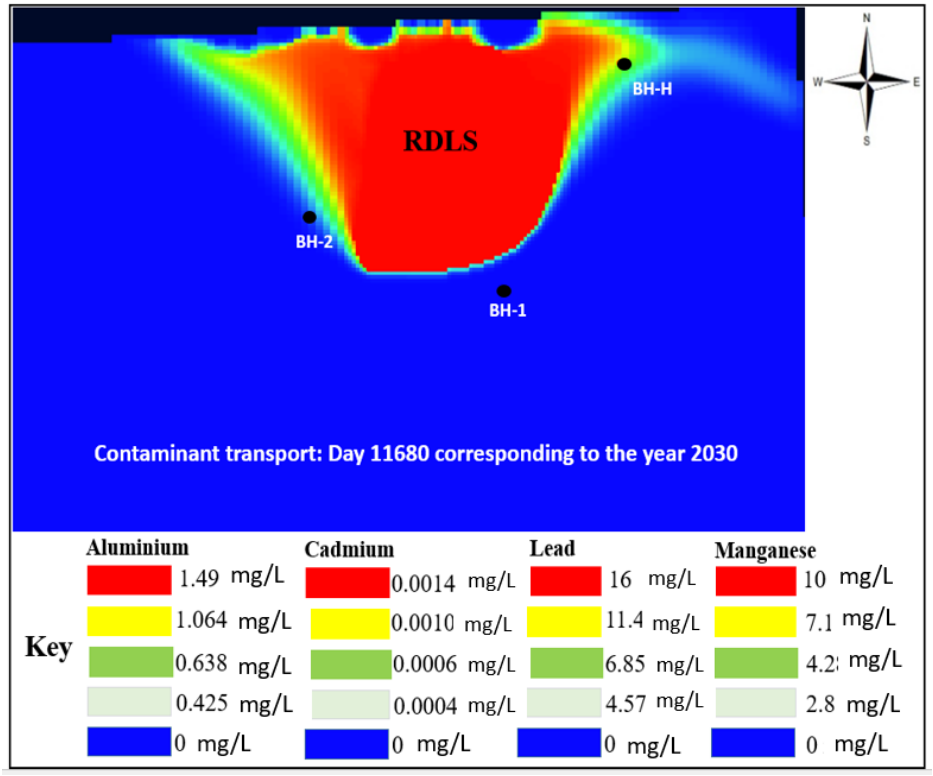

Fig. 7: Predictive simulation result showing plume spread.

The groundwater quality of the BH-H is predicted to have heavy metal concentrations of 0.638 mg/L, 0.0006 mg/L, 6.85 mg/L, and 4.2 mg/L for Al, Cd, Pb, and Mn, respectively. All other predicted concentrations at BH-H were above the permissible limit except for the Cd concentration. Figure 8 (a-d) shows predicted concentrations of the heavy metals versus the time graph of BH-H from day one, from January 1 1998 to day 11680, to January 1 2030.

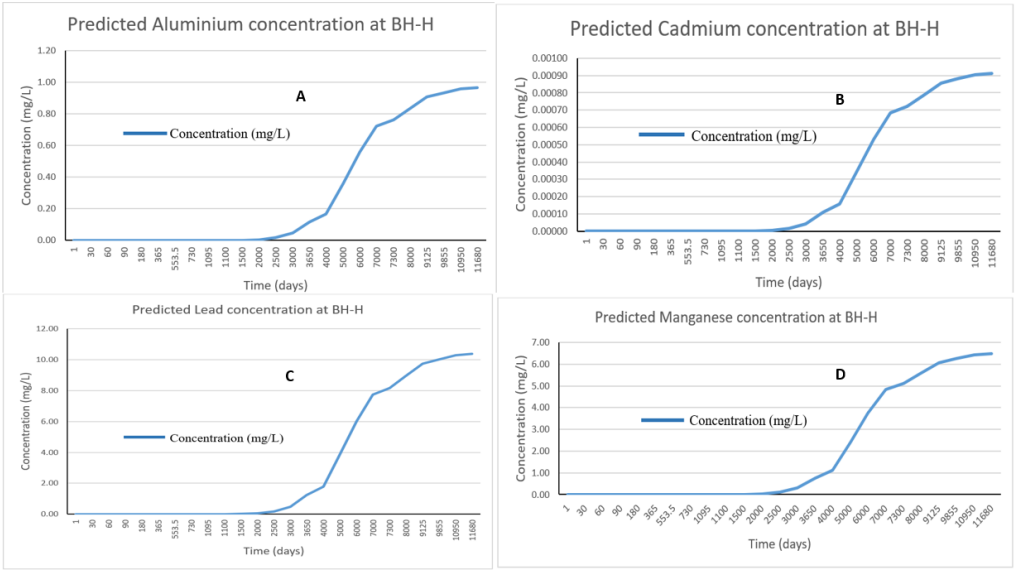

Fig. 8: Predicted heavy metal concentrations versus time graph for the BH-H.

JDFEWS 5 (2): 65 - 82, 2024
ISSN 2709-4529

Although the rate of contaminant migration in underground environments is spatially and temporally variable, the findings of this study align well with other studies on contaminant transport modelling. The studies [24] and [26] found a contaminant plume migration rate in the range of 10m to 300m per year, while the current study found a plume migration rate of 12m to 60m per year. The migration rate of heavy metals observed in this study is slow, indicating the need for long-term groundwater monitoring strategies. The developed CTM's predictive simulations highlight the potential risks of heavy metal contamination, particularly Mn and Pb, which are projected to exceed permissible limits by 2030. Furthermore, the study's emphasis on the need for post-closure care and monitoring facilities for the RDL echoes the recommendations of [9] and [10], highlighting the importance of continuous monitoring to protect groundwater from landfill-related contamination. Finally, Policymakers can utilise these findings to formulate regulations that mandate groundwater monitoring practices for landfill sites nearing closure.

4. Conclusion

The overall objective of this study was to establish a calibrated, validated groundwater flow and contaminant transport model for the Robinson Deep landfill area located in Johannesburg, South, to predict groundwater quality in and around the RDL. The transport modelling results showed that the heavy metals released at the RLD moved at 60 m/year to reach the BH-H and a rate of 12 m/year to reach BH-2. However, the leachate plume or the highly contaminated groundwater could not reach boreholes BH-1 and BH-3, and generally, the leachate leaked by the RDL did not travel southwards.

The predictive simulation shows that in 2030, the concentrations of Pb, Mn, Al, and Cd in the groundwater of the BH-H can reach up to 6.85 mg/L, 4.2 mg/L, 0.638 mg/L, and 0.0006mg/L respectively. All other predicted concentrations at BH-H were above the permissible limit except for the Cd concentration.

In summary, the results indicate that the RDL threatens the groundwater quality of its proximate areas, particularly in the northern direction of the landfill site. It is expected that the RDL will close; however, even after closure, it may adversely affect the groundwater quality of the proximate areas soon.

One of the limitations of this study was limited funding, which did not allow the research to obtain more data to cover the complexities of groundwater-leachate interactions in the study area. However, the findings of this study may support the post-closure care of the landfill site so that management can ensure that this landfill safely stabilises without damaging the groundwater. In addition, because the landfill is on the verge of closure, post-closure groundwater monitoring facilities should be installed, and future groundwater flow and transport modelling studies should focus more on the northern direction of the landfill, where the present study has predicted elevated concentrations of heavy metals. Further, it is recommended that precautionary preventive measures be implemented to mitigate possible contamination of groundwater in the northern areas of the landfill.

Declaration of competing interests

"We declare that there are no conflicts of interest to disclose."

Acknowledgements

The Vaal University of Technology is acknowledged for providing financial support and purchasing Visual MODFLOW Flex Pro.

JDFEWS 5 (2): 65 - 82, 2024
ISSN 2709-4529

References

[1] D. Sheng, X. Meng, X. Wen, J. Wu, H. Yu, and M. Wu, Contamination characteristics, source identification, and source-specific health risks of heavy metal(loid)s in groundwater of an arid oasis region in Northwest China, Sci. Total Environ. 2022;841:156733. https://doi.org/10.1016/j.scitotenv.2022.156733
[2] D. Abiriga, l. Vestgarden, H. Klempe, Groundwater contamination from a municipal landfill: effect of age, landfill closure, and season on groundwater chemistry. Sci. Total Environ. 2020;737:140307. https://doi.org/10.1016/j.scitotenv.2020.140307
[3] P. Ravenscroft, L. Lytton, Seeing the invisible: A strategic report on groundwater quality. Report no. 169674. Washington, DC: World Bank; 2022.
[4] United Nations, The United Nations World Water Development Report 2024: Water for Prosperity and Peace. UNESCO, Paris. https://doi.org/10.18356/9789210050000
[5] I.V. Sibiya, O.I. Olukunle, Okonkwo, Seasonal variations and the influence of geomembrane liners on the levels of PBDES in landfill leachates, sediment and groundwater in Gauteng Province, South Africa. Emerg. Contam. 2017;3(2):76–84. https://doi.org/10.1016/j.emcon.2017.05.002
[6] J.N. Edokpayi, O.S. Durowoju, J.O. Odiyo, Assessment of heavy metals in landfill leachate: A case study of Thohoyandou landfill, Limpopo Province, South Africa. Heavy Met. 2018;16:214–227. https://doi.org/10.5772/intechopen.74009
[7] V. Nevondo, A.P. Daso, O.J. Okonkwo, T. Malehase, Leachate seepage from landfill: a source of groundwater mercury contamination in South Africa. Water Sa. 2019;45(2):225-231. https://hdl.handle.net/10520/EJC-15974e82c8
[8] I. Sibiya, G. Poma, M. Cuykx, A. Covaci, P. Adegbenro, J. Okonkwo, Targeted and non-target screening of persistent organic pollutants and organophosphorus flame retardants in leachate and sediment from landfill sites in Gauteng Province, South Africa. Sci. Total Environ. 2019;653:1231–1239. https://doi.org/10.1016/j.scitotenv.2018.10.356
[9] R. Makhadi, S.A. Oke, O.O. Ololade, The influence of non-engineered municipal landfills on groundwater chemistry and quality in Bloemfontein, South Africa. Molecules. 2020;25(23):5599. https://doi.org/10.3390/molecules25235599
[10] S. Mepaiyeda, K. Madi, O. Gwavava, O. Baiyegunhi, Geological and geophysical assessment of groundwater contamination at the Roundhill landfill site, Berlin, Eastern Cape, South Africa. Heliyon. 2020;6(7):E04249. https://doi.org/10.1016/j.heliyon.2020.e04249
[11] T.K. Boateng, F. Opoku, O. Akoto, Heavy metal contamination assessment of groundwater quality: A case study of Oti landfill site, Kumasi. Appl. Water Sci. 2019;9:33. https://doi.org/10.1007/s13201-019-0915-y
[12] Y. El-mouine, Amal el H, Moad M, Vincent V, Hasna Y, Houria D. Groundwater contamination due to landfill leachate—A case study of Tadla Plain. Environ. Sci. Proc. 2020;16(1):53. https://doi.org/10.3390/environsciproc2022016053
[13] L. Lindamulla, Nanayakkara N, Othman M, Jinadasa S, Herath G, Jegatheesan V. Municipal solid waste landfill leachate characteristics and their treatment options in tropical countries. Curr. Pollut. Rep. 2022;8:273–287. https://doi.org/10.1007/s40726-022-00222-x
[14] A. Wdowczyk, szymańska-pulikowska A. Analysis of the possibility of conducting a comprehensive assessment of landfill leachate contamination using physicochemical indicators and toxicity test. Ecotoxicol. Environ. Saf. 2021;221:112434. https://doi.org/10.1016/j.ecoenv.2021.112434
[15] C. Teng, Chen W. Technologies for the treatment of emerging contaminants in landfill leachate. Curr. Opin. Environ. Sci. Health. 2023;31:100409. https://doi.org/10.1016/j.coesh.2022.100409
[16] M. Bakker, Post V. Analytical groundwater modelling—Theory and applications using Python. London, UK. Taylor & Francis Group; 2022.
[17] A.M. Gahala, Bristow ELD, Sharpe JB, Metcalf BG, Matson LA. Simulation of groundwater and surface-water interaction and lake resiliency at Crystal Lake, City of Crystal Lake, Illinois. Reston, VA: USGS; 2024. https://doi.org/10.3133/sir20245007
[18] C.P. Kumar, An overview of commonly used groundwater modelling software. Int. J. Adv Res. Sci. Eng. Technol. 2019; 6(1):7854-7865.
[19] C.D. Langevin, Hughes JD, Banta ER, Niswonger RG, Panday S, Provost AM. Documentation for the MODFLOW 6 groundwater flow model. Reston, VA: USGS; 2017. https://doi.org/10.3133/tm6A55
[20] C.P. Kumar, modelling of groundwater flow and data requirements. Int. J. Mod. Sci. Eng. Technol. 2015;2(2):18-27.
[21] M.G. Mcdonald, Harbaugh AW. A modular three-dimensional finite-difference groundwater flow model. USGS. Book 6, Chapter A1:586; 1988. https://doi.org/10.3133/twri06A1
[22] S. Rwanga, Ndambuki J. Solving groundwater problems fraught with uncertain recharge: An application to Central Limpopo, South Africa. Groundw. sustain. dev. 2020;10:100305. https://doi.org/10.1016/j.gsd.2019.100305
[23] J. Doherty, Calibration and uncertainty analysis for complex environmental models. Brisbane, Australia: Watermark Numerical Computing; 2015. https://doi.org/10.1111/gwat.12360
[24] N. Jovanovic, Bugan RD, Tredoux G, Israel S, BIshop R, Marinus V. Hydrogeological modelling of the Atlantis aquifer for management support to the Atlantis Water Supply Scheme. Water S.A. 2017;43(1):122-138. https://doi.org/10.4314/wsa.v43i1.15

JDFEWS 5 (2): 65 - 82, 2024
ISSN 2709-4529

[25] C. Zheng, Wang PP. MT3DMS: A modular three-dimensional multispecies transport model for simulation of advection, dispersion, and chemical reactions of contaminants in groundwater systems; documentation and user's guide. Contract report SERDP-99-1. Vicksburg, USA. US Army Corps of Engineers Engineer Research and Development Centre; 1999.
[26] C. Sundararaj, Muthukaruppan K, Mariappan D, Veluswamy K. Groundwater contaminant transport modelling using Visual MODFLOW: A case study of corporation sewage farm in South Madurai, Tamil Nadu, India. Arab. J. Geosci. 2022;15(18):1538. https://doi.org/10.1007/s12517-022-10804-0
[27] Akinsulie OO. Material flow analysis on a landfill site in Johannesburg. Dissertation (M.Sc.). Johannesburg: The University of the Witwatersrand; 2016.
[28] Musekiwa C, Majola K. Groundwater vulnerability map for South Africa. S.A. J. Geomat. 2013;2(2):152–162.
[29] Barnard HC. Hydrogeological map of Johannesburg 2526 (1:500 000). Department of Water Affairs and Forestry, Pretoria, Johannesburg, South Africa; 1999.
[30] Coetzee LE. Geological series 2628 East Rand (1:250000). South African Department of Mineral and Energy Affairs, Pretoria; 1986.
[31] De Beer JH. Geology of Johannesburg, Republic of South Africa. Bulletin of the Association of Engineering Geologists. 1986;23(2):101-137. https://doi.org/10.2113/gseegeosci.xxiii.2.101
[32] Wilkinson KJ. Geological Series 2626 West Rand (1:250000). South African Department of Mineral and Energy Affairs, Pretoria; 1986. Downloadable Material - Council for Geoscience
[33] Johnson MR, Wolmarans LG. Simplified geological map of the Republic of South Africa and the kingdoms of Lesotho and Swaziland. 1:2 000 000. Council for Geoscience, Pretoria; 2008.
[34] Burger M, Vermeulen PD. The groundwater interaction of a deeper lying gold mine and a shallower lying coal mine through the presence of naturally occurring as well as induced preferential flow paths. Presented at: 11th International Mine Water Association Congress–Mine Water–Managing Challenges Conference. Aachen, Germany. IMWA; 2011.63-567.
[35] Mokhahlane LS, Mathoho G, Gomo M, Vermeulen D. Qualitative hydrogeological assessment of vertical connectivity in aquifers surrounding an underground coal gasification site. J. South. Afr. Inst. Min. Metall. 2018;118(10):1047-1052.
[36] Waterloo Hydrogeologic. Visual MODFLOW version 8.0 user's manual-integrated conceptual and numerical groundwater modelling software. Ontario, Canada: Waterloo Hydrogeologic Inc.; 2022. Visual MODFLOW Flex 8.0 Product Release (waterloohydrogeologic.com)
[37] Niswonger RG, Panday S, Motomu I. MODFLOW-NWT, A newton formulation for MODFLOW-2005: US Geological Survey techniques and methods.2011;6–A37:44p. http://pubsdata.usgs.gov/pubs/tm/tm6a37/index.html
[38] Leketa k. Abiye T. Using environmental tracers to characterise groundwater flow mechanisms in the fractured crystalline and karst aquifers in Upper Crocodile River basin, Johannesburg, South Africa. Hydrology. 2021;8(1):50–50. https://www.mdpi.com/2306-5338/8/1/50
[39] Vermaak JJG. Geotechnical and hydrogeological characterization of residual soils in the vadose zone. Thesis (Doctoral). Pretoria: University of Pretoria; 2000. http://hdl.handle.net/2263/30093
[40] Osman OA, Ochieng GM, Rwanga S. Assessment of groundwater quality correlation to proximate landfill leachate: A case study on a selected landfill in Johannesburg, South Africa. [Unpublished manuscript]. Department of Civil Engineering, Vaal University of Technology; 2024.
[41] Xu M. Eckstein Y. Use of weighted least-squares method in evaluation of the relationship between dispersivity and field scale. Groundwater. 1995;33(6):905-908. https://doi.org/10.1111/j.1745-6584.1995.tb00035.x
[42] Khadri SFR. Pande C. Groundwater flow modelling for calibrating steady state using MODFLOW software: A case study of Mahesh River Basin, India. MESE. 2016;2(1):39. https://doi.org/10.1007/s40808-015-0049-7
[43] Shamsi UMS, Koran J. Continuous calibration. JWMM. 2017;25:C414. https://doi.org/10.14796/JWMM.C414
[44] Baalousha HM, Fahs M, Ramasomanana F, Younes A. Effect of pilot-points location on model calibration: Application to the northern karst aquifer of Qatar. Water. 2019;11(4):679. https://doi.org/10.3390/w11040679
[45] DWAF (Department of Water Affairs, South Africa). South African water quality guidelines, volume 1, 2nd edn. Domestic water use. Pretoria, South Africa: Department of Water Affairs and Forestry; 1996.
[46] SABS (South African Bureau of Standards). SANS 241:1 Drinking Water. Pretoria, South Africa: SABS Standards Division; 2015.
[47] WHO (World Health Organization). Guidelines for drinking-water quality: Incorporating the first and second addenda. Geneva, Switzerland: WHO; 2022.